

Tu-PM-Sym 1

ROLE OF HYDROPHOBIC, HYDRATION AND STERIC FORCES IN ADHESION AND FUSION OF BILAYERS

Jacob N. Israelachvili, Department of Chemical and Nuclear Engineering, and Materials Department, University of California, Santa Barbara, CA 93106

The surface forces apparatus technique was used to directly measure the force-laws between supported lipid bilayers in aqueous solutions. By changing the types of lipids used, the solution conditions, and the way the bilayers were adsorbed onto the surfaces it was possible to regulate the hydration, electrostatic charge and hydrophobicity of the bilayers. The results were compared with electron microscope freeze-fracture images of adhering vesicles. The aim was to identify the main forces responsible for the adhesion and fusion of bilayers and to monitor the molecular rearrangements associated with the adhesion and fusion processes in real time. The results show that the major force leading to the direct fusion of bilayers is the hydrophobic interaction, and that short-range repulsive steric and hydration forces are not "overcome" during fusion but are "bypassed" via local molecular rearrangements. The results of direct force measurements quantitatively correlate with the deformed shapes of adhering vesicles in solution as monitored by freeze fracture electron microscopy. Our findings indicate that the hydrophobic adhesion forces between bilayers can be significantly enhanced by stretching them osmotically, compressing them electrically or via local packing mismatch stresses.

Tu-PM-Sym 3

TOTAL INTERNAL REFLECTION FLUORESCENCE MICROSCOPY OF SUBSTRATE-SUPPORTED PLANAR MEMBRANES. N. L. Thompson, C. L. Poglitsch, M. L. Pisarchick, M. M. Timbs, M. T. Sumner, K. H. Pearce and H. V. Hsieh, Department of Chemistry, University of North Carolina, Chapel Hill, NC, 27599-3290.

Total internal reflection fluorescence microscopy (TIRFM) has been used to examine the behavior of fluorescently labelled ligands at model membranes deposited on transparent planar substrates. In TIRFM, a laser beam is internally reflected at the membrane/solution interface, creating an evanescent field that penetrates approximately 900 Å into the solution and selectively excites surface-bound fluorescent ligands. This technique has been used to examine monoclonal and polyclonal IgG on supported planar membranes containing the mouse Fc receptor mFcγRII; anti-dinitrophenyl monoclonal antibodies and their Fab fragments on phospholipid Langmuir-Blodgett films containing dinitrophenyl-conjugated phospholipids; bovine prothrombin fragment 1 on supported planar membranes containing negatively-charged phospholipids; and RGD-containing proteins and peptides on planar membranes containing the human platelet receptor GPIIb-IIIa. TIRFM has been used to measure equilibrium binding curves, has been combined with fluorescence photobleaching recovery to measure surface binding kinetic rates, and has been combined with fluorescence polarization to measure the orientation distributions of fluorophore absorption dipoles.

This work was supported by NIH grant GM-37145 and NSF grant DCB-8552986.

Tu-PM-Sym 2

INTERNAL AND INTERFACIAL STRUCTURE OF MEMBRANES USING X-RAY STANDING WAVES

Martin Caffrey

Department of Chemistry, The Ohio State University
Columbus, OH 43210

The x-ray standing wave (XSW) method developed in the mid-Sixties was used then to determine the position of heavy atoms in and on crystals of silicon and germanium with subångström resolution. The advent of layered synthetic microstructures, used primarily as wide-bandpass x-ray monochromators, heralded in a new era in the use of XSW to study biologically relevant structures with a length scale of order tens of ångströms. The original measurements were performed on model membrane Langmuir-Blodgett films and served to establish the utility of the XSW approach in determining heavy atom location in such systems with subångström resolution and in tracking the heavy atom layer as it moves during a thermotropic transition (Bedzyk *et al.* 1988, *Science* 241, 1788-1791). Recent results show that the XSW is well defined at close to a thousand ångströms from the XSW generating surface. Thus, the useful probing distance of XSW is of this length scale also without a compromise in resolution. In addition to the above measurements on well ordered systems the XSW method is being used to "directly" profile ion distribution at the membrane/aqueous interface (Bedzyk *et al.* 1990, *Science* 248, 52-56). Recent results show that the diffuse double layer can be established reversibly by suitably adjusting pH of the aqueous phase next to a phospholipid membrane. The advantages and disadvantages of this new surface technique as applied to the study of membrane structure and interfacial phenomena will be discussed and other likely uses for the method will be described.

Tu-PM-Sym 4

LENSLESS METHODOLOGIES FOR SUBWAVELENGTH IMAGING WITH LIGHT Aaron Lewis, Division of Applied Physics, The Hebrew University of Jerusalem, Jerusalem, Israel.

The lens has been the focusing element of choice for the past 400 years of light microscopy. However, this optical element imposes fundamental constraints on resolution that is associated with the wavelength of light and this practically limits the light microscope to 0.2μ resolution. Cellular biophysics is increasingly interested in imaging molecular associations in cells that form microdomains, microclusters and macromolecular aggregates. Thus, the resolution limit of lens-based light microscopes is a serious limitation to imaging cellular molecular aggregates with light even though light can probe cells non-destructively and with high contrast using standard staining procedures. In view of these advantages of light microscopy in cellular imaging my laboratory has been engaged over the last decade in the development of new methodologies for microscopy with light that are not limited in resolution by wavelength considerations. In this lecture three methodologies will be described that use as the optical imaging element the hole at the tip of a glass micropipette which can vary in size from 75Å to several microns depending on the resolution desired. In the first approach to be described called near-field scanning optical microscopy (NSOM) the small hole at the pipette tip is brought close, within the near-field (~equivalent to the size of the hole) of a surface and this hole either illuminates or detects light from the surface to form an image with the aid of a computer as it is scanned. In a second approach called molecular exciton microscopy (MEM) a crystal is grown in the tip of a pipette and light transmitted through the pipette generates excitons in the tip of the pipette which can tunnel to an acceptor in a surface. The acceptor in the surface can then fluoresce at its wavelength with an image being formed by instrumentation that is similar to NSOM. Molecular resolution is expected from MEM. Finally, high energy beams of electromagnetic radiation such as x-rays have been focused through tapered glass pipettes and this can be combined with x-ray or particle beam induced luminescence to allow the resolution of NSOM to be extended to structures beneath the surface.

Tu-PM-Sym 5

SCANNING TUNNELING MICROSCOPY OF NUCLEIC ACIDS AND NUCLEOPROTEIN COMPLEXES. Victor A. Bloomfield and Patricia G. Arscott, Department of Biochemistry, University of Minnesota, St. Paul MN 55108.

Scanning tunneling microscopy (STM) shows great promise as a tool for obtaining structural information about biopolymers and their functionally active complexes. We will review STM images of DNA obtained in our laboratory, and present a progress report on our studies of three DNA-binding proteins and their interactions with DNA. These are (1) C/EBP, a member of the class of leucine zipper binding proteins; (2) M_CABZ22, an immunoglobulin of the class IgG₂, with specificity for Z-DNA; and (3) the virE protein of *Agrobacterium tumefaciens*, a single-strand DNA binding protein. We will also point out some of the difficulties in these studies. In addition to problems of sample deposition and efficient scanning, which are generic to all STM studies of biopolymers, studies on DNA-protein complexes are particularly prone to artifacts arising from dehydration, which can both distort the structures of the biopolymers and, by raising the salt concentration, greatly weaken the ionic bonds which stabilize protein-nucleic acid association. Also, the general problem of the uncertain mechanism of STM image formation with deposited biomolecules is exacerbated in these complex systems, where there are few clear indications of the identity of the molecules being imaged. Notwithstanding these difficulties, which are inevitable at this early stage of development of STM, the technique holds great promise for structural studies of complex biomolecular systems at the atomic level.

Tu-PM-A1

Ca²⁺-ACTIVATED K⁺ CHANNELS IN RESTING AND ACTIVATED HUMAN PERIPHERAL T LYMPHOCYTES. Stephan Grissmer and Michael D. Cahalan. Dept. Physiology & Biophysics, UCI, Irvine, CA 92717.

During mitogenic stimulation of lymphocytes, cytosolic calcium $[Ca^{2+}]_i$ rises and the membrane potential hyperpolarizes. We have previously shown in a leukemic T-cell line, Jurkat, that the rise in $[Ca^{2+}]_i$ activates two components of voltage-insensitive K⁺ currents; a large population (~800 per cell) of apamin-sensitive K(Ca) channels, along with a very small population (~1.5 per cell) of charybdotoxin-sensitive K(Ca) channels. Here we report on K(Ca) channels in normal human peripheral T cells before and after activation with the mitogenic lectin, phytohemagglutinin (PHA). Whole-cell dialysis with pipette solutions containing a Ca-EGTA mixture with free $[Ca^{2+}]_i$ of 1 μ M activates a voltage-independent K⁺-selective conductance (g_{KCa}) within 2-4 seconds of break-in. Unlike the Jurkat T cells, g_{KCa} in both resting and activated human T cells is highly sensitive to charybdotoxin ($K_d < 4$ nM), not very sensitive to tetraethylammonium ($K_d \sim 40$ mM), and insensitive to apamin. Changing from normal Ringer to isotonic K⁺ Ringer shifted the reversal potential by ~80 mV and increased the slope conductance by a factor of 5. In most of the resting T cells, g_{KCa} in normal Ringer solution was less than 0.5 nS. Activated cells displayed a large increase in the number of K(Ca) channels; in cells treated with PHA for > 2 days, g_{KCa} averaged 6.7 nS. During activation, the T cells enlarge; in the cells sampled for whole-cell recording C_m values rose from 2.4 to 8.5 pF. Thus, the larger increase in g_{KCa} represents an increase in the surface density of K(Ca) channels. Supported by NIH grant NS14609 and GM41514.

Tu-PM-A3

CALCIUM AND LONG-LIVED CLOSED STATES IN A Ca²⁺-ACTIVATED K⁺ CHANNEL FROM SKELETAL MUSCLE. Natalien Malebran, Ramon Latorre, and Ximena Cecchi. Depto. de Biología, Facultad de Ciencias, Universidad de Chile and Centro de Estudios Científicos de Santiago, Santiago, Chile.

Calcium-activated K⁺ [K(Ca)] channels of high unitary conductance are blocked by internally added Ba²⁺. Blocked periods in the presence of Ba²⁺ can last several seconds. In the absence of Ba²⁺, K(Ca) channels also show long-lived closed events that have been interpreted in terms of a Ca²⁺ blockade. However, Neyton and Miller [*J. Gen. Physiol.* 92:549 (1988)] have proposed that most of the "Ca²⁺ blockade" is due to Ba²⁺ contamination of the solutions. In the present work we have restudied the characteristics of the slow kinetic process in K(Ca) channels incorporated into planar lipid bilayer membranes. When the internal solution was 100 mM KCl, 5 mM MOPS-NMDG, pH 7 the Ba²⁺ contamination is in the 1 μ M range. In these conditions and when the external solution was 5 mM MOPS-NMDG, pH 7 both, burst and long-lived closed dwell times are distributed exponentially. The mean burst and long-lived closed times were about 6 s at 0 mV and they were found to be voltage dependent. They decreased and e-fold per a 50 mV change in voltage in the depolarizing direction. When sulfate is added to the internal side to a final concentration of 10 mM ($[Ba^{2+}] \approx 10$ nM), the mean burst time was 7.6 s and the mean long-lived closed time was 4.8 s. If the Ba²⁺ concentration is further lowered by adding sulfate to a final concentration of 30 mM ($[Ba^{2+}] \approx 3$ nM) the mean times were 3 and 4.9 s for the burst and long-lived closed states respectively. These results suggest that the slow kinetic process showed by the K(Ca) channel, in the absence of external K⁺, is not due to a Ba²⁺ blockade. However, it was also found that the slow channel kinetic is independent of internal Ca²⁺ concentration in the 30 to 1000 mM range. Therefore, the long quiescent periods that the K(Ca) shows appear to be the result of a voltage-dependent gate. Supported by NIH and FNI 451/1988 and 1112/1989.

Tu-PM-A2

INHIBITION BY TOXINS OF CHARYBDOTOXIN BINDING TO THE VOLTAGE-GATED POTASSIUM CHANNEL OF LYMPHOCYTES: CORRELATION WITH BLOCK OF ACTIVATION OF HUMAN PERIPHERAL T-LYMPHOCYTES. R. S. Slaughter, J. L. Shevell, J. P. Felix, C. S. Lin, N. H. Sigal and G. J. Kaczorowski, Merck Institute for Therapeutic Research, Rahway, NJ 07065

Noxiustoxin (NxTX), alpha-dendrotoxin (α -DaTX), iberiotoxin (IbTX) and unlabeled charybdotoxin (ChTX) were compared for their ability to inhibit binding of [¹²⁵I]ChTX to voltage-gated K⁺ channels of purified human peripheral lymphocytes, of Jurkat cells (a human leukemia cell line) and of plasma membranes purified from Jurkat cells. Inhibition of [¹²⁵I]ChTX binding to T-lymphocytes and to Jurkat cells by the toxins was identical, but, due to different binding conditions, the potencies of the toxins varied slightly when tested on Jurkat plasma membranes. For Jurkat plasma membranes, NxTX and ChTX were the most potent with K_i's of 3 and 5 pM, respectively, while α -DaTX exhibited a K_i of 100 pM, and IbTX, a potent inhibitor of Ca²⁺-activated K⁺ channel of vascular smooth muscle, was not inhibitory. These same compounds were tested on highly purified quiescent human T-lymphocytes which were activated by Concanavalin A, or an anti-CD3 antibody in combination with the phorbol ester, PMA. They inhibited the proliferative response measured by [³H]thymidine incorporation, and inhibited the release of IL-2 determined by the CTLL bioassay. The rank order of inhibition of T-cell activation by the toxins is identical to that for [¹²⁵I]ChTX binding, while the potency was reduced. ChTX inhibited at 6 nM, NxTX at 11 nM and α -DaTX at 210 nM, while IbTX was not inhibitory. The [¹²⁵I]ChTX binding assay is normally performed in low salt, and elevated salt concentrations reduce the potency of the toxins from pM to nM levels, comparable to levels in T-cell activation assays. The toxins do not block lymphocyte activation by IL-2, a non Ca²⁺-dependent pathway. These data suggest that inhibition of voltage-gated K⁺ channels in lymphocyte is sufficient to block activation of lymphocytes by mediators that act through Ca²⁺-dependent pathways.

Tu-PM-A4

IBERIOTOXIN BLOCKADE IN A LARGE CONDUCTANCE Ca²⁺-ACTIVATED K⁺ CHANNEL FROM SKELETAL MUSCLE. Sebastian Candia, Maria L. Garcia, and Ramon Latorre. Depto. de Biología, Fac. de Ciencias, Univ. de Chile, Santiago, Chile, Dept. of Membrane Biochemistry and Biophysics, Merck Institute for Therapeutic Research, Rahway, New Jersey 07065, and Centro de Estudios Científicos de Santiago, Santiago 9, Chile.

Iberiotoxin (IbTX) is a peptide toxin purified from the venom of the scorpion *Buthus tamulus*. The toxin has a molecular weight of 4.3 kDa and shows a high degree of homology with charybdotoxin (CTX). The effect of IbTX on a Ca²⁺-activated K⁺ [K(Ca)] channel of high unitary conductance incorporated into planar lipid bilayers was studied. IbTX at nanomolar concentrations was able to induce very long periods in which the K(Ca) remain quiescent. These long-lived nonconducting states separate bursts of channel activity and can be interpreted as periods of time in which the channel remains blocked by IbTX. Channel gating during the burst periods was not different of that showed by the K(Ca) channel in the absence of IbTX. As the [IbTX] was raised bursts became shorter. Active and blocked dwell times were exponentially distributed. At 3 nM IbTX dwell times can be described by exponential functions with a mean burst time of 154 s and the a mean blocked time of 530 s. It was found that the reciprocal of the mean active time increased linearly whereas the mean blocked time was independent of [IbTX]. The data can be interpreted in terms of a simple two state model of the type: active + IbTX \rightleftharpoons blocked, with forward and backward rates constants k_{on} and k_{off} respectively. The calculated rate constants were $k_{on} = 4.4 \times 10^6$ M⁻¹s⁻¹ and $k_{off} = 4.9 \times 10^{-3}$ s⁻¹ when the channel external medium contained 2.5 mM K⁺, 300 mM Na⁺. Therefore, in these conditions $K_d = 0.82$ nM. It was also found that 1 mM external TEA increased the mean active time about 4-fold suggesting that IbTX block is due to channel occlusion at a site near the TEA external receptor. Thus, the mode of action of IbTX is similar to that of CTX, but IbTX needs to overcome a larger energy barrier in order to leave the channel external mouth. Supported by NIH and FNI-451/1988.

Tu-PM-A5

A ROLE OF Ca^{++} IN THE MUSCARINIC SUPPRESSION OF THE M-CURRENT IN BULLFROG SYMPATHETIC GANGLION CELLS. A. Kirkwood and J. Lisman. Dept. of Biology, Brandeis Univ., Waltham MA 02254.

The muscarinic action of acetylcholine suppresses the M-current in B cells of bullfrog sympathetic ganglia. Previous work has shown that muscarinic agonists induce Ca^{++} release from internal stores, and that caffeine-induced Ca^{++} release from these stores suppresses M-current. However, the failure of intracellular application of Ca^{++} buffer to block the suppression of M-current argues against a role for Ca^{++} (Pfaf-finger et al., 1988. *Neuron* 1,477). We have reexamined the role of Ca^{++} by intracellularly injecting BAPTA through a microelectrode in the intact ganglion. The cells were voltage-clamped with 1 or 2 microelectrodes and muscarinic synaptic responses were evoked by preganglionic stimulation (in 0.1mM curare) above the 7th ganglion. BAPTA injections greatly reduced (40-90%) the synaptic suppression of the M-current. Similarly, BAPTA (with free Ca set from $\sim 10^{-9}$ to 1.6×10^{-7} M) reduced the effect of the muscarinic agonist, betamechol. The amount of BAPTA in the cell was determined by coinjecting a dye (fast green) and measuring the changes in cell's absorbance with video microscopy. We found that concentrations higher than 5 mM BAPTA were required to reduce the agonist effect. To further examine the role of Ca^{++} , we depleted the internal Ca^{++} stores by applying 10 mM caffeine in 0 Ca^{++} Ringer. After caffeine was removed, the effect of agonist was tested and found to be reduced by 50% (compared to control prior to depletion). Restoration of external Ca^{++} rapidly restored the effect of agonist. Taken together, these results strongly suggest that an increase in intracellular Ca^{++} is necessary for the muscarinic suppression of M-current.

Tu-PM-A7

DELAYED RECTIFIER AND MAXI K^{+} CHANNELS IN CEREBELLAR GRANULE CELLS
Søren-Peter Olesen, NeuroSearch A/S, Smedeland 26, DK-2600 Glostrup, Denmark

Cerebellar granule cells constitute the largest population of neurons in the CNS, but little has been known about their electrophysiology, and single K^{+} channels of this neuronal cell have not yet been identified.

Granule cells from 7-8 days old mice were cultured and studied with patch-clamp technique in the cell-attached and inside-out mode. The intra- and extracellular solutions contained 145 mM and 4 mM K^{+} , respectively. Two different K^{+} channels were identified.

Voltage steps from a holding potential of -70 mV activated an outward rectifying channel with a reversal potential of -81 mV and a single channel conductance of 19 pS ($\text{SD}=2$ pS; $n=14$). The channel was K^{+} selective, and the average number of channels per patch was 1.8. Depolarizing steps from $V_m = -70$ mV to -40 mV, -20 mV, and 0 mV activated the channel with the most positive pulses being the strongest stimuli. The half-time of inactivation following steps to 0 mV ranged 3-9 sec ($n=6$). The channel activity was not influenced by changing the internal calcium concentration from 100 to 1000 nM.

Following inactivation of the 19 pS channel brief openings of a larger channel was observed at membrane potentials of -40 to +60 mV. In the standard solutions the channel had a conductance of 76 pS ($\text{SD}=4$ pS; $N=7$) and a reversal potential of -76 mV. The single channel conductance in a 145 mM symmetric potassium solution was 105 pS ($\text{SD}=6$ pS; $n=4$). The channel did not inactivate, but the opening frequency was increasingly higher, the more positive the membrane potential was. Changing the calcium concentration at the cytosolic side from 100 to 1000 nM increased the opening probability by $8-60 \times$ ($n=4$) at $V_m=0$.

In conclusion, the cultured cerebellar granule cells express a delayed rectifier K^{+} channel with a single channel conductance of 19 pS as well as a large-conductance Ca^{++} activated K^{+} channel.

Tu-PM-A6

FUNCTIONAL RECONSTITUTION OF THE LARGE CONDUCTANCE Ca^{++} -ACTIVATED K^{+} CHANNEL PURIFIED FROM BOVINE AORTIC SMOOTH MUSCLE. K.M. Giangiacomo, M. Garcia-Calvo, M.L. Garcia and O. B. McManus. Merck Sharp & Dohme Research Laboratories, P.O. Box 2000, Rahway, NJ 07065.

The Charybdotoxin (ChTX) receptor from bovine aortic sarcolemmal membranes has been purified to apparent homogeneity (Garcia-Calvo et al, this meeting). SDS-PAGE of the purified receptor shows a major band of ~ 35 kDa; a protein of similar molecular weight was specifically cross-linked with [125 I]ChTX. The purified ChTX receptor was reconstituted into liposomes and fused with planar lipid bilayers. Fusion of the proteoliposomes produced large conductance Ca^{++} -activated K^{+} (BK) channels with properties similar to the native channel. The purified channel had a single channel conductance of ~ 320 pS in symmetric 150 mM KCL, and was highly selective for K^{+} over Na^{+} ($\text{PNa}/\text{PK} < 0.05$) or chloride. The open probability (P_o) of the channel was increased by micromolar concentrations of internal calcium ($\sim 4 \mu\text{M}$ CaCl_2 yielded a P_o of 0.5 at 0mV) and by depolarizing membrane potentials (e-fold increase in P_o per ~ 11 mV). The purified channel was blocked by ChTX and by Iberiotoxin with inhibitor dissociation constant (K_i) values of 22 nM and 1 nM, respectively, in symmetric 150 mM KCL. External tetraethylammonium (TEA) caused a voltage dependent decrease in apparent single channel conductance, consistent with TEA binding to a site that sensed 0.19 of the voltage drop across the membrane with a K_i (at 0mV) of 300 μM . These results suggest that the purified ChTX receptor is sufficient to reconstitute functional large conductance Ca^{++} -activated K^{+} channels.

Tu-PM-B1

INTERACTIONS OF A SYNTHETIC TARGETING PEPTIDE WITH MEMBRANE CRYSTALS OF THE OUTER MITOCHONDRIAL MEMBRANE CHANNEL, VDAC. C.A. Mannella*, X.W. Guo[†], S. Yan, B. Cognon, J.A. Dias*, Wadsworth Center, NYS Dept of Health, Box 509, Albany, NY 12201-0509, and Depts of *Biomedical Sciences and [†]Physics, State Univ of NY at Albany.

The cationic, amphipathic N-terminal sequences of mitochondrial precursors have been implicated in the targeting of these proteins to mitochondria. A peptide corresponding to residues 3-22 of the precursor of subunit IV of cytochrome oxidase of *Neurospora crassa* has been synthesized and incubated with 2D crystals of the mitochondrial outer membrane channel (VDAC, porin). Following incubation (20-60 min) of the membrane crystals with 0, 10 or 100 μ M peptide, specimens were embedded in uranyl acetate or aurothioglucose and electron microscopic images were recorded. Membrane arrays in images of the peptide-treated specimens are coated with patches of thread-like, stain-excluding particles, presumably composed of the synthetic targeting peptide. Binding of the peptide to membrane crystals of the mitochondrial channel also causes a lateral phase transition in the 2D crystals, corresponding to contraction of the parallelogram lattice. Comparison of average projection images of control and peptide-coated arrays (obtained by correlation analysis) suggests that the peptide attaches to the same sites in the crystalline channel arrays as apocytochrome c (Mannella et al, Biophys.J. 51:221). These sites are a subset of the lipid domains bordering the channels which, in the non-contracted lattice, are occupied by protein "arms" that extend laterally between the channels. While amphipathic peptides are generally lipophilic, the indication of specificity in the binding of mitochondrial precursors to the periphery of outer-membrane channels suggests that such binding might be significant, perhaps preceding diffusion of the polypeptides through the channel lumens. (Supported by NSF grants DMB-8916315, DIR-8914757 and NIH grant 1S15 GM4344301.)

Tu-PM-B3

INFERRING THE STRUCTURAL CHANGES IN VDAC, ASSOCIATED WITH THE CHANNEL'S GATING PROCESS, THROUGH SITE-DIRECTED MUTAGENESIS Songzhi Peng*, Elizabeth Blachly-Dyson[†], Marco Colombini*, Michael Forte[‡]. * Cell Biology Labs., Zoology Dept., Univ. of Maryland, College Park, MD 20742. [†] Vollum Inst. for Advanced Biomedical Research, Oregon Health Sciences Univ., Portland, OR 97201. (Intro. by Lynn M. Amende)

An identification of protein strands forming the wall of the aqueous pore of the mitochondrial channel, VDAC, in its open state, has been performed and published (Science 247:1233-36, 1990). We extended this work to a low-conducting, "closed", state (still allows KCl to pass but probably not ATP). König's polyanion was used to restrict the variability in the selectivity of the closed state. This state has a large pore diameter (1.8 nm) and therefore, as was the case for the open state, we expect charge on the walls of the pore to dominate the ion selectivity (for the small ions used: K⁺ and Cl⁻). Channels with charge changes at specific locations were obtained by site-directed mutagenesis. Protein regions in which charge changes resulted in appropriate selectivity changes in VDAC were interpreted as forming the wall of the pore. Some mutations had no effect on the selectivity of either the open or closed state (interpretation: located outside the pore); some changed the selectivity of both states in the same direction (interpretation: forming the wall in both states); some changed the selectivity of the open state, leaving that of the closed state unaltered. The last type of mutant indicates the movement of a domain(s) from the wall of the pore, in the open state, to a location outside the pore in the closed state. A reduction in the amount of matter forming the wall of the pore must result in a reduced pore radius and volume. This could be the structural change associated with the gating process in VDAC. (Supported by NIH grant # GM35759 and ONR grant # N00014-90-J-1024)

Tu-PM-B2

PROJECTION IMAGES OF MEMBRANE CRYSTALS OF THE MITOCHONDRIAL OUTER MEMBRANE CHANNEL, VDAC, EMBEDDED IN AUROTHIOGLUCOSE. X.W. Guo*, H. Chen*, C.A. Mannella[†], Wadsworth Center, NYS Dept of Health, Box 509, Albany, NY 12201-0509, and Depts of *Physics and [†]Biomedical Sciences, State Univ of NY at Albany.

High resolution electron microscopic images of phospholipase A₂-induced 2D crystals of mitochondrial outer-membrane channels (VDAC, porin) from *Neurospora crassa* are obtained with specimens embedded in aurothioglucose. Correlation averages computed from such membrane crystals typically contain strong Fourier components out to 1/(1.3 nm). Correspondence analysis has been used to classify 53 projection images of control crystals and those treated with effectors of the VDAC channel to detect possible systematic differences in the images. The results described here relate only to the "oblique" polymorph (lattice angle = 109°) of VDAC crystals. Most control images fall into two classes, characterized primarily by differences in the mean projected diameters of the pore lumens (1.4 and 2.2 nm). This wide-vs-narrow pore distinction is the main feature of the first factor axis in correspondence analysis, accounting for 24% of the total interimage variance. The second factor axis (13% of total variance) is associated primarily with the absence or presence of density at the corners of the unit cells in the arrays, i.e. between the channel hexamers. (Dense protein "arms" in these regions were previously observed only with unstained, frozen-hydrated VDAC arrays.) There appears to be a general correlation between presence of lateral arms and large pore size for most of the control images. Images of arrays treated with a polyanion effector or high pH fall into a third class, characterized by intermediate pore size and very prominent density away from the pores. Arrays treated with aluminum have variable pore size and weak or no "arms". (Supported by NSF grant DMB-8916315.)

Tu-PM-B4

PROBING FOR THE VOLTAGE SENSOR OF THE VDAC ION CHANNEL BY SITE-DIRECTED MUTAGENESIS.

*L. Thomas, +E. Blachly-Dyson, *M. Colombini and +M. Forte, *Univ. of Maryland, College Park, MD 20742, +Oregon Health Sciences University, Portland, OR 97201 (Intro. by Susan F. Wood)

VDAC is a voltage-dependent channel found in mitochondrial outer membranes. The channel adopts an open conformation (high conductance state) at low or zero membrane potential, and a closed conformation (low conductance state) at transmembrane potentials above 30-40 mV. To probe for the voltage sensor, site-directed mutagenesis was used to generate mutant proteins differing in charge from the wild-type protein. The rationale was that if a portion of the protein was involved in voltage sensing then a change in charge at this region should affect the voltage sensitivity of the protein. VDAC's sensor appears to carry a net positive charge. Therefore, by increasing positive charge on the sensor, the voltage dependence of the channel should be increased and vice-versa. The substitution of glutamate for lysine at position 19 from the N-terminus resulted in a 2.5 fold reduction in the steepness of voltage dependence when compared to the wild-type channel under the same conditions. A lysine substitution for an aspartic acid residue at position 51 resulted in a 2 fold increase in the steepness of voltage dependence. By contrast, substitution of glutamic acid for lysine at positions 132, 205, 211, 248 and 267 had little or no effect on voltage dependence. Thus, it appears that identification of protein domains involved in voltage sensing is possible using this approach. (Supported by NIH grant #GM35759 and ONR grant #N0004-90-J-1024)

Tu-PM-B5

CLONING OF A HUMAN VDAC cDNA

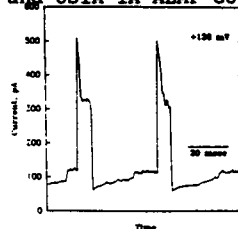
E. Blachly-Dyson and M. Forte, Vollum Institute, Oregon Health Sciences University, Portland, OR 97201

VDAC is a small (~30 kD) protein which forms large voltage-dependent channels in the outer mitochondrial membranes of eukaryotes of all kingdoms. Recently, a human VDAC protein has been purified (surprisingly, from plasma membranes of a B-lymphocyte cell line), and its entire polypeptide sequence determined (F. P. Thirnes et al., Biol. Chem. Hoppe-Seyler 370, 1253-1264, 1989). We used the published amino acid sequence to design two nested pairs of degenerate oligonucleotide primers, and used these primers to amplify by polymerase chain reaction a specific fragment from transcripts expressed in a human lymphocyte cell line. This 450 b.p. fragment was sequenced to verify that it encoded the expected peptide sequence, and was used to probe a human pituitary cDNA library in lambda gt10. A single hybridizing clone was identified, which contained a 1.8 kb insert. This insert contained a 283 codon open reading frame encoding a polypeptide that perfectly matched the published protein sequence with the addition of a methionine residue at the amino terminus. We will use RNA transcribed in vitro from this clone to inject *Xenopus* oocytes, in order to determine whether VDAC-like channels are produced in the plasma membrane. We also plan to express the cDNA in yeast cells lacking an endogenous VDAC gene to determine whether the protein reaches the mitochondria and if so, how its biophysical characteristics compare with VDAC from other species. (Supported by NIH grant #GM35759)

Tu-PM-B6

CHARACTERISTICS OF HIGH CONDUCTANCE CHANNELS IN RAT HEART INNER MITOCHONDRIAL MEMBRANES. Dmitry B. Zorov¹, Kathleen W. Kinnally^{2,3}, Sean Perini² and Henry Tedeschi². ¹A.N. Belozersky Laboratory, Moscow State University, ²Dept. of Biological Sciences, State University of New York at Albany, ³Siena College, Loudonville, N.Y.

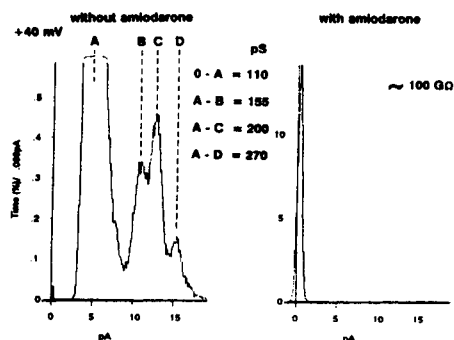
We have observed channels of high conductance in rat heart mitochondria with single transitions as high as 3 nS (see figure). Usually these transitions have been seen at high potential (e.g. ± 130 mV) although they also have been seen at lower voltages. These transitions have not been seen with liposomes devoid of proteins. Some observations suggest that the transitions correspond to channels produced from the assembly of subunits capable of subsequently acting in concert. The model is supported by the following observations: (a) although the opening (or closing) may be in a single step, the closing (or opening) may be in several lower conductance steps, (b) in some experiments (some with mouse liver mitochondria) small transitions were replaced by progressively larger ones in a graded manner, (c) the opening is frequently preceded by small steps (pre-steps) (d) The intermediate steps of the nS transitions are of the same size as the closing steps induced by the inhibitor amiodarone. Supported in part by grants from NSF DCB-8818432 and USIA 1A-AEMP-G8193395.



Tu-PM-B7

EFFECT OF INHIBITORS ON INNER MITOCHONDRIAL MEMBRANE CHANNELS. Yuri N. Antonenko¹, Kathleen W. Kinnally^{2,3}, Sean Perini² and Henry Tedeschi². ¹A.N. Belozersky Laboratory, Moscow State University, ²Dept. of Biol. Sci., SUNY Albany and ³Siena College, Loudonville, N.Y.

Amiodarone, propranolol and quinine were found to block two conductance pathways of the inner mitochondrial membrane. One corresponds to the anion-selective pathway induced by alkaline pH and the other to a cation-selective pathway hitherto unsuspected. The data are consistent with the presence of two different channels involved in these two pathways. Amiodarone was also found to eliminate the multi-conductance channel activity first described by Kinnally et al. (1989). This drug increases the conductance of a channel we ascribe to the ~110 pS channel of Sorgato et al. (1987). The effect on other conductance levels of similar size appears to be complex. Supported in part by grants from NSF DCB-8818432 and USIA 1A-AEMP-G 193692.



Tu-PM-B8

CYCLOSPORIN A INHIBITS THE MEGACHANNEL OF THE INNER MITOCHONDRIAL MEMBRANE

Mario Zoratti and Ildiko Szabo¹
CNR, CS Fisiologia Mitochondri, Via Trieste 75,
Padova, Italy

In patch-clamp experiments, cyclosporin A inhibits the activity of the giant (1.3 nS in 150 mM KCl) channel of the inner mitochondrial membrane (or of the contact sites) at concentrations in the 10^{-8} M range. The inhibition takes place only if cyclosporin is present on the matrix side of the membrane. Cyclosporin does not inhibit the 107 pS anion-selective channel. Millimolar concentrations of Ca^{++} elicit megachannel activity from a high proportion of the "silent" patches. The effect is reversed by EGTA. The "permeability transition" of mitochondria (1) is caused by high Ca^{++} and it is inhibited by cyclosporin in the same concentration range we used. It has been attributed to the opening of a giant pore, which may be tentatively identified with the megachannel observed in electrophysiological experiments.

(1) Denton, R.M. and McCormack, J.G. (1990) Am. J. Physiol. 258, C755-C766.

Tu-PM-B9**SUBSTRATE TRANSPORT PROTEINS OF THE INNER MITOCHONDRIAL MEMBRANE**

F. Palmieri, F. Bisaccia, L. Capobianco, V. Dolce, V. Iacobazzi, C. Indiveri and V. Zara (Intro by C.H. Chen)
Department of Pharmacology-Biology, University of Bari and CNR
Unit for the Study of Mitochondria, Bari (Italy)

In the last years we have purified and reconstituted into liposomes the phosphate (PIC), the oxoglutarate (OGC), the dicarboxylate and the tricarboxylate carriers from heart or liver mitochondria. We have now purified the carnitine carrier (CAC) by chromatography on hydroxyapatite and celite of Triton X-100 solubilized rat liver mitochondria. Once bound to celite the CAC was eluted in pure form by application of the Triton X-100 buffer containing cardiolipin and no salts. The purified celite fraction consisted of a single band with a Mr of 32.5 kDa. Incubation of newly synthesized PIC precursor with bovine heart or rat liver mitochondria resulted in an efficient transfer of the protein into mitochondria. The topology of the membrane-bound PIC was investigated by studying the interaction between antibodies specific for the N-terminal and the C-terminal ends of the PIC and freeze-thawed mitochondria or SMP. It was found that both the N-terminal and the C-terminal regions are located on the cytosolic side of the inner membrane. The amino acid sequence of the OGC was deduced from the cDNA sequence obtained by PCR. The protein sequence contains three tandem repeats of related sequences. Moreover, these repeats are related to those found in the AAC and the PIC indicating that these carriers belong to the same protein family. The kinetic mechanism of the exchange reaction catalyzed by the reconstituted OGC is consistent with a sequential mechanism including a ternary complex.

Tu-PM-C1

CHARACTERIZATION OF THE Ca^{2+} -INDUCED CONFORMATIONAL CHANGE IN TROPONIN-C BY SITE-DIRECTED MUTAGENESIS, PYRENE EXCIMER EMISSION AND RESONANCE ENERGY TRANSFER. Z. Wang, J. Gergely and T. Tao. Dept. of Muscle Research, Boston Biomedical Research Institute, 20 Staniford St. Boston MA 02114.

A key event in the regulation of vertebrate striated muscle contraction is the binding of Ca^{2+} to troponin-C (TnC). Comparison of the atomic structure of the Ca^{2+} -free N-terminal domain with that of the Ca^{2+} -bound C-terminal domain led to the hypothesis that binding of Ca^{2+} to the low affinity "triggering sites" of TnC gives rise to a separation of the B- and C-helices from the N-, A- and D-helices, thereby exposing a patch of residues that can serve as an additional interaction site with troponin-I (Herzberg, Moulton & James, *J. Biol. Chem.* 261, 2638-2644, 1986) (HMJ model). Although recent site-directed mutagenesis studies strongly indicate that this conformational transition is important for the function of TnC (Grabarek et al. *Nature* 345, 132-135, 1990; Fujimori et al., *Nature* 345, 182-184, 1990), primary experimental evidence for the proposed conformational change has been lacking.

In this work we synthesized a recombinant rabbit skeletal TnC containing a pair of Cys's, one at position 49 in the loop linking helices B and C, the second at position 12 at the beginning of the A helix (designated as TnC12/49). The HMJ model predicts that while residue 12 does not undergo any Ca^{2+} -induced movement residue 49 moves away from residue 12 by ~11 Å. Our results show firstly that the excimer emission of pyrene maleimide labeled TnC12/49 decreases when Ca^{2+} bind to the low affinity sites, indicating separation of the pyrene moieties. Secondly, the resonance energy transfer efficiency of TnC12/49 labeled with a donor-acceptor pair decreases when Ca^{2+} bind to the low affinity sites. Application of the Förster equations and assuming $\kappa^2=2/3$ yielded distances of 26 and 39 Å in the absence and presence of Ca^{2+} , respectively. Thus, both sets of results are in agreement with the HMJ model, and provide quantitative experimental evidence for the Ca^{2+} -induced movement of helices B and C. (Supported by NIH and MDA).

Tu-PM-C3

MUTATION OF CALCIUM BINDING SITES III AND IV IN CARDIAC TROPONIN C. John A. Putkey, H. Lee Sweeney and Judy Negele. Biochem. and Mol. Biol., Univ. Texas Med. School, Hou. and Dept. Physiol., Univ. Penn. Med. School, Phil.

Cardiac TnC (cTnC) has two high affinity Ca^{2+} -binding sites in the C-terminal domain and a single low affinity site in the N-terminus. To study the high affinity sites, mutagenesis was used to generate proteins with a single inactive site III or IV (CBM-III and CBM-IV, respectively), or with both sites inactive (CBM-III-IV). Direct Ca^{2+} binding demonstrated that the mutants had the predicted Ca^{2+} binding characteristics. Circular dichroism and fluorescence studies suggest that the mutated sites III and IV may still bind Mg^{2+} but that the conformational change induced by Mg^{2+} is not the same as for the normal protein. Calcium titration of the monomeric proteins labeled at Cys residues with the fluorescence probe IAANS showed that mutation of site III or both sites III and IV greatly affected fluorescent emissions. However, these differences observed in the monomeric proteins may be minimized within the troponin complex since Ca^{2+} titration of complexes formed with IAANS-labeled normal and mutant proteins gave similar fluorescence emissions. Both CBM-III and CBM-IV could effectively substitute for cTnC in skinned muscle and myofibril ATPase assays. The mutant CBM-III-IV, which has both high affinity Ca^{2+} -binding sites inactivated, is also capable of regulating actomyosin ATPase activity but only at concentrations that are 10-20-fold greater than the normal protein. The activation characteristics of CBM-III-IV are similar to calmodulin. The elevated levels of CBM-III-IV necessary for activation of muscle contraction is consistent with a reduced affinity of CBMIII/IV for the troponin complex. Therefore, although neither high affinity site is absolutely essential for regulation of muscle contraction in vitro, at least one active high affinity site is required for normal functional characteristics. This requirement can be satisfied by either site III or IV.

Tu-PM-C2

MUTATION OF CALCIUM BINDING SITES I AND II IN CARDIAC TROPONIN C. H. Lee Sweeney and John A. Putkey, Dept. of Physiology, Univ. of Pennsylvania, Philadelphia, PA and Dept. of Biochemistry & Molecular Biology, Univ. of Texas Medical School, Houston, TX.

Fast skeletal TnC has two low-affinity Ca^{2+} -binding sites (sites I and II), while in cardiac/slow skeletal TnC site I is inactive. Using protein engineering, we directly demonstrated that binding of Ca^{2+} to the low-affinity site(s) initiates muscle contraction [Putkey, J.A., Sweeney, H.L. & Campbell, S.T. (1989) *J. Biol. Chem.* 264, 12370-12378]. In this study, we use mutagenesis to determine whether either of the low-affinity sites in cardiac TnC can trigger contraction. In one calcium binding mutant, Ca^{2+} -binding to the dormant low-affinity site I was restored (CBM+I). In a second mutant, site I was activated while site II was inactivated (CBM+I-IIA). Both proteins had the predicted Ca^{2+} -binding characteristics, and both were able to associate with TnI and TnT to form a troponin complex and integrate into permeabilized slow and fast skeletal muscle fibers. CBM+I supported force generation in skinned slow skeletal muscle fibers but with Sr^{2+} and Ca^{2+} sensitivities similar to fast skeletal TnC. CBM+I-IIA was unable to restore Ca^{2+} -dependent contraction to TnC-depleted skinned slow muscle fibers. However, CBM+I-IIA was able to recover approximately 20% of the normal ATPase activity in fast skeletal myofibrils and approximately 20% of force in permeabilized psoas (fast) fibers. The $p\text{Ca}_{50}$ for CBM+I-IIA in fast skeletal muscle is approximately 0.5 pCa units lower than that of either fast skeletal TnC or cardiac/slow TnC and the apparent Hill coefficient is more similar to that of fast skeletal TnC. The data directly demonstrate that low-affinity sites I and II have distinct functions, and that only site II in cardiac TnC can trigger muscle contraction in slow skeletal muscle. In fast skeletal muscle, which normally has a TnC that binds four Ca^{2+} , the isoforms of TnT and TnI can translate the signal initiated by binding Ca^{2+} to site I in the absence of Ca^{2+} binding to site II, but the activation of ATPase activity and force is only a fraction of that obtained with normal TnC.

This work was supported by grants from the NIH (H.L.S. and J.A.P.), grants from the American Heart Association and the Texas and Pennsylvania Affiliates of the American Heart Association.

Tu-PM-C4

THE CARBOXYL-TERMINAL EXON 9 OF α -TROPOMYOSIN IS IMPORTANT FOR ISOFORM SPECIFIC FUNCTIONS. Young-Joon Cho and Sarah E. Hitchcock-DeGregori. Dept. of Neuroscience and Cell Biology, UMDNJ-Robert Wood Johnson Medical School, Piscataway, NJ 08854

In order to determine the functional significance of alternatively spliced exons of α -tropomyosin, we constructed two chimeras from striated and smooth α -tropomyosin c-DNA (gift of B. Nadal-Ginard) in which the striated tropomyosin has a smooth exon 2 (residue 39-80, chimera sm2) or a smooth exon 9 (residue 258-284, chimera sm9). We previously reported preliminary results showing that the 9th exon is responsible for isoform specific functions (Cho and Hitchcock-DeGregori, 1990, *Biophysical J.*, 57, 153a). To understand the role of the exon 9 in detail we quantitatively measured actin binding affinities of four nonfusion tropomyosins: striated, smooth, chimera sm2, and chimera sm9. Smooth ($K_{app}=4.9 \times 10^5 \text{ M}^{-1}$) and chimera sm9 ($K_{app}=6.1 \times 10^5 \text{ M}^{-1}$) bound to actin with much higher affinities than striated ($K_{app}<10^5 \text{ M}^{-1}$) and chimera sm2 ($K_{app}<<10^5 \text{ M}^{-1}$). This indicates that the increased actin affinity of smooth and chimera sm9 is primarily due to the presence of smooth exon 9. Exon 2 also influences actin affinity since the tropomyosins with striated exon 2 bind with slightly higher affinity than those with smooth exon 2. The higher actin affinity of tropomyosins with the smooth 9th exon cannot be explained by head-to-tail association since all 4 recombinant tropomyosins polymerized poorly. In the presence of 0.2 mM CaCl_2 , troponin increased the actin affinity of striated ($K_{app}=4.6 \times 10^6 \text{ M}^{-1}$) and chimera sm2 ($K_{app}=1.3 \times 10^5 \text{ M}^{-1}$) at least 50 fold while smooth ($K_{app}=6.4 \times 10^5 \text{ M}^{-1}$) and chimera sm9 ($K_{app}=7.7 \times 10^5 \text{ M}^{-1}$) showed only a slight increase. In the absence of CaCl_2 (0.5 mM EGTA) the affinity of all four tropomyosins for actin was further increased 10-fold except for striated which showed a 3.5-fold increase. The results indicate that striated exon 9 is specialized for interaction with troponin. Of the 9 tropomyosin isoforms encoded by the α -tropomyosin gene, the striated exon 9 is restricted to striated muscles, the only tissues known to contain troponin. Supported by AHA

Tu-PM-C5

FUNCTIONAL PROPERTIES OF THE C-TERMINAL ACTIN-BINDING FRAGMENTS OF CALDESMON. L. Velaz, and J.M. Chalovich. East Carolina University School of Medicine; Greenville, NC 27858.

Caldesmon, a putative smooth muscle regulatory protein, binds to actin, tropomyosin, myosin, and calmodulin. We have digested [14 C]-caldesmon with chymotrypsin and purified a family of three actin-binding peptides from the C-terminal region of caldesmon. Like intact caldesmon, the binding of these fragments to actin is competitive with the binding of both myosin subfragments and Ca^{2+} -calmodulin to actin. Inhibition of ATPase activity is primarily due to the inhibition of the binding myosin-ATP complexes to actin. In addition, these 20 kDa fragments bind to tropomyosin and their inhibitory activity is increased about 3-fold by smooth muscle tropomyosin. However, in contrast to caldesmon, the binding of these fragments to actin is not enhanced by tropomyosin. This is further evidence that the effect of tropomyosin on the inhibitory activity of caldesmon is not directly the result of an increase in the strength of binding of caldesmon to actin. In the presence of tropomyosin, caldesmon and its fragments, inhibit actin-activated ATP hydrolysis by reversing the potentiating effect of tropomyosin (about 2-3 fold), as suggested by others, in addition to reversing the binding of myosin-ATP to actin.

The 20 kDa caldesmon fragments bind to actin and to actin-tropomyosin with an stoichiometry of 1 fragment per 2 actin monomers and in the absence of tropomyosin maximum inhibition of ATPase activity occurs when 1 fragment is bound per 3 actin monomers. Like intact caldesmon, the degree of inhibition, in the absence of tropomyosin, is related to the number of actin monomers covered with caldesmon; this is in agreement with a competitive binding mechanism. There appear to be no long range effects of caldesmon on the actin filament.

Tu-PM-C7

ABSENCE OF CALPONIN PHOSPHORYLATION IN RESTING OR CONTRACTING ARTERIAL SMOOTH MUSCLE. M. Bárány, A. Rokolya, C. Koncz, and K. Bárány. Departments of Physiology and Biophysics and Biochemistry, College of Medicine, University of Illinois, Chicago, IL 60612.

Winder and Walsh have reported (JBC, 265, 10148, 1990) that *in vitro* the inhibition of smooth muscle actomyosin MgATPase by calponin is reversed by its phosphorylation. We have tested their suggestion that the contractile state of smooth muscle is regulated by calponin phosphorylation. Porcine carotid arterial muscles were incubated in physiological salt solution (PSS) containing 2 mCi [32 P] orthophosphate at 37 °C for 90 min. 32 P-labeled muscles were contracted with 100 mM K^+ in PSS for 1, 30 or 60 min. For determination of protein phosphorylation, resting or contracted muscles were frozen in liquid nitrogen, pulverized, washed with TCA containing phosphate and dissolved in SDS. The total muscle proteins were separated either by 1D gel electrophoresis, or by 2D gel electrophoresis, pH 3-10 in the first dimension and 10 or 15% polyacrylamide gels containing SDS in the second dimension. For identification of calponin bands on the gels pure calponin was isolated according to a modified procedure of Abe et al. (J. Biochem. 107, 507, 1990). No radioactivity was detected in calponin from muscle, resting or contracted with K^+ for 1, 30, or 60 min. Under these conditions a large number of 32 P-labeled proteins were found both in resting and contracted muscles, some of them showed changes in their radioactivity depending on the contractile state of the muscle. Thus, our results do not support the idea of calponin phosphorylation playing a role in the regulation of arterial muscle contractility. (Supported by NIH, AR 34602 and AHA).

Tu-PM-C8

LOCALIZATION OF THE CALMODULIN- AND THE ACTIN-BINDING SITES OF CALDESMON. C.-L. Albert Wang, Li-Wen C. Wang, Shuang Xu, Renné C. Lu, Victor Saavedra-Alanis[§] and Joseph Bryan[§], Dept. of Muscle Research, Boston Biomedical Research Inst., Boston, MA 02114 and [§]Dept. of Cell Biology, Baylor College of Medicine, Houston, TX 77030

Expression of the C-terminal third of chicken gizzard caldesmon in *E. coli* produces a cII-caldesmon fusion protein (27 kDa) with caldesmon sequence beginning at Lys⁵⁷⁹. Degradation during purification yields five peptides with molecular masses of 24 kDa (beginning at Phe⁵⁸¹), 22 kDa (beginning at Leu⁵⁹⁷), 19 kDa (two peptides; 19K-a and 19K-b, beginning at Phe⁵⁸¹ and Val⁶²⁹, respectively) and 15 kDa (also beginning at Val⁶²⁹). We estimate that the 15 kDa and one of the 19 kDa peptides (19K-a) end at or near Leu⁷¹⁰, whereas the other peptides end at or very near the C-terminus, Pro⁷⁵⁶. Site-directed mutagenesis was used to produce truncated peptides with known C-termini; one such peptide (17 kDa) terminates at Asn⁶⁷⁵. Digestion of the fragments with chymotrypsin generates a second 15 kDa fragment (15K') that begins at Ser⁶⁶⁶. All of these peptides, with the exception of 15K', bind Ca^{2+} -calmodulin-Sepharose and have a common peptide sequence between Val⁶²⁹ and Ser⁶⁶⁶, suggesting that this is the calmodulin-binding site. All of the fragments, except the two 15 kDa peptides, co-sediment with F-actin, indicating that there are at least two actin-binding sites in this region of caldesmon, located between Leu⁵⁹⁷ and Val⁶²⁹ and between Arg⁷¹¹ and Pro⁷⁵⁶. These two sites, although separated in the primary sequence, may very well interact with the calmodulin-binding region in the folded structure. (Supported by grants from NIH and AHA)

Tu-PM-C8

RESULTS OF PRELIMINARY STUDIES OF TROPOMYOSIN RADIAL MOVEMENT USING NEUTRON SCATTERING. R. A. Mendelson, D.B. Stone, P.A. Timmins[†], E.R. Johnston. C.V.R.I., Univ. of Calif., San Francisco CA 94143 and [†] Institut Laue-Langevin, 38042 Grenoble Cedex, France.

We are currently investigating changes in the average (cross-helix) distance between tropomyosin molecules (Tm) in reconstituted thin filaments using neutron scattering. In this approach the entire thin filament except (deuterated) tropomyosin is rendered "invisible" by solvent density-matching of the protonated protein. This method eliminates many of the problems present in conventional structural techniques of unambiguously resolving Tm.

Highly deuterated tropomyosin was obtained by expressing a Factor X_a-cleavable fusion protein in *E. coli* grown on deuterated algal hydrolysate in D₂O. (The clone used was a gift of F. Reinach and the late A.R. MacLeod.) We have found that reconstituted thin filaments made with the product (D)Tm regulate S1 ATPase almost identically to native thin filaments in H₂O and D₂O.

Because the structure of Tm is known at low resolution and its radial extent is small compared to the Tm distance from the filament axis, the cross-sectional radius of gyration (R_g) is a good measure of this radius. Preliminary measurements of R_g under conditions of low ionic strength with and without Ca^{2+} indicate that any changes in the average inter-Tm distance are small (< 0.5 nm). Early formulations of the steric-blocking hypothesis suggested that changes in this distance could be as large as 2.5 nm.; however, more recent notions of regulation (Phillips *et al.*, JMB 192: 111, 1986) are more consistent with our observations.

Supported by NSF grant DMB 8716091.

Tu-PM-C9

SEQUENCE LOCATION OF Ca IN F-ACTIN. K. Ue¹, A. Muhrad¹, C. G. Edmonds¹, D. Bivin¹, W. Piechowski¹, A. Perez², & M.F. Morales², from U. of the Pacific, San Francisco^(*), Hebrew U. ([#]), and Battelle Pacific Northwest Laboratory ([@])

It is suggested from Dervan (*Proc. Natl. Acad. Sci.* 82, 968, 1985) and Stadtman (*J. Biol. Chem.* 260, 15394, 1985) that short-ranged, chain-cutting free radicals generated by Fenton cycles at bound redox metal ions may mark the metal locations in the macromolecule that binds them. This idea was tested in F-actin. Fe²⁺ was exchanged with the Ca²⁺ of G-actin. The protein was then polymerized, passed through AG-50 columns, and analyzed for Ca²⁺ (by counting ⁴⁵Ca) and Fe²⁺ (by phenanthroline colorimetry). [Tight binding of ca 3.6 Fe/actin is achieved, but back titration with Ca indicates that only a single Ca-displaceable Fe/actin is effective in the chain cutting described below]. Such F-actin was exposed to reductant and samples were then drawn for PAGE or for HPLC. Besides the 42kDa band of intact actin, PAGE showed heavy bands at 24kDa (containing C-) and at 18kDa (containing N-) and light bands at 34kDa (containing the N-) and 8kDa (containing C-). There was also a light band at 16kDa containing neither terminus. We surmised that the actin chain had been cut at 2 points. End group analysis of 24kDa showed that its N-terminus was Thr-160; similar analysis of 8kDa showed that its N-terminus was Gly-302. 16kDa had the same N-terminus as 24kDa, indicating that it was the "internal" fragment arising in a double cut. Electrospray ionization mass spectrometry measurement gave the theoretically expected MW (from amino acid composition) for intact actin, and also showed that HPLC-purified 18kDa had the MW expected from only one bond cutting (Between Val-159 and Thr-160). Using HPLC-purified 16kDa, work is underway to establish the same for the cut near position 302. This work suggests that bonds 159-160 and 301-302 are very near to the tightly-held Ca²⁺ of actin, and is consistent with the idea that the actin chain passes the metal location twice (in order to achieve proximity between termini). Our technique and result seem validated by the crystallography of Kabsch, et al. (*Nature*, 347, 37, 1990) that appeared after our work was completed: The cited bonds are very near to the most proximal atoms identified by Kabsch, et al; they are not identical, but note that the crystallography refers to the actin-DNAse I complex, and our work refers to F-actin in solution. It is noteworthy also that Fe²⁺ incorporated into G-actin and supplied with reductant fails to catalyze chain cutting, and that Fe²⁺ cannot be directly incorporated into the effective site of F-actin. (Supported by R37 NHLBI-44200¹ & HG00327¹)

Tu-PM-D1

LEU-ZERVAMICIN: CRYSTAL STRUCTURE OF FOUR POLYMORPHS; PROBABLE ION CHANNEL CONFIGURATION. Isabella L. Karle,^a Judith L. Flippen-Anderson,^a K. Umab and P. Balaram,^b ^aLaboratory for the Structure of Matter, Naval Research Laboratory, Washington, D. C. 20375-5000, and ^bIndian Institute of Science, Bangalore 560 012, India

Crystal structure analyses have been obtained for four polymorphs of the naturally occurring ionophore, Ac-Leu-Ile-Gln-Iva-Ile⁵-Thr-Aib-Leu-Aib-Hyp¹⁰-Gln-Aib-Hyp-Aib-Pro¹⁵-Phe: from MeOH/H₂O, (a) P₂₁, a = 23.068(6) Å, b = 9.162(3), c = 26.727(9), β = 108.67(2)° and (b) P₂₁, a = 21.857(4), b = 9.381(3), c = 26.744(6), β = 105.22(2); from ethylene glycol, (c) P₂₁2₁2₁, a = 10.337(2), b = 28.389(7), c = 39.864(11); crystal (c) soaked in KCl, (d) P₂₁2₁2₁, a = 10.160(3), b = 28.252(9), c = 40.338(13). Resolution 0.9 to 1.3 Å, respectively. In all four crystals, the molecule has a banana shape with a completely helical backbone. The molecule is amphiphilic with all the polar side-chains extended on the convex side. Furthermore, the molecules associate in an antiparallel motif with two intermolecular hydrogen bonds involving the OH group on Hyp¹⁰. The differences in the four structures involve the amount of bend in the backbone which is correlated with the quantity of cocrystallized water, 8 to ~17 molecules/peptide, residing in a channel. The channels are closed at one point by the side-chain of a glutamine residue which appears to be the gate that opens and closes the channel. Supported by NIH Grant GM30902, ONR and Dept. of Science and Technology, India.

Tu-PM-D3

THE pH DEPENDENCE OF THE HELICITY OF PEPTIDES acetyl-YEAAAKEAXAKEAAKAamide. Soon-Ho Park, Gene Merutka, John Rovang and Earle Stellwagen, Department of Biochemistry, University of Iowa, Iowa City, IA 52242.

The far ultraviolet circular dichroic spectrum of the peptide acetylY(EAAAK)₃amide in a reference solvent, 10 mM NaCl at pH 7.0 and 0°, indicates the presence of a significant fractional content of helical residues. The helical content of solutions of this peptide is diminished by incremental adjustment of either the pH or the NaCl concentration of the reference solvent. Replacement of the three lysine residues or the three glutamate residues with alanine residues alters both the fractional helical content observed in the reference solvent and its response to changes in pH and salt concentration. Similarly, replacement of alanine residue 9 with each of the other 19 amino acid residues causes marked changes in the fractional helical content of the peptide in the reference solvent and its response to changes in pH and salt concentration. These observed changes in fractional helical content are interpreted in terms of the helical preference of the amino acid residues, the interaction of the charged residues with the helical macrodipole and ion-pair formation among oppositely charged residues. This investigation was supported in part by PHS grants HE14388 and GM22109 and NSF grant DMB8413658.

Tu-PM-D2

THE ENERGETICS OF STABILIZATION OF α HELIX STRUCTURE IN PEPTIDES BY SALT BRIDGES.

Pingchiang C. Lyu and Neville R. Kallenbach
Department of Chemistry, New York University
New York, NY 10003.

Salt bridges or ion pairs that link charged residues of opposite sign play an important role in stabilizing protein conformations. Two *de novo* designed peptides, succinyl-TyrSer(Glu₄Lys₄)₂-NH₂ (E₄K₄) and succinyl-TyrSer(Glu₂Lys₂)₄-NH₂ (E₂K₂), were synthesized and characterized. These two peptides that have identical composition but different sequence allow us to evaluate the contribution of salt bridges in stabilizing intramolecular α helical structure. The E₄K₄ peptide permits formation of helix stabilizing salt bridges between Glu⁻ and Lys⁺ spaced at i, i+4 intervals; it reveals a high degree of helical structure at neutral pH (63±4%, 4°C). On the other hand, E₂K₂ has very little (0-3%), both based on UV circular dichroism measurements. High salt concentrations diminish the helix content of the E₄K₄ but affect the second peptide only to a minor extent. The two peptides have nearly identical helix content at pH 12, following titration of Lys side chains. Analysis of the secondary structure as a function of pH and temperature in these two peptides using a multi-state transition model affords an estimate of the free energy contribution of a single salt bridge to the stability of an isolated α helix.

This work was supported by a grant from NIH, GM 40746.

Tu-PM-D4

RE-ASSESSING THE STRENGTH OF THE HYDROPHOBIC EFFECT: Kim Sharp, Anthony Nicholls, Rick Fine*, Xiangshan Ni⁺, and Barry Honig, Department of Biochemistry, Columbia University, New York, NY (*Dept. of Biological Sciences, Columbia University, Biosym Corp, La Jolla, Ca). Liquid hydrocarbon/water surface tension gives an estimate of 72 cal/mole/Å² for the hydrophobic strength, while solubility data gives 25-30 cal/mole/Å². This remarkable 3-fold discrepancy, first pointed out by Tanford in 1979, remains unresolved. Reassessment of the solubility data using classical solution thermodynamics shows that contributions from entropy of mixing and solute-solvent interactions were not completely separated out. The solution theories of Flory and Hildebrand provide a prescription for such a separation via the molar volume difference between solute and solvent. Experiments by De Young and Dill on solute partition between water and alkane solvents, and comparison of solvent partition and protein stability measurements confirm these theories, and lead to a much larger hydrophobic effect for solutes: 46-47 cal/mole/Å². The remaining discrepancy between this value and 72 cal/mole/Å² can be resolved if the hydrophobic strength depends upon the radius of curvature of the solute/water interface. Geometric arguments based on solvent packing and molecular simulations of water at nonpolar interfaces predict very similar curvature dependences. This curvature dependence is also remarkably similar to an early thermodynamic model developed by Tolman and also to scaled particle theory. That these four quite different models provide very similar pictures of the curvature dependence supports this explanation, and relates microscopic and macroscopic measures of hydrophobic strength. Corrected hydrophobicity scales for the twenty amino acids, based on cyclohexane to water and octanol to water transfer energies are derived. The agreement between these scales, particularly the octanol scale, and mutant protein stability measurements is good. The increased estimate of the strength of the hydrophobic interaction for solutes, and its curvature dependence will have important consequences for calculations of the energetics of protein folding, protein binding and nucleic acid base stacking.

Tu-PM-D5

STRUCTURE-FUNCTION RELATIONSHIPS IN THE TOXIC DOMAIN OF THE E. COLI HEAT-STABLE ENTEROTOXIN STIb. Bruce W. Carpick and Jean Gariépy, Department of Medical Biophysics, University of Toronto and The Ontario Cancer Institute, Toronto, Canada, M4Y 1M4.

STIb is a 19 amino acid peptide produced by enterotoxigenic *E. coli*, and is a major cause of diarrheal disease in humans and animals. The biological properties of the STIb toxin are encoded in a 13 amino acid C-terminal domain, abbreviated STIb(6-18). This tridecapeptide contains six cysteine residues within its sequence, and its conformation can be modeled as a series of three reverse turns stabilized by the three intramolecular disulphide bridges. In order to study the relationship between primary sequence and biological function in this molecule, we prepared synthetic analogues of STIb(6-18) containing single amino acid replacements at non-cysteine sites and assayed each peptide for its ability to (i) inhibit the binding of an 125 I-labelled STIb analogue to membrane receptors on rat intestinal cells, and (ii) cause a diarrheal response in infant mice. Analogues containing L-amino acid replacements generally showed moderate reductions in receptor binding activity which correlated with reductions in enterotoxicity, although this correlation may not be linear. An analogue with an L-alanine for asparagine substitution at position 12 showed no binding activity, suggesting the importance of the asparagine side chain at this site. The weakest active analogue tested was dA¹⁴STIb(6-18), which contains a D-alanine for L-alanine replacement. These results, in conjunction with those of other researchers, suggest that D-amino acid replacements, which alter the peptide backbone orientation, have a much greater effect on the biological activity of STIb(6-18) than do L-amino acid replacements, which alter only the side chain identity. It is possible that certain D-amino acid substitutions affect the ability of the enterotoxin to fold into a biologically active conformation, perhaps through disruption of one or more of the three reverse turns. A truncated analogue of STIb(6-18) missing the three C-terminal residues and one disulphide bridge also showed no binding activity, indicating that the full 13 amino acid sequence of STIb(6-18) is required for activity.

Tu-PM-D7

ANALYSIS OF SIZE-EXCLUSION CHROMATOGRAPHIC PROFILES OF MONOMERIC PROTEINS IN DENATURING SOLVENTS. William Shalongo and Earle Stellwagen, Department of Biochemistry, University of Iowa, Iowa City, IA 52242.

The elution position of a persistent native protein, bovine pancreatic trypsin inhibitor, or a persistent unfolded protein, oxidized pancreatic ribonuclease, from a HPLC size exclusion column is dependent upon the concentration of denaturants such as urea or guanidinium chloride at neutral pH and 4°. This dependence observed in isocratic equilibrium chromatographic profiles can be modeled using the partition equations obtained from plate theory assuming proteins bind reversibly with the column matrix. As the concentration of denaturant increases, the affinity of a protein for the matrix decreases and the exchange time for its binding increases. As the size of a native or denatured protein increases, its affinity for the matrix in an isocratic denaturant concentration increases while its exchange time remains about the same. No evidence is found for denaturant dependent configurational or conformational changes at equilibrium which perturb the hydrodynamic volume of proteins in either the native or the denatured baseline zones.

By contrast, non-equilibrium chromatographic profiles can be analyzed to obtain the rates for the change in hydrodynamic volume accompanying the folding and unfolding of a monomeric protein in isocratic denaturant concentrations. This is done by superimposing the conformational isomerization on matrix binding using plate theory. Simulations of the unfolding profiles for thioredoxin and for ribonuclease in isocratic concentrations of guanidinium chloride yield unfolding and refolding rates which predict the exchange times observed for the unfolding of these proteins obtained from tryptophan fluorescence measurements. This research was supported in part by PHS grant GM22109.

Tu-PM-D6

RELATIONSHIP BETWEEN PARTIAL UNFOLDING AND THE HYDROPHOBICITY AND MEMBRANE TRANSLLOCATION OF DIPHTHERIA TOXIN AND PSEUDOMONAS EXOTOXIN A

Jean Xin Jiang, Domenico Tortorella, Franklin Abrams and Erwin London, Dept. of Biochemistry and Cell Biology, SUNY at Stony Brook, Stony Brook, NY 11794-5215

One of the major questions in the area of protein translocation across membranes is the role of unfolding and refolding in the translocation process. Diphtheria toxin and the exotoxin are useful protein models for this process because they appear to undergo major changes in folding during their translocation across cell membranes. In the case of both toxins it has been possible to demonstrate that exposure to the low pH these toxins encounter within acidic organelles *in vivo* causes partial unfolding and vastly increased hydrophobicity. Interestingly, other conditions that induce partial unfolding, such as high temperature or high pH, also induce hydrophobic behavior in these proteins. This is especially surprising in the case of the exotoxin, which lacks obviously hydrophobic sequences. We also now find that each of these toxins can take on two distinct low pH conformations. In both cases there is one conformation that contains at least one folded domain, and another that seems to be more folded. In the case of diphtheria toxin the more unfolded state that contains an unfolded catalytic A domain is the one that seems to dominate under physiological conditions. Significantly, upon release of the A domain from membrane-inserted toxin it can be shown to refold and regain activity. Supported by NIH grant GM 31986.

Tu-PM-D8

REFOLDING OF DENATURED APOCYTOCHROME C BY MAMMALIAN HSC73

K.P.Ritchie¹, C.Zhang¹, S.Sadis², L.Hightower², J.R.Lepock¹, ¹Guelph-Waterloo Program for Graduate Work in Physics, Waterloo campus, Waterloo, Ont., Canada, ²Dept. of Molecular and Cell Biology, The Univ. of Connecticut, Storrs, CT, USA

In response to stress, synthesis of a class of proteins known as the heat shock proteins (HSP's) increases. Inducers of HSP's (i.e. elevated temperature, ethanol, heavy metals) are known to damage cellular proteins. It is also known that HSP's bind preferentially to misfolded or unfolded protein rather than the native structure and are released on addition of ATP. It has been proposed that HSP's aid in refolding unfolded proteins, both newly synthesized protein and protein denatured during heat shock. The constitutively expressed $M_r = 73000$ heat shock cognate (HSC73) and apocytochrome c, a heme-free derivative of cytochrome c that is denatured during isolation, were used to test this proposal. Differential scanning calorimetry (DSC) was used to show that HSC73 alone has a major denaturation peak at about 53 °C which on addition of ATP is shifted to about 60 °C. A smaller peak is usually found at 70 °C which is also shifted by ATP. In addition, ATP causes a change in the fluorescence spectrum of trp90 and trp580, indicating a conformational change induced by ATP. Apocytochrome c alone was found to have no well defined structure but after incubation with HSC73 and ATP at room temperature for 1 hour, a component was found with a T_m of about 53 °C. When apocytochrome c, HSC73 and ATP were incubated in the presence of hemin then the refolded component is more stable with a T_m of about 65 °C. ATP is required for refolding of the apocytochrome c.

Tu-PM-E1

RYANODINE BINDING BY JUNCTIONAL SARCOPLASMIC RETICULUM. EFFECTS OF TEMPERATURE, CROSSLINKING, AND REDUCING AGENTS. J. Gomez-Skarmeta, K. Collins and G. Inesi, Dept. of Biochem., U. of MD Sch. of Med. Balto., MD.

Binding of ryanodine vesicular fragments of junctional terminal cisternae (JTC) was found to be very slow and highly temperature dependent ($Q_{10}=4$). Prolonged incubation at 37°C, or even at 25°C, produced partial denaturation of the receptor, as revealed by dissociation of bound ligand. On the other hand, satisfactory characterization was obtained at 4°C, yielding a 7×10^{-9} M dissociation constant, a 6.2×10^{10} M⁻¹ hr⁻¹ "on" rate constant, and a 4×10^3 hr⁻¹ "off" rate constant. The maximal amounts of binding varied between 25 and 40 picomoles per mg of JTC protein, corresponding to one site per RR tetramer. The non saturable association of relatively large amounts of ryanodine with JTC was observed at high concentrations of ryanodine.

Although the subunits of the RR tetramers do not appear to be linked by native disulfide interactions, covalent stabilization of RR oligomers by -SH crosslinking was readily obtained with the bifunctional -SH reagent 1,6-bismaleimido-hexane (BMH). This crosslinking reaction maintained the receptor in a high affinity state for ryanodine. In contrast, treatment of JTC with the reducing agent dithioerythritol (DTT) decreased the binding affinity by one order of magnitude, and produced a prominent time lag in the ryanodine association kinetics when binding was measured at 4°C. This effect was likely due to reduction of disulfide linkages with the RR monomers. DTT had no effect if crosslinking with BMH was carried out first. We conclude that the ryanodine binding kinetics and association constant can be altered by partial denaturation of the receptor protein resulting from reduction of native disulfide linkages, or exposure to high (25-37°C) temperature. On the other hand, the high affinity conformation of the RR is stabilized by receptor oligomerization.

Tu-PM-E3

WITHDRAWN

Tu-PM-E2

THE ROLE OF FACILITATED DIFFUSION OF CALCIUM BY CALCIUM-BINDING PROTEIN (CALBINDIN) IN INTESTINAL CALCIUM TRANSPORT. Joseph J. Feher, Dept. of Physiology, Medical College of Virginia, Richmond, VA 23298

Computer simulations of trans-cellular Ca^{2+} transport in enterocytes were carried out using the electronic network simulation program, SPICE. The program incorporated a negative-feedback entry of Ca^{2+} at the brush-border membrane which was characterized by a K_d of 0.5 μM cytosolic $[\text{Ca}^{2+}]$. The baso-lateral Ca^{2+} -ATPase was simulated by a four-step mechanism which resulted in Michaelis-Menten kinetics with a K_m of 0.2 μM $[\text{Ca}^{2+}]$. The cytosolic diffusion of Ca^{2+} was simulated by dividing the cytosol into ten slabs of equal width. Ca^{2+} binding to calbindin was simulated in each slab, and diffusion of free Ca^{2+} , free calbindin, and Ca^{2+} -laden calbindin was simulated between each slab. The cytosolic $[\text{Ca}^{2+}]$ of the simulated cells was regulated within the range of what is expected physiologically. The presence of calbindin alone was sufficient to increase Ca^{2+} entry into the cell by reducing the free $[\text{Ca}^{2+}]$ immediately adjacent to the brush border, thereby removing the negative feedback inhibition of Ca^{2+} entry. At the same time, the calbindin increased the efflux of Ca^{2+} from the baso-lateral membrane by increasing the free $[\text{Ca}^{2+}]$ immediately adjacent to the pump. The increased fluxes at the two cell borders was exactly matched by the increased diffusional flux through the cytosol provided by calbindin. The enhancement of trans-cellular Ca^{2+} transport was nearly linearly dependent on [calbindin]. The values of K_d for calbindin which were used in these simulations were previously obtained experimentally in the presence and absence of KCl. The simulations show that the K_d obtained in the presence of KCl produces considerably greater stimulation of Ca^{2+} transport than the K_d obtained in the absence of KCl. This result suggests that the physiological K_d of calbindin is optimal for the enhancement of trans-cellular Ca^{2+} transport. The markedly elevated $[\text{Ca}^{2+}]$ predicted by this model in the absence of calbindin suggests an experimental test of the model.

Tu-PM-E4

PHOSPHORYLATION STUDIES OF ENVZ, A PUTATIVE OSMOSENSOR IN *E. coli*. By Linda J. Kenney and Thomas J. Silhavy. Department of Molecular Biology, Lewis Thomas Laboratory, Princeton University, Princeton, N.J. 08544.

E. coli regulate their outer membrane porins in response to osmolarity. At low osmolarity *ompF* is preferentially expressed, at high osmolarity *ompF* is inhibited and *ompC* is expressed. Expression of *ompC* and *ompF* is regulated by the *ompB* locus containing the two regulatory genes *envZ* and *ompR*. EnvZ is a 45 KDa integral inner membrane protein; OmpR is a soluble protein of 25 KDa and a specific regulator of the *ompF* and *ompC* genes. EnvZ is presumed to be the osmosensor and communicates with OmpR via a phosphotransfer reaction. Based on similarity to other two-component regulatory systems, it has been suggested that the phosphoryl group is transferred from a phosphohistidine on EnvZ to an aspartate on OmpR.

We have overexpressed a truncated form of *envZ* in which the first 38 codons have been replaced with 8 codons of *lacZ*. As a result, EnvZ localizes to the cytoplasm and can be purified by cell disruption and ultracentrifugation on a sucrose step gradient. We can thus isolate 50-100 mg of protein which is >95% pure (SDS PAGE). We measured the initial rate of EnvZ phosphorylation and report an apparent affinity between 100-200 μM for ATP. 50 mM KCl increases the steady state phosphorylation level by 2-fold. The slow turn-over rate of the EnvZ phosphoenzyme yields a low basal ATPase activity, addition of OmpR stimulates the EnvZ-ATPase ten-fold. The stimulatory effect of OmpR on the EnvZ-dependent ATPase activity is saturable and neither the EnvZ-dependent ATPase nor the OmpR-stimulated EnvZ-ATPase are inhibited by 1 mM vanadate. Understanding the interplay of the phosphotransfer reactions will help elucidate the mechanism underlying osmoregulation. Supported by GM35791.

Tu-PM-E5

THE ELEVATION OF CYTOSOLIC Ca^{2+} ($[\text{Ca}^{2+}]_i$) IN RAT CHROMAFFIN CELLS BY MUSCARINE AND CAFFEINE. C.J. Lingle & A. Neely; Dept. Anesthesiology, Wash. Univ. Sch. Med., St. Louis, MO 63110.

In single rat chromaffin cells, muscarine induces a transient elevation of $[\text{Ca}^{2+}]_i$, measured either by fura-2 in non-dialyzed cells or by the time course of a voltage-independent, Ca^{2+} -activated K^+ current (I_{SK}) in voltage-clamped cells. In the sustained presence of muscarine, the $[\text{Ca}^{2+}]_i$ elevation is complete in about 15-30 seconds. Caffeine evokes a similar transient elevation in $[\text{Ca}^{2+}]_i$.

The second response to paired muscarine applications is suppressed for about 2-3 minutes. Paired applications of caffeine show a qualitatively similar effect, but there is a 10-30 sec period when caffeine is totally unable to elevate $[\text{Ca}^{2+}]_i$. Recovery of the muscarine response is promoted by factors which increase Ca^{2+} influx during the recovery period including 1. action potentials elicited by either 10 μM nicotine or 15 mM KCl in non-dialyzed cells and 2. depolarizing commands sufficient to activate Ca^{2+} current in voltage-clamped cells. Slow refilling of intracellular Ca^{2+} stores appears to account for a portion of the slow recovery in the ability of muscarine to elevate $[\text{Ca}^{2+}]_i$.

Within 20-30 seconds after an initial response to muscarine, caffeine is totally unable to elevate $[\text{Ca}^{2+}]_i$ at a time when the response to muscarine is only reduced. Within 20-30 seconds following a response to caffeine, the response to muscarine is reduced, but present. This result is consistent with the view that a portion of the muscarine-induced elevation of $[\text{Ca}^{2+}]_i$ involves release of Ca^{2+} from a caffeine-sensitive Ca^{2+} pool. Muscarine can completely empty this pool, thereby abolishing the response to caffeine. In contrast, caffeine releases only a portion of Ca^{2+} available for release by muscarine.

Supported by DK-37109.

Tu-PM-E7

EFFECTS OF PROTEIN KINASE C ACTIVATORS ON THE ATP-INDUCED Ca^{2+} RESPONSE OF RAT VENTRICULAR MYOCYTES. Zheng, J-S; Christie, A.; Levy, M.N.; and Scarpa, A. Dept. of Physiology and Biophysics, School of Medicine, Case Western Reserve University, Cleveland, OH 44106 (Introduced by G. Dubyak)

We have previously shown that ATP transiently increases the intracellular Ca^{2+} concentration in rat ventricular myocytes loaded with Fura-2. Norepinephrine (NE), forskolin, and 3-isobutyl-1-methyl xanthine (IBMX) potentiated the ATP-induced Ca^{2+} response and increased intracellular cAMP. Thus, cAMP appears to be the second messenger that mediates the potentiation. In the present study, we investigated the role of protein kinase C by pretreating the myocytes with the protein kinase C activators, phorbol-12,13-dibutyrate (PDBU) (200 nM) and 1-oleoyl-2-acetyl-sn-glycerol (OAG) (25 μM). We found that pretreatment of the myocytes with PDBU, attenuates the ATP-induced mobilization of intracellular Ca^{2+} and its potentiation by NE. Under these conditions, PDBU and OAG significantly decreased the basal intracellular cAMP level and the elevated cAMP levels induced by NE (1 μM), forskolin (1 μM) and IBMX (100 μM). The inhibitory effects of PDBU and OAG were reversed by the protein kinase C inhibitor, staurosporine (100 μM). In patch clamp studies, we found that extracellular ATP (100 μM) induced a non-selective inward cation current (I_{ATP}), and shifted the Ba^{2+} activation curve to the left by about 10 mV. These responses to ATP were not modified by pretreating the myocytes with PDBU or OAG. The time course of inactivation of the Ba^{2+} current could be fit by a single exponential regression equation. Pretreatment with PDBU or OAG decreased the inactivation time constant, which suggests that protein kinase C modulates the Ca^{2+} channel. NE (1 μM) increased the Ba^{2+} current, but did not shift the activation curve. Pretreatment with PDBU decreased the NE-induced Ba^{2+} current, which is consistent with our cAMP measurement. Our results suggest that protein kinase C is a key component in a negative feedback system that regulates intracellular cAMP production in cardiac myocytes. (This work is supported by NIH Grants HL15758, HL18708 and HL07653).

Tu-PM-E6

MODULATORY EFFECTS OF PARATHYROID HORMONE ON CALCIUM CHANNEL CURRENTS IN VASCULAR SMOOTH MUSCLE CELLS AND VENTRICULAR MYOCYTES ARE MEDIATED BY CYCLIC AMP. Rui Wang, Edward Karpinski and Peter K.T. Pang. Department of Physiology, University of Alberta, Edmonton, Alberta, Canada T6G 2H7.

Using the whole cell configuration of the patch clamp technique, the mediation of the effects of bovine parathyroid peptide, [bPTH-(1-34)], on L-type voltage-dependent calcium channels by cyclic AMP (cAMP) was investigated in vascular smooth muscle cells and ventricular myocytes. In smooth muscle cells, both bPTH-(1-34) and dibutyl cAMP (db-cAMP) decreased the amplitude, but had no effect on the I-V relationship or the kinetics of L channel currents. On contrast, both bPTH-(1-34) and db-cAMP increased the amplitude, shifted the peak of the I-V relationship toward more negative potentials and slowed down the kinetics of L channel current activation in ventricular myocytes. 1 μM bPTH-(1-34) maximally increased L channel currents by $73 \pm 13\%$ ($n=13$, $p<0.05$) in ventricular myocytes, and decreased L channel currents by $37 \pm 3\%$ ($n=14$, $p<0.05$) in smooth muscle cells. However, the sequential application of db-cAMP (1 mM) and bPTH-(1-34) (1 μM) did not lead to an additional increase in L channel currents in ventricular cells ($68 \pm 20\%$, $n=5$), or an additional decrease in smooth muscle cells ($36.8 \pm 5\%$, $n=5$). The lack of the summation of effects of db-cAMP and bPTH-(1-34) suggested that these two agents acted on the same end sites. Furthermore, the intracellular application of 100 μM Rp-cAMPs, which competitively inhibits the cAMP-dependent protein kinase, prior to the application of bPTH-(1-34) totally abolished the effects of bPTH-(1-34) on L channel currents in both vascular smooth muscle cells and ventricular myocytes. These results suggest that cAMP is the second messenger which mediates effects of bPTH-(1-34) on L-type calcium channel currents in vascular smooth muscle cells and ventricular myocytes.

Tu-PM-E8

SUBSTANCE P AND VIP INDUCE CONDUCTANCE TRANSIENTS IN RBL-2H3, A MUCOSAL MAST CELL LINE.

J. Janiszewski, J. Bienenstock and M.G. Blennerhassett (Intr. by R.E. Garfield). Dept. of Pathology, McMaster University, Hamilton, Ontario, Canada L8N 3Z5.

Mast cell (MC) activation and release of inflammatory mediators may be regulated by nerves in vivo, since histamine release follows application of certain neurotransmitters in vitro. We used whole-cell patch clamp methods to study the action of substance P (SP) and vasoactive intestinal polypeptide (VIP) on RBL-2H3 cells to define better the mechanisms involved in nerve/MC interactions.

The whole-cell current was measured in RBL cells with membrane voltage (V_m) clamped to different potentials in the range of ± 160 mV from V_m hold = 0 mV. Control cells were characterized by a strong potassium-dependent inward rectified current. Following recording of baseline conductances, individual RBL were exposed to a 20 sec pulse of either SP (10^{-6} to 10^{-12} M) or VIP (10^{-9} to 10^{-18} M). Both SP and VIP caused a transient (0.5-2 min), fully reversible increase in conductance. The magnitude of that increase (slope conductance) was highest in the V_m range of -60 mV to 80 mV, with a maximum change from 0.24 nS to 28.76 nS ($n=32$ cells). During the transient, the equilibrium potential shifted from -80 mV at rest to 0 mV, and the whole-cell current had both inward and outward components. The transients could be repetitive and usually were followed by a sustained increased conductance. They were characterized by a 2-3 min delay of onset following stimulation with SP at 10^{-6} M, or VIP at 10^{-9} M, with increasing delay at lower concentrations of neuropeptides. These changes in conductance resembled the pattern of increase in intracellular calcium in MC that follows antigen stimulation (Neher, Almers, EMBO J. 5:51-53). Therefore, the neuropeptide-dependent conductance changes may contribute to MC activation leading to release of allergic and inflammatory mediators.

Supported by M.R.C. of Canada.

Tu-PM-E9

CRITICAL RESIDUES OF MUSCARINIC RECEPTORS DETERMINE G PROTEIN SPECIFIC PATTERNS OF INTRACELLULAR CALCIUM RELEASE. James Lechleiter, Steven Girard, Ernest Peralta* and David Clapham, Dept. of Pharmacology, Mayo Foundation, Rochester, MN 55905 *Depts of Biochemistry and Molecular Biology, Harvard University, Cambridge, MA 02138

Calcium release from intracellular stores constitutes a massive point of convergence for a broad class of receptors coupled to guanine nucleotide binding (G) proteins. A central question concerning this form of transmembrane communication relates to the mechanism(s) by which cells differentiate between individual receptor signals. Possible candidates which may encode receptor-specific information are variations in magnitude, spatial and/or temporal release of Ca^{2+} . We have recently demonstrated that the m2 and m3 muscarinic acetylcholine receptor (mAChR) subtypes differentially modulate the magnitude and kinetics of Ca^{2+} sensitive Cl^- current activation in *Xenopus* oocytes (Lechleiter et al. *EMBO J* 9, 1990). Significantly, the G protein specificity of these actions was attributable to residues occurring within the same region of the third cytoplasmic domain for the m2 and m3 receptors. Using confocal microscopy, we now show that the Ca^{2+} release pathways of m2 and m3 mAChRs can also be distinguished in the spatial domain. Oocytes were individually assayed 48 hours after injection of SP6 generated RNA transcripts encoding either m2, m3 or hybrid mAChRs. Each oocyte was injected with the Ca^{2+} dye indicator Fluo-3 (50 nl of 1 mM; Molecular Probes) prior to image analysis (30-120 minutes). In addition, intracellular Ca^{2+} was simultaneously monitored with two-electrode voltage clamp. Submaximal acetylcholine (ACh) concentrations applied to either receptor stimulated Ca^{2+} release from discrete foci in random, periodic and frequently bursting patterns of activity. Maximal stimulation of m2 receptors increased the number of foci, while m3 receptors invariably evoked a propagating Ca^{2+} wave. These distinctive Ca^{2+} release patterns could be attributed to different G protein coupled pathways by analysis of pertussis toxin (PTX) sensitivity. Furthermore, analysis of hybrid m2-m3 mAChRs demonstrated that these characteristic signals were due to critical G protein specific residues. Funded by AHA (J.L. & D.C.), by NIH (D.C. & E.P.), by the Whitaker Foundation (D.C.).

Tu-Pos1

MYOSIN ATPASE INHIBITOR AND ITS EFFECT ON THE CONFORMATION OF MYOSIN HEAD. Takayuki MIYANISHI, Mitsuki WATANABE[†], and Genji MATSUDA, Department of Biochemistry, School of Medicine and [†]Center for Instrumental Analysis, Nagasaki University, Nagasaki 852, Japan.

Tridecylresorcylic acid (TRA) isolated from a primula (*Lythamachia japonica*) inhibits cerebral cortex $\text{Na}^+\text{-K}^+\text{-ATPase}$ (Shoji, N. et al., 1984) and myosin $\text{EDTA(K}^+)\text{-ATPase}$ (Kobayashi, M. et al., 1984). We synthesized this chemical and examined its effect on the ATPase activity and on the conformation of myosin subfragment-1 (S-1).

At 10 μM TRA, $\text{EDTA(K}^+)\text{-ATPase}$ activity and P_i -burst size of $\text{Mg}^{++}\text{-ATPase}$ were both suppressed to half of the control while at 100 μM TRA to less than 10 % of the control. At a very similar concentration dependency, TRA suppressed the fluorescence emission at 340 nm of tryptophan residues of S-1. Circular dichroism of S-1 at 222 nm showed an increased alpha helices content at 10 μM TRA followed by its gradual decrease at higher concentration of TRA. The $\text{Mg}^{++}\text{-ATPase}$ activity was enhanced at 10 μM TRA followed by its gradual decrease (becoming less than 10 % of the control at 100 μM TRA). Even at 100 μM TRA, S-1 was able to bind to actin and to dissociate from actin by ATP addition as well as in the absence of TRA, examined by ultracentrifuge method. At 100 μM TRA, superprecipitation and ATPase activity of actomyosin were suppressed significantly. These results suggest that 100 μM TRA broke alpha helices in S-1 and possibly inhibited $\text{Mg}^{++}\text{-ATPase}$ reaction by blocking the transition of myosin-ATP complex to myosin-ADP complex in a rapid equilibrium with myosin-P-ADP complex, and that 10 μM TRA increased alpha helices content in S-1 and reduced myosin-P-ADP complex formation partly by accelerating its decomposition and/or by suppressing transition of intermediates to myosin-P-ADP complex. The change of alpha helices content in S-1 may be closely related to kinetic parameters of the $\text{Mg}^{++}\text{-ATPase}$ reaction.

Tu-Pos3

PHOTOCHEMICAL EVIDENCE THAT SER-243 OF MYOSIN'S HEAVY CHAIN IS NEAR THE PHOSPHATE BINDING SITE FOR ATP

Jean Grammer and Ralph G. Yount

Department of Biochemistry and Biophysics
Washington State University, Pullman, WA 99164-4660

The photochemical modification of myosin subfragment one (S-1) by irradiation of the $\text{MgADP}\cdot\text{vanadate (VI)-S1}$ complex has been studied further. Earlier studies (Grammer et al., (1988), *Biochemistry* 27, 8408; Cremo et al., (1988), *Biochemistry* 27, 8415, and (1989) *J. Biol. Chem.* 264, 6608) have shown that the hydroxymethyl side chain of Ser-180 in myosin's heavy chain is specifically photooxidized to an aldehyde when the $\text{MgADP}\cdot\text{Vi}\cdot\text{S1}$ complex is irradiated by UV light. The resulting photomodified S1 (pm-S1) retraps $\text{MgADP}\cdot\text{Vi}$, albeit at a slower rate. Irradiation of this $\text{MgADP}\cdot\text{Vi}\cdot\text{pmS1}$ complex leads to photocleavage at Ser 180. The photocleaved S1 was briefly trypsinized and reduced with NaB^3H_4 in an effort to characterize the chemistry of the photocleavage. Surprisingly all the radioactivity was present in the 50 kDa heavy chain peptide and none at the site of photocleavage. Exhaustive thermolysin digestion of the labeled 50 kDa fragment, followed by HPLC purification of labeled peptides and gas phase peptide sequencing gave Val-Arg-Asn-Asp-Asn-Ser-Ser-Arg corresponding to residues 238-245 in which all the label was with Ser-243. These results suggest Ser-243 is at or near the vanadate-binding site of pm-S1 and likely binds close to the γ -phosphate of ATP in native myosin. The complete conservation of residues 242-250 in all myosins sequenced to date suggest their role may be to contribute part of the ATP binding site. Supported by MDA and NIH (DK05195).

Tu-Pos2

PHOTOAFFINITY LABELING OF SKELETAL AND SMOOTH MUSCLE MYOSIN S1 WITH VANADATE TRAPPED $[\text{H}]2',3'\text{-O-(3-[N-(4-AZIDO-2-NITRO-PHENYL)AMINO] PROPIONYL) ADP (NANPAP-ADP)}$

Daniel L. Kennedy, Douglas G. Cole, and Ralph G. Yount

(Intr. by Leonard B. Kirschner)

Department of Biochemistry/Biophysics

Washington State University, Pullman WA 99164-4660

$[\text{H}]\text{NANPAP-ADP}$ was stably trapped at the active site of skeletal and smooth muscle myosin subfragment 1 (S1) with Co^{2+} and vanadate (V_i). Replacement of Mg^{2+} with Co^{2+} was essential to prevent a vanadate dependent photooxidation of the enzyme and release of nucleotide (Grammer et al., (1988) *Biochemistry* 27, 8408-8415). Irradiation of purified skeletal and gizzard myosin $\text{S1}\cdot\text{Co}^{2+}\cdot[\text{H}]\text{NANPAP-ADP}\cdot\text{V}_i$ complexes gave 40-50% covalent incorporation of the trapped nucleotide analog. Analysis of the major tryptic peptides of skeletal S1 by SDS gel electrophoresis showed that both the 50-kDa and 23-kDa fragments were labeled. Parallel experiments with gizzard myosin S1 indicated that the 50-kDa tryptic peptide was also prominently labeled. These results are in contrast to earlier photolabeling studies with NANPAP-ADP reversibly bound to skeletal heavy meromyosin in which only the 23-kDa fragment was photolabeled (Szilagyi et al., (1979) *Biochem. Biophys. Res. Comm.* 87, 936-945). These different photolabeling patterns may reflect differences in conformation of S1 in the trapped versus untrapped states, but provide additional evidence that both the 50-kDa and 23-kDa fragments contribute to the ATP-binding site. Supported by MDA and NIH (DK 05195)

Tu-Pos4

ROTARY SHADOWED HEAVY MEROMYOSIN/F-ACTIN.

K. Mabuchi, and J. Gergely. Dept. of Muscle Res., Boston Biomedical Research Institute, Boston, MA, Dept. of Neurology, Mass. General Hosp., and Dept. of Biol. Chem. and Mol. Pharmacol., Harvard Med. School, Boston MA, 02114.

We developed a new method not requiring deep-freeze drying at or below -90°C to preserve actin filaments (AFs) for rotary shadowing. Combination of this technique with low angle shadowing enabled us to visualize individual heavy meromyosin (HMM) molecules and the AFs in the same field. The use of buffered uranyl acetate (pH ~6) in 30% glycerol and removal of liquid after rinsing were necessary to preserve AFs. Electron micrographs of mixtures of HMM and AFs (HMM/AF 1:8) taken within 2 min of mixing show many single AFs and some partially decorated paired AFs. On longer (15 min) incubation the number of paired AFs increases and multiple bundles appear, with very few free HMM molecules. If such mixture is allowed to stand overnight at 4°C the number of bundled AFs increases and single undecorated AFs appear suggesting that decorated bundles are more stable than single decorated AFs. HMM appears to be bound to single AFs by only one head, the contact with actin occurring at its tip. In contrast, in bundled AFs the two heads of many HMM's appear to be bound to two different AFs (cf Offer & Elliott, *Nature* 271, 325, 1978). At the stage when single AFs predominate the decoration of AFs by HMM is not uniform. The presence of many poorly decorated as well as heavily decorated AFs suggests cooperativity in binding to the same AF. (Supported by grants from NIH (HL 5949) and MDA).

Tu-Pos5

FLUORESCENCE STUDIES WITHIN THE REGULATORY LIGHT CHAIN (LC2) OF SKELETAL MYOSIN. W. Boey, B.D. Hambly, E. Moisidis and C.G. dos Remedios. Anatomy Dept., Sydney University, 2006 Australia.

The regulatory light chain of rabbit skeletal myosin (LC2) appears to lie within 3.5 nm of the head-rod junction (Kato & Lowey, 1989 J. Cell Biol. 109:1549), binds one mole of cation per mole LC2 and can be phosphorylated. It also appears to be involved in modulating Ca^{2+} sensitivity of cross-bridge cycling in skeletal muscle (Persechini et al., 1985 J. Biol. Chem. 260:7951). LC2 contains two reactive Cys residues (125 and 154) which can be selectively labeled with probe molecules (Hambly et al., 1991 Biophys. J. [in press]). We have bound a donor-acceptor pair to these two Cys to use fluorescence resonance energy transfer (FRET) spectroscopy to measure the distance between these residues in solution. Using 1,5-IAEDANS as a donor and 5-IAF as an acceptor we obtained >90% quenching, indicating the distance to be very close, in agreement with crosslinking studies (Huber et al., 1989 Biochem. 28:9116). Additionally, we find that the fluorescence intensity of these probes in solution does not change in the presence and absence of divalent cations, consistent with structure predictions that the cation binding site is located in the other (N-terminal) domain of the putative dumbbell shaped molecule (Bechet & Houadjeto, 1989 BBA 996:199). Approximately 50% of the LC2 of myosin has been successfully exchanged with fluorescently labeled LC2. This preparation will be used to continue to study the spatial relationships between residues within LC2 and other myosin probe sites.

Supported by the NH&MRC of Australia.

Tu-Pos7

EFFECT OF CATIONS AND NUCLEOTIDES ON TEMPERATURE-DEPENDENT ASSOCIATION OF MYOSIN SUBFRAGMENT-1. Umesh Ghodke and Paul Dreizen. Graduate Program in Physiology & Biophysics, State University of New York Health Science Center at Brooklyn, Brooklyn, New York 11203.

Myosin subfragment-1 (S1) of skeletal and cardiac muscle is known to undergo temperature-dependent aggregation. We have examined this phenomenon by means of turbidity measurements on rabbit fast-twitch muscle myosin S1 isoforms with heavy chain and LCI or LC3. The rates and extent of turbidity changes are greatest in the presence of Mg-ATP and Mg-AMP/PNP, less in the presence of Mg-ADP-Pi and Mg-ADP, and least in the presence of Mg^{++} or ATP alone. The changes in turbidity are partially reversible under appropriate conditions, suggesting that the phenomenon involves equilibrium association of S1-S1, followed by their irreversible aggregation. Similar findings are obtained for the two light chain isoforms of myosin S1. The rates and extent of turbidity changes can be crudely fit to a Michaelis-Menten scheme, with apparent Michaelis constant approximately 100 μM for Mg-ATP and comparable values in the cases of other nucleotides. The overall data suggest that S1-S1 association depends upon specific nucleotide binding at the hydrolytic site of myosin S1, with greatly different extent of self-association among the sequential kinetic intermediates of myosin ATPase. Further studies on thermal incubation of myosin S1 in the presence of Ca^{++} show a selective effect of Ca^{++} on S1 self-association. The rate and extent of turbidity change are augmented by addition of Ca^{++} in the presence of Mg-ADP-Pi. Ca^{++} has much less effect on S1 self-association in the presence of Mg-ATP or Mg-ADP, and no effect on S1 in the absence of nucleotide. These findings are of particular interest in that a possible extrapolation to the intact myofibril suggests that association/dissociation equilibria involving the kinetic intermediates of myosin S1 may play a central role in the primary contractile event.

Tu-Pos6

ORIENTATION OF SPIN LABELED LC2 BOUND TO CROSSBRIDGES IN GLYCERINATED MUSCLE FIBERS AT ZERO OVERLAP. B. Hambly*, K. Franks & R. Cooke. Biochemistry Department & CVRI, University of California, San Francisco CA 94143 and *Anatomy Department, Sydney University 2006, Australia

We have covalently spin labeled Cys-125 of skeletal myosin light chain-2 (LC2) and exchanged SL-LC2 into glycerinated muscle fibers. Electron paramagnetic resonance (EPR) spectra show that in rigor the probe is oriented with respect to the fiber axis and in relaxation changes to a highly disordered angular distribution, consistent with myosin heads being detached from the thin filament and undergoing large angular motions. EPR spectra of fibers during active force generation are indistinguishable from relaxed fibers, in contrast to EPR spectra obtained from the region proximal to the actin filament (SH-1 and ATP sites), which are ordered as in rigor in at least part of the attached population of force generating crossbridges. EPR spectra obtained from rigor fibers whose sarcomere length has been stretched to no overlap (3.65 μm) are found to be indistinguishable from spectra obtained from fibers with normal overlap (2.4 μm) in rigor buffer, contrasting with EPR data obtained from the SH-1 and ATP sites, where non-overlapping crossbridges are randomly oriented in rigor buffer. These data imply that the orientation of the LC2 binding region of the cross-bridge in rigor results from an interaction with thick filament structures, rather than the binding of the crossbridge to the thin filament and that this region becomes flexible and disordered when the crossbridge binds ATP. Supported by USPHS AM 30868 & NH&MRC of Australia.

Tu-Pos8

A CROSS-BRIDGE MODEL INVOLVING THE CYCLIC INTERACTION OF NEIGHBORING MYOSIN MOLECULES. Paul Dreizen and Umesh Ghodke. Physiology & Biophysics Program, State University of New York Health Science Center at Brooklyn, New York.

The cross-bridge cycle involves interaction between actin and myosin, coupled with ATP hydrolysis, resulting in shortening and force generation. It has long been accepted that force generation results from a conformational change within each myosin head, but direct experimental evidence for a major structural change has been lacking. Recent evidence on self-association of myosin S1 suggests that myosin-myosin interactions are implicated in shortening and force generation, without need to postulate a major conformational change within each myosin head during the cross-bridge cycle. The proposed model is consistent with x-ray diffraction evidence that the myosin filament forms an 8/3 helical rigor pattern, with change of cross-bridge repeat from 14.3nm to 14.45nm during activation of muscle fibers stretched beyond filament overlap. This suggests that neighboring myosin molecules may interact to form n-mers along a helical path. According to the present evidence on S1-S1 self-association, in the relaxed, Ca^{++} -off state, M-ATP may form low n-mers which dissociate after ATP hydrolysis and before strong binding to actin. In the Ca^{++} -on state, S1 n-mers may persist through ATP hydrolysis. The terminal S1 of an n-mer interacts with actin, undergoes product release, and then dissociates from the residual n-mer. The acto-S1 dissociates following ATP attachment to S1, and the free S1-ATP head undergoes random movement until interaction with a neighboring myosin head. Cyclic repeat of this process would result in mass transport of myosin heads along the thin filament axis, consistent with geometric constraints imposed by cross-bridge and actin periodicities. This model provides a straightforward explanation of shortening and tension, and is also consistent with some of the classical physiological findings that are not readily explained by the independent force generator model.

Tu-Pos9

TEMPERATURE-JUMP RELAXATION STUDY OF A TWO-STATE EQUILIBRIUM OF MYOSIN SUBFRAGMENT-1. Shwu-Hwa Lin^a and Herbert C. Cheung^b. Graduate Program in Biophysical Sciences^a and Department of Biochemistry^b, University of Alabama at Birmingham, Birmingham, AL 35294.

We have performed temperature-jump relaxation measurements on myosin subfragment-1 covalently labeled at SH₁ with 5-iodoacetamido-fluorescein (S1-AF). The relaxation experiment was carried out in 60 mM KCl, 30 mM TES, 2 mM MgCl₂, and pH 7.5 at two temperatures. The reaction was monitored by following the increase in the fluorescein emission intensity after a jump of 5.8 °C. A single relaxation process was observed at both temperatures, with relaxation time 102 ± 5 s⁻¹ and 182 ± 9 s⁻¹ at 19 and 25 °C, respectively. We (Lin, S.-H and Cheung, H. C., (1990) Biophys. J. 58(#2, pt.2), 332a) previously showed that the temperature dependence of the fluorescence of S1-AF was compatible with a two state transition, (S1-AF)_L $\xrightleftharpoons[k_{-1}]{k_{+1}}$ (S1-AF)_H, with $\Delta H^\circ = 12.7$ kcal/mol and $\Delta S^\circ = 46$ cal/deg/mol. We interpret the present relaxation results in terms of this two-state transition and the observed relaxation time equals $k_{+1} + k_{-1}$. The forward isomerization rate constant (k_{+1}) for the formation of the high-temperature state of S1-AF, (S1-AF)_H, is 12.5 and 7.4 ms at 19 and 25 °C, respectively, and the rate constant for the reverse transition (k_{-1}) is 45.4 and 36.8 ms at the corresponding temperatures. The present work provides for the first time kinetic evidence for a two-state transition of S1 in the absence of bound nucleotide and supports our previous two-state model. (Supported in part by NIH AR31239 and Muscular Dystrophy Association)

Tu-Pos11

SCALLOPED STRIATED AND SMOOTH ADDUCTOR MUSCLE MYOSIN HEAVY CHAIN ISOFORMS ARE PRODUCED BY ALTERNATIVE RNA PROCESSING L. Nyitray, E.B. Goodwin & A.G. Szent-Gyorgyi, Brandeis University, Dept. of Biology, Waltham, MA 02254

We have previously characterized myosin heavy chain (MHC) clones from scallop muscles (Nyitray et al. Biophys. J. 1990, 57:144a). We present here the complete sequence of the striated adductor muscle MHC. The 6.8 kb mRNA encodes 1938 amino acid residues. Conserved region in the globular head includes the ATP-binding site (residues 106-192), the reactive thiols (693-707) and regions with unidentified functions. Proteolytically sensitive sites are located in the least conserved regions (200-213, 623-638 & 557-573). Interestingly, the C-terminal two-thirds of the regulatory domain (occupying the neck region; 755-835) has higher homology with regulated myosins than with unregulated ones, indicating that certain MHC sites might be critical for regulation. Other parts of the head and the coiled-coil rod resemble sarcomeric myosins. The rod ends in a Ser-rich non-helical tail piece containing 16 residues.

We have isolated a distinct MHC cDNA (C/2-7) from a smooth adductor (catch) muscle library, which encodes part of the rod (1161-1560). A 78 nucleotide stretch, within the hinge region (1213-1239), differs from the striated MHC sequence by 48%, while the remainder of the sequences are identical. The presence of two alternative exons in the *Drosophila* MHC gene at exactly the same position (George et. al., Mol. Cell. Biol. 1989, 9:2957) strongly supports the conclusion that the scallop muscle MHC isoforms are also produced by alternative RNA splicing. The C/2-7-specific sequence is expressed exclusively in the catch muscle. PCR studies of catch muscle mRNA revealed no additional differences from the regulatory domain coding region to the 3'-end of the message. The presence of additional splice sites at the 5'-end of the gene remains to be demonstrated. These results suggest that the hinge may have a key role in the isoform-specific functions of MHCs.

Supported by NIH AR15963 and MDA

Tu-Pos10

THE COMPLETE AMINO ACID SEQUENCE OF CHICKEN SKELETAL MYOSIN HEAVY CHAIN. Tetsuo MAITA, Shuichi NAGATA, Takayuki MIYANISHI, Eiko YAJIMA, and Genji MATSUDA, Department of Biochemistry, Nagasaki University School of Medicine, Nagasaki 852, Japan

From chicken breast muscle myosin, 1) Subfragment-1 (S-1) and rod obtained by digesting myosin filaments with α -chymotrypsin or papain, 2) Heavy meromyosin (HMM) and light meromyosin (LMM) obtained by digesting myosin monomers with trypsin, 3) Three characteristic fragments of 23, 50, and 20 or 22 kDa obtained by digesting the S-1 with trypsin, 4) Subfragment-2 (S-2) and LMM obtained by digesting the rod with α -chymotrypsin in the presence of 0.5 M KCl, 5) A carboxyl terminal fragment obtained by cleaving the heavy chain with cyanogen bromide, 6) Cyanogen bromide-peptides overlapping the 23- and 50-kDa fragments and also the 50- and 20-kDa fragments from the S-1, that overlapping the S-1 and S-2 from the HMM, and that overlapping the S-2 and LMM from the rod, were isolated, respectively, and sequenced completely or partially. Thus, the complete 1938-residue sequence of the myosin heavy chain was determined, and the precise cleavage-sites by the limited proteolyses were revealed.

The papain S-1 contained 837 residues including four methylated amino acids: *N*-monomethyllysine at position 35, *N*-trimethyllysines at 130 and 551, and 3-*N*-methylhistidine at 755. The longest S-2 of 448 residues obtained by redigestion of the chymotrypsin rod for 10 min spread positions 842 to 1289. The chymotrypsin LMM started at position 1304 and ended at 1880, while the trypsin LMM started at 1306 and ended at 1897. It was remarkable that the all of the rods and LMMs were lacking the carboxyl terminal part of the heavy chain.

Tu-Pos12

CHANGES OF THE *IN VIVO* LEVEL OF MYOSIN P-LIGHT CHAIN PHOSPHORYLATION (MPLC-P) IN THE HUMAN AND ANIMAL HEART MORANO, I, AGOSTINI B, KATUS H, GANTEN D, RUEGG JC. UNIVERSITY OF HEIDELBERG, DEPARTMENT OF PHYSIOLOGY II, INF 326, D-6900 HEIDELBERG

The level of MPLC-P in the left ventricle of the heart of male and female rats (WKY and spontaneously hypertensive rats of the stroke prone strain (SHRSP)), male European Hamster (*Cricetus cricetus*) and patients with severe cardiac failure were investigated. MPLC-P was determined using a 2D-PAGE technique. In the human ventricle two MPLC isoforms exist in the completely dephosphorylated state having the same molecular weight but different isoelectric points designated as V₂ and V₂*. Both forms may be monophosphorylated. In the partially phosphorylated state, therefore, 4 different forms could be analyzed by 2D-PAGE: two unphosphorylated (V₂ and V₂*) and their respective monophosphorylated derivatives (V₂P and V₂*P). In 80% of the patients investigated (42 total), a partial MPLC-P of $39.7 \pm 4.4\%$ (V₂) and $25.9 \pm 6\%$ (V₂*) was measured. MPLC of 20% of the patients investigated, however, were completely dephosphorylated. In the ventricle of the rat and hamster only one MPLC exists leading to two different MPLC forms in the partially phosphorylated state. In male and female WKY (7 animals per group) MPLC-P was $38 \pm 3\%$ and $40 \pm 3.8\%$ up to 64 weeks of age. There was no difference in MPLC-P between male SHRSP and WKY (7 animals per group) up to 30 weeks of age but MPLC-P of SHRSP decreased to $22 \pm 4\%$ at the age of 44 weeks ($p < 0.001$). In female SHRSP (7 animals) MPLC-P was normal up to 52 weeks but decreased to $18 \pm 2.3\%$ at the age of 64 weeks ($p < 0.001$). During summer activity of hamster MPLC-P was $45 \pm 4\%$. This level decreased during hibernation to $23 \pm 2\%$ ($p < 0.001$; 6 animals per group).

Tu-Pos13

REGULATION OF MOVEMENT OF ACTIN FILAMENTS BY ACANTHAMOEBA CASTELLANI MYOSIN II.

C.L. Ganguly, J.R. Sellers, E.D. Korn, NHLBI, NIH, Bethesda, MD 20892 (Sponsored by Robert S. Adelstein)

Myosin II from *Acanthamoeba castellanii* is a conventional myosin composed of two heavy chains of M_r 172,000 and two pairs of light chains. The heavy chains can be phosphorylated at 3 sites near the carboxy terminus by a heavy chain kinase and this phosphorylation inhibits the actin-activated MgATPase activity. Maximal activity occurs when the heavy chain is completely dephosphorylated and in filamentous form. Previous studies have shown that phosphorylation-dependent regulation is cooperative. Filaments that are copolymers of phosphorylated and dephosphorylated myosin have lower actin-activated MgATPase activity than that predicted by the sum of the individual components. (J.Biol.Chem. 258:6011, 1983). Here we show that similar cooperative behavior is obtained in the sliding actin *in vitro* motility assay. Dephosphorylated filaments move actin at a rate of 0.24 ± 0.05 μ m/s whereas phosphorylated filaments move at the much lower rate of 0.08 ± 0.009 μ m/s. A 1:1 copolymer of phosphorylated and dephosphorylated myosin filaments moved actin at 0.11 ± 0.03 μ m/s. Copolymers containing 67% phosphorylated myosin moved actin filaments at the same rate as phosphorylated myosin filaments alone. We also observe that dephosphorylated myosin monomers bound to the glass surface move actin filaments at the same rate as do myosin filaments.

Tu-Pos15

cDNA CLONING AND PARTIAL SEQUENCING OF A CELLULAR MYOSIN II POSSESSING A LONG NON-HELICAL TAIL-PIECE, RESTRICTED TO CEREBRAL CORTEX.

WEIDONG SUN & PETER D. CHANTLER. Department of Anatomy, Medical College of Pennsylvania, Philadelphia, PA 19129

Using an affinity-purified polyclonal antibody directed against myosin II purified from a neuroblastoma cell line (Neuro-2A)(Chantler et al, 1988. Abstracts 4th Intl. Conf. Cell Biol. p265), we have screened 5×10^5 plaques from a rat brain cDNA expression library in λ -Zap II (Stratagene) and are sequencing the 16 positive clones (0.3 - 2.0 kb) obtained. One of these clones, CT1, includes the coding region for the heavy-chain casein kinase II phosphorylation site (Murakami et al, (1990). J. Biol. Chem. 265, 1041-1047) and extends through to the poly-A tail. Another clone, C4, contained entirely within CT1, overlaps the carboxy terminus of the heavy-chain and part of the 3' non-coding region. The derived amino-acid sequence shows that this brain myosin possesses 39 additional amino-acids within its non-helical tail-piece, which are not found in other cellular myosins. This tail-piece, which features a hydrophobic region flanked by stretches of hydrophilic sequence, may have functional significance. On Northern blots, C4 hybridizes with a single band of RNA from rat brain, ~7.2 kb in size, consistent with that expected for a myosin II probe. No hybridization is observed with RNA from liver or kidney, consistent with the anticipated specificity for this neuronal myosin probe. When RNA is prepared from different brain regions (cortex, cerebellum or a preparation of brain from which cortex has been dissected away), C4 only hybridizes with a single 7.2 kb band from cerebral cortex, indicating a restricted localization of this myosin within the central nervous system.

Supported by NIAMS Grant # AR 32858 awarded to P.D.C.

Tu-Pos14

STUDIES ON CELLULAR MYOSIN II HEAVY CHAIN ISOFORMS USING ISOFORM-SPECIFIC ANTIBODIES Noriko Murakami, Pankaj Mehta, and Marshall Elzinga, NYS Institute for Basic Research in Developmental Disabilities, Staten Island NY 10314

Comparison of the amino acid sequences of the COOH-termini of myosin heavy chains from bovine brain (Murakami et al, JBC 265 1041, 1990) and human macrophage (Saez et al, PNAS 87 1164, 1990) indicates that these myosins are genetically distinct isoforms; they are related, but the sequences are very different at the end of the heavy chain. We prepared antisera against synthetic peptides having sequences that are isoform-specific; the immunogen for anti-IIA was a macrophage sequence and for anti-IIIB a sequence from brain myosin. These antisera did not recognize muscle myosins, but did recognize cellular myosins from several mammalian species. On Western blots of tissue extracts, in which the cellular myosin heavy chain isoforms were electrophoretically separated, we found that anti-IIA and anti-IIIB stained different myosin heavy chain bands, and did not crossreact. Most tissues contained both isoforms, but the ratios between them varied. Brains from bovine, mouse, and rat showed a weak band stained by anti-IIA, and two strong bands stained by anti-IIIB. These myosin heavy chain bands are designated MIIA, MIIIB₁, and MIIIB₂. Blood platelets contained only MIIA, while kidney showed MIIIB₂ and MIIA bands of equal intensity. We observed the MIIIB₁ isoform only in brain, and the MIIIB₁:MIIIB₂ ratio varied in different regions of the brain. A commercial anti-platelet myosin antibody stained MIIA but not MIIIB₁ or MIIIB₂. Immunohistochemistry of brain sections showed that anti-IIA and anti-platelet myosin antibodies stained only blood vessels, while anti-IIIB stained most neuronal cells. These results indicate that mammalian cells contain the MIIA and MIIIB isoforms of cellular myosin in variable ratios, and that the MIIIB isoform has subtypes (perhaps resulting from alternative splicing), one of which is brain-specific. (Supported by the NY State Office of Mental Retardation and Developmental Disabilities, and by NIH grant HL-21471.)

Tu-Pos16

A NEW MEMBER OF THE MYOSIN I PROTEIN FAMILY FROM BOVINE BRAIN.

DEQIN LI & PETER D. CHANTLER. Department of Anatomy, Medical College of Pennsylvania, Philadelphia, PA. 19129. Sponsored by John Woodhead.

Myosin I is known as a motor which powers amoeboid motion and the propulsion of intracellular organelles. In vertebrates, the location of myosin I has been limited, so far, to the lateral bridges found in intestinal epithelial cell microvilli. Here, we report isolation of a protein fraction from bovine brain enriched for a 150 kD protein. We consider this protein to be a myosin I for the following reasons:

1. Upon western blotting, this protein is immunoreactive to a polyclonal antiserum raised against purified myosin I from chicken brush border (generously provided by Drs. Kathy Collins and Paul Matsudaira, Whitehead Institute, Cambridge, MA). This band does not recognize an antibody raised against a neuronal myosin II (Chantler et al, 1988. Abstracts 4th Intl. Conf. Cell Biol. p265), making it unlikely that it is a breakdown product of a myosin II.
2. The single peak of immunoreactivity eluting after passage through a hydroxyapatite column coincides with a peak of K⁺-EDTA ATPase activity. Myosin II, which gives rise to another peak of K⁺-EDTA ATPase activity, is well separated from myosin I on this column.
3. The MgATPase activity of this material is stimulated ~3-fold by the addition of F-actin.
4. Upon electrophoretic transfer of the protein fraction from an SDS gel to nitrocellulose, the 150 kD band associates with biotinylated calmodulin, similar to results seen with brush border myosin I.
5. Using a novel gel filtration assay (Adams & Pollard, 1989. *Nature*. 340 565-568), the 150 kD immunoreactive protein is found to associate with pure phospholipid vesicles made from phosphatidyl serine, as seen for other myosin Is.

The combination of the above properties, together with the higher molecular weight of 150 kD (most myosin I molecules found to date are 110 kD), suggest the presence of a new member of the myosin I family within mammalian brain.

Supported by NIAMS Grant # AR 32858 awarded to P.D.C.

Tu-Pos17

A MYOSIN I-LIKE ENZYME IN EXTRACTS OF RABBIT ALVEOLAR MACROPHAGES. Mark A L Atkinson and Dorothy M Peterson. Dept. of Biochemistry, University of Texas Health Science Center, Tyler, Texas. 75710.

We have examined extracts of rabbit alveolar macrophages for the presence of myosin I-like enzymes. A peak of K^+ /EDTA ATPase activity eluted from a gel filtration column with a Stokes radius of 5.5 nm (*Acanthamoeba* Myosins IA and IB have Stokes radii of 6.2 nm and 5.9 nm respectively). Due to the low yield of this enzyme further purification and characterization by conventional means has proved elusive. A polyclonal antibody raised to *Acanthamoeba* myosin IB did not cross react with this enzyme.

To test the hypothesis that this enzyme is a myosin I we have taken a different approach and synthesized a number of peptides corresponding to regions of sequence which appear to be conserved in myosins I but differ from the corresponding regions in myosins II. Polyclonal antibodies raised to one of these peptides, -GAGNRRSTYNV-, the heavy chain phosphorylation site of myosins I, reacted with a protein of approximate Mr 110,000. This protein co-eluted with the peak of K^+ /EDTA ATPase activity from the gel filtration column. The antibody did not react with the conventional myosin II from macrophages but did react with a protein of similar molecular weight purified to homogeneity from the intestinal brush border of rabbits. Using this antibody crosslinked to Sepharose CL-4B we have been able to affinity purify small amounts of the molecule for further characterization.

[This work was done during the tenure of an Established Investigatorship from the American Heart Association and was supported by a Grant-in-Aid from the American Heart Association and by NIH Grant # GM40423]

Tu-Pos18

Ca^{2+} STIMULATES THE MG-ATPASE ACTIVITY OF BRUSH BORDER MYOSIN I WITH THREE OR FOUR CALMODULIN LIGHT CHAINS BUT INHIBITS WITH LESS THAN TWO BOUND. Helena Swanljung-Collins and Jimmy H. Collins, Dept. of Biochemistry, Eastern Virginia Medical School, Norfolk, VA 23501.

Intestinal brush border myosin I ATPase and contractile activities have been reported to be either activated or inhibited by calcium at micromolar levels. Towards resolving these controversial effects of calcium, we have linked the MgATPase and contractile activities to the effects of temperature and calcium on the structure of myosin I. The subunit stoichiometry of myosin I as isolated in the presence of EGTA was determined to be four calmodulin light chains per myosin I heavy chain by amino acid compositional analysis of the separated subunits. At 30 °C the actin-activatable ATPase activity is stimulated two-fold at 10-700 μM Ca^{2+} . Dissociation of one calmodulin occurs at 25-50 μM Ca^{2+} , but this has no effect on actin activation. The contractile activity of myosin I, expressed as superprecipitation, is greatly enhanced by Ca^{2+} under conditions in which one calmodulin is dissociated. This calmodulin is thus not essential for actin activation or superprecipitation. Myosin I was found to be highly temperature sensitive, with an increase to 37 °C resulting in dissociation of one calmodulin at below 10^{-7} M Ca^{2+} and an additional 1.5 calmodulins at 1-10 μM Ca^{2+} . A complete loss of actin activation accompanies the Ca^{2+} -induced calmodulin dissociation at 37 °C. Our conclusion is that physiological levels of Ca^{2+} can either stimulate or inhibit the mechanoenzyme activities of brush border myosin I *in vitro*, with the mode of regulation determined by the number of associated calmodulin light chains. This work was supported by National Institutes of Health Grants GM 32567 and GM 35448.

Tu-Pos19

DOMAIN STRUCTURE OF SMOOTH MUSCLE MYOSIN LIGHT CHAIN KINASE
Masaaki Ito, Vince Guerriero, Jr., and David J. Hartshorne.
Muscle Biology Group, Department of Animal Sciences,
University of Arizona, Tucson, AZ 85721

Our studies are focused on the inhibitory domain of smooth muscle myosin light chain kinase (MLCK). It has been suggested that inhibition is due to binding to the active site of a pseudosubstrate sequence where H 805 of MLCK is aligned with S 19 of the 20,000-dalton light chain. This hypothesis is not universally accepted. One of our objectives was to define the boundaries of the inhibitory sequence and challenge the pseudosubstrate hypothesis. Using limited proteolysis it was shown that several proteases could convert MLCK initially into an inactive fragment that lacked CaM-binding ability and subsequently into an active constitutively-active fragment. This is due to cleavage only at the C-terminal end of MLCK. From these studies the boundaries of the inhibitory sequence were determined as K 779 to K 802. More precise boundaries were required. Studies involving site-directed mutagenesis of MLCK, therefore, were initiated. Feasibility of this approach was tested using a partial cDNA (corresponding to residues 447 through 972) inserted into the expression vector pRIT2T (Pharmacia). The expressed protein was fused to a fragment of protein A, to assist in purification via binding to IgG. The plasmid was transformed into *E. coli* strain N4830, carrying the temperature sensitive cl_{857} repressor integrated into its genome. The expressed MLCK was purified and exhibited Ca^{2+} -calmodulin-dependence and an activity close to native MLCK. Other mutants contained the same initiation point but were truncated at various points along the C-terminal sequence, i.e. T 778, K 793 and W 800. These studies demonstrated that a constitutively-active MLCK can be obtained with the T 778 mutant. The K 793 mutant was constitutively-active and did not contain the inhibitory sequence. In contrast, the W 800 mutant was partially inhibited and was subject to autoinhibition. Our tentative conclusion therefore is that the sequence Y 794 to W 800 is critical for the inhibition of the apoenzyme. Supported by NIH grants HL-43651 and HL-23615.

Tu-Pos21

MYOSIN LIGHT CHAIN KINASE AND PHOSPHATASE
RECOGNITION SITES OF THE 20 kDa LIGHT CHAIN OF
SMOOTH MUSCLE MYOSIN. M. Ikebe, Dept. of
Physiology and Biophysics, Case Western Reserve
University, Cleveland, OH 44106.

Smooth muscle actomyosin ATPase activity is regulated by the reversible phosphorylation of the 20 kDa light chain of myosin catalyzed by myosin light chain kinase (MLCK) and phosphatase (MLCP). The primary phosphorylation site is identified as serine 19 of the light chain. We studied the MLCK and MLCP recognition sites of the 20 kDa light chain using various proteolyzed light chains as substrates. H-meromyosin prepared by *S. aureus* protease digestion was subjected to the lysine endopeptidase proteolysis and trypsin proteolysis. Lysine endopeptidase initially cleaved at the C-terminus of lysine 6 (Lys 1 HMM) and subsequently the C-terminus of lysine 12 (Lys 2 HMM). Trypsin cleaved the C-terminus of arginine 16 (Try HMM). The rate of phosphorylation of Lys 1 HMM by MLCK was the same as intact HMM. Although the rate of phosphorylation was significantly slower than the intact HMM, Lys 2 HMM was phosphorylated by MLCK. In contrast, Try HMM was never phosphorylated by MLCK. This suggests that the amino acid sequence from arginine 13 to arginine 16 is important as a MLCK recognition site. The rate of dephosphorylation of Lys 1 HMM by MLCP was 40 times slower than the intact HMM. The rates of dephosphorylation of Lys 2 HMM and Try HMM were the same as the Lys 1 HMM. Therefore, the amino acid sequence from serine 1 to lysine 6 is important to determine the rate of dephosphorylation of 20 kDa light chain. (Supported by NIH, AHA and Glaxo).

Tu-Pos20

CONFORMATIONS OF SMOOTH MUSCLE MYOSIN LIGHT
CHAIN KINASE. Louise M. Garone and John H.
Collins, Med. Biotech. Center and Dept. of
Biol. Chem., School of Medicine, Univ. of
Maryland, Baltimore, MD 21201.

Myosin light chain kinase (E.C. 2.7.1.37) isolated from turkey gizzard myofibrils (tgMLCK) and purified by conventional liquid chromatography has been resolved into a "cluster" of peaks by high performance liquid chromatography on a 1000 Å pore polymer-based anion exchange column (Bio-Rad DEAE-5-PW). The cluster comprises at least five peaks, the first three of which we have begun to characterize. The protein in these peaks is not obviously degraded when observed by SDS-PAGE and they differ from one another with respect to specific activity. We have preliminary evidence that decreasing specific activity is correlated with increasing retention time. In addition, the more anionic tgMLCKs require higher concentrations of calmodulin to achieve equivalent enzyme activation suggesting that the protein may be phosphorylated at the site which perturbs calmodulin binding (Ser 814) and at additional sites. A possible reason that phosphorylation states of tgMLCK were not previously observed is that protease inhibitors have not been included in the isolation and purification buffers of other HPLC studies on MLCK isolated from frozen gizzard tissue. Work is currently under way to test this hypothesis.

Tu-Pos22

INHIBITION OF SMOOTH MUSCLE MYOSIN LIGHT CHAIN
KINASE BY SYNTHETIC PEPTIDE ANALOGS. M. Ikebe,
S. Reardon and F.S. Fay. Dept. of Physiology
and Biophysics, Case Western Reserve University,
Cleveland, OH 44106, University of
Massachusetts, MA 01605.

Smooth muscle myosin light chain kinase (MLCK) is calmodulin dependent protein kinase which specifically phosphorylates 20 kDa smooth muscle myosin light chain and it is known that this phosphorylation activates smooth muscle contractile apparatus. It has been proposed that MLCK contains the intramolecular inhibitor sequence right next to the N-terminus side of the calmodulin binding region. We studied the structural requirement of the inhibition using the synthetic peptide analogs. Peptide 783-799 and 786-801 inhibited calmodulin independent MLCK at the same potency as the peptide 783-804. Substitution of arginine 797, 798 and lysine 799 to alanine increased K_i approximately 100 times, while the substitution of lysine 792 and 793 to alanine did not significantly alter the K_i . The peptide 783-799 also inhibited calmodulin dependent native MLCK, and the inhibition was completed by calmodulin. The results suggest that the cluster of basic amino acid residues, arginine 797-lysine 799 is important for the inhibitory activity while tryptophan-800 and the cluster of basic amino acid residue lysine 792-lysine 793 are not important for the inhibitory activity. (Supported by NIH, AHA and Glaxo).

Tu-P023

PHOSPHORYLATION OF PREGNANT SHEEP MYOMETRIUM MYOSIN LIGHT CHAIN KINASE BY CYCLIC AMP-DEPENDENT PROTEIN KINASE.

Mary D. Pato, Steve J. Lye* and Ewa Kerc. Dept. of Biochemistry, University of Saskatchewan, Saskatoon, SK, Canada, S7N 0W0, *Division of Perinatology, Samuel Lunenfeld Research Institute, Mount Sinai Hospital, Toronto, ON, Canada, M5G 1X5

Contractile activity in smooth muscle cells is initiated and regulated primarily by the phosphorylation of the 20,000 Da Light chains of myosin by Myosin Light Chain Kinase (MLCK). It has been proposed that contraction is also modulated by the reversible phosphorylation of MLCK. Phosphorylation of MLCK by cAMP-dependent protein kinase in the absence of bound Ca^{2+} -calmodulin decreases its activity. This provides a mechanism for the relaxing effect of β -adrenergic agents. We have purified myometrium MLCK from pregnant sheep. Like other smooth muscle MLCK, it requires Ca^{2+} and calmodulin for activity but its molecular weight (160,000) is higher than most MLCK. Since the function of the uterine muscle is influenced by a number of hormones and agents some of which alter the intracellular level of cyclic AMP, we studied the phosphorylation of psm-MLCK by the catalytic subunit of the cAMP dependent protein kinase. We observed that psm-MLCK is a substrate for PKA but unlike other smooth muscle MLCK studied, the extent of phosphorylation in the presence and absence of bound Ca^{2+} -calmodulin are similar (1.0-1.3 mole Pi/mole MLCK). Phosphoamino acid analysis identified serine as the residue modified. The enzyme phosphorylated under both conditions exhibits a lower enzyme activity than the unphosphorylated MLCK due to a 4-fold increase in K_{CM} . These results suggest that the binding of Ca^{2+} -calmodulin to psm-MLCK does not interfere with the action of cAMP-dependent protein kinase. Moreover, an increase in intracellular cAMP level in pregnant sheep myometrium will inhibit contractile activity in both contracting and relaxing Ca^{2+} concentrations. (Supported by the Medical Research Council of Canada).

Tu-P024

 Ca^{2+} -DEPENDENT PHOSPHORYLATION OF MYOSIN LIGHT CHAIN KINASE IN TRACHEAL SMOOTH MUSCLE. M.G. Tansey, Y. Kubota, R.A. Word, K.E. Kamm, and J.T. Stull Dept. of Physiology, U.T. Southwestern Med. Ctr., Dallas, TX. 75235

Smooth muscle contraction is initiated by the Ca^{2+} /calmodulin-dependent phosphorylation of myosin light chain (MLC) by myosin light chain kinase (MLCK). Phosphorylation of purified MLCK at a regulatory site (site A) by any of several protein kinases increases the concentration of Ca^{2+} /calmodulin required for half-maximal activation of MLCK (K_{CM}). We have investigated MLCK phosphorylation in tracheal smooth muscle, since it may affect the Ca^{2+} sensitivity of MLC phosphorylation. Because site A is phosphorylated in contracting tracheal smooth muscle, we also tested the hypothesis that this phosphorylation is Ca^{2+} -dependent in smooth muscle cells. The MLCK activity ratio assay was used to assess the extent of phosphorylation of MLCK at site A (Stull *et al.*, JBC 265:16683, 1990). Stimulation of tracheal smooth muscle strips with carbachol results in a rapid (1 min) decrease in MLCK activity ratio (from 0.77 ± 0.01 to 0.47 ± 0.01). This decrease did not occur in Ca^{2+} -depleted tissues. Stimulation of cultured tracheal smooth muscle cells with the Ca^{2+} ionophore ionomycin resulted in an increase in cytosolic Ca^{2+} and a rapid (3 sec) decrease in MLCK activity ratio. Ca^{2+} -free conditions inhibited these responses. Because phosphorylation of MLCK at site A would be expected to decrease the Ca^{2+} sensitivity of MLC phosphorylation, we evaluated whether alterations in the MLC phosphorylation/ Ca^{2+} relationship are associated with changes in MLCK phosphorylation. Although stimulation of tracheal smooth muscle strips with either carbachol or KCl rapidly increased cytosolic Ca^{2+} , MLC phosphorylation and tension while decreasing MLCK activity ratios, there were quantitative differences. At 25 min the relative cytosolic Ca^{2+} concentration was greater with KCl than with carbachol, yet the extent of MLC phosphorylation was similar. However, MLCK activity ratio was significantly lower with KCl treatment than with carbachol. Thus the apparent desensitization of MLC phosphorylation to Ca^{2+} was associated with MLCK phosphorylation. These results suggest that the Ca^{2+} -dependent phosphorylation of MLCK may be involved in regulation of smooth muscle contractility. [Supported in part by HL23990 and GM07062]

Tu-Pos25

NOREPINEPHRINE INCREASES INOSITOL PHOSPHATE LEVELS IN VASCULAR SMOOTH MUSCLE WITHIN 3 SECONDS

Hong Gu and Edward LaBelle (Intro. by Eric Murer). Bockus Research Institute, The Graduate Hospital, Philadelphia, PA

In order to determine whether or not IP_3 can mediate the effects of agonists on the contractions of vascular smooth muscle, the effects of norepinephrine on inositol phosphate levels in rat tail artery were measured. Segments of tail artery were preincubated for 180 min with $[^3H]$ inositol and then pretreated with $LiCl$ (10 mM) before being dipped into norepinephrine (10^{-5} M) for 3-10" intervals. The segments were then quick-frozen in dry ice/acetone and thawed in trichloroacetic acid. After removal of the trichloroacetate with ether, the tissue extracts were applied to Dowex resin in order to separate IP_1 , IP_2 , and IP_3 . Levels of IP_2 and IP_3 were stimulated in the tissue after 3" of norepinephrine treatment. Levels of IP_3 increased significantly after 5" of norepinephrine treatment. Analysis of tissue extracts by means of HPLC demonstrated that the only isomer of IP_3 present in any tissue extract was the 1,4,5 isomer of IP_3 . When segments were stimulated to contract by norepinephrine and the amount of force measured, it was determined that nearly all of the force generated by the segments was generated between 3-10" after norepinephrine treatment. This provides evidence that IP_3 does increase rapidly enough in agonist-stimulated smooth muscle to be responsible for the release of SR calcium that produces the rapid phase of smooth muscle contraction. (Supported by NIH Grant HL 37413).

Tu-Pos27

MEASUREMENT OF INTRACELLULAR pH (pH_i) WITH FLUORESCENT DYE IN CANINE BASILAR ARTERIES J. Yu, R. Rose, B.Y. Ong. Departments of Pharmacology and Anesthesia, University of Manitoba, Winnipeg, MB R3E 0W3, Canada

In previous studies on tracheal muscle strips, we have successfully monitored pH_i with a fluorescent dye (BCECF) by measuring the ratio of emitted (540 nm) fluorescent intensities (FI) of 2 excitation wavelengths at 500 and 440 nm. In the present study we measured pH_i of basilar artery rings using the same technique. Unlike in the tracheal strip, in the artery ring there was a significant dye loss from the tissue ($31 \pm 6.7\%$; $P < 0.005$) exhibited by a decrease in FI_{440} . FI_{440} was positively correlated with BCECF concentration ($r = 0.9997$; $P < 0.0001$) in free BCECF solutions. A calibration curve of the ratio versus pH_i was constructed for each artery ring by permeabilizing the tissue to hydrogen with a nigericin-containing solution. The slope and intercept of the calibration curves depended on the intracellular concentration of BCECF which could be determined by FI_{440} . The linear regression lines for plots of the slope and intercept values from the calibration curve versus FI_{440} values, and their correlation coefficients were

$$\text{slope} = 0.00343 \times FI_{440} + 0.32484 \quad (r = 0.96; P < 0.0001)$$

$$\text{intercept} = -0.02048 \times FI_{440} - 0.80123 \quad (r = -0.97; P < 0.0001)$$

These results agreed well with those from the free BCECF solutions, in which the slope of the ratio versus pH of the solution was steeper at high concentrations of BCECF. In addition when two calibration curves were constructed the slope of second calibration curve would be flatter if there was a significant dye loss between the two periods. Thus, pH_i was calculated from the ratio (FI_{500}/FI_{440}) by determining the slope and intercept from FI_{440} with the above formula. The corrected pH_i was 0.63 ± 0.12 lower than uncorrected pH_i at pH 7.4 and $37^\circ C$ in bicarbonate buffered solution. We conclude that the slope of ratio versus pH_i is BCECF concentration dependent, thus a correction for pH_i calibration is necessary when a substantial loss of intracellular BCECF occurs during experiments. (Supported by Canadian Lung Association and MRC of Canada)

Tu-Pos26

Regulation of Intracellular Ca^{2+} Release by Acetylcholine in Single Smooth Muscle Cells. Peter L. Becker, Fredric S. Fay, Joshua J. Singer, Valerie G. Montana, and John V. Walsh, Jr. Dept. of Physiology, Univ. of Mass Medical Center, Worcester, MA 01655.

The mechanism whereby ACh induces release of Ca^{2+} from intracellular stores in isolated toad gastric smooth muscle cells was studied by combining the single microelectrode voltage-clamped technique with simultaneous monitoring of $[Ca^{2+}]$ with a high-time resolution microfluorimeter. When the membrane potential was held negative to -80 mV to preclude activation of voltage-dependent calcium current (I_{Ca}), ACh (10^{-4} M) caused a transient rise in $[Ca^{2+}]$ (peak elevation of 265 ± 32 nM by 4.5 sec; $n=16$) with no detectable change in membrane current, indicating Ca^{2+} release from internal stores.

The transient nature of the $[Ca^{2+}]$ response, even with continued ACh exposure, indicated the presence of a mechanism that limits the duration of the Ca^{2+} transient. This mechanism appears to operate by limiting Ca^{2+} release, not by stimulating Ca^{2+} removal. This follows from the observation that the rate of fall of $[Ca^{2+}]$ after its increase due to depolarization-induced I_{Ca} was not affected by ACh. A recovery of 1-3 minutes in the absence of ACh was required before another marked ACh-induced Ca^{2+} transient could be observed. Depolarization-induced I_{Ca} and attendant rise in $[Ca^{2+}]$ during this recovery period did not shorten the period, suggesting that the Ca^{2+} stores were not depleted during a single ACh exposure. The $[Ca^{2+}]$ itself does not appear to turn off the $[Ca^{2+}]$ response via a negative feedback mechanism since a depolarization-induced increase in $[Ca^{2+}]$ prior to ACh application did not block ACh-induced Ca^{2+} release. However, the phorbol ester PMA (but not the inactive α -phorbol) blocked the ACh-induced rise in $[Ca^{2+}]$, whereas it had no effect on the depolarization-induced $[Ca^{2+}]$ rise. Thus, activation of protein kinase-C, as a consequence of muscarinic stimulation, may play a role in terminating the release of Ca^{2+} from internal stores. Support: NIH HL4523 (P.S.F.), DK31620 (J.V.S. + J.V.W.), AHA Grant-in-Aid (P.L.B.).

Tu-Pos28

 Ca^{2+} ACTIVATED K^+ CHANNEL ACTIVITY IN CELL-ATTACHED PATCH-CLAMP IN SMOOTH MUSCLE CELLS SKINNED BY β -ESCIN. Yuji Imaizumi, Katsuhiko Muraki and Minoru Watanabe. (Intro. by N.M. Anderson). Dept. of Chemical Pharmacology, Faculty of Pharmaceutical Sciences, Nagoya City University, Nagoya 467, Japan.

Activity of single Ca^{2+} activated K^+ channels was recorded under cell attached patch clamp conditions from single smooth muscle cells freshly isolated from urinary bladder of the guinea-pig and trachea of the swine. Cells were superfused with a solution consisting of 126 mM K^+ , 4 mM ATP, 4 mM EGTA (pCa 6). After the cell-attached patch configuration was achieved, β -escin, a saponin-like detergent, was puffed for 10-40 sec onto the cell from a pipette containing 1-3 mM β -escin (diameter of approx. 5 μ m) placed downstream from the cell. During this procedure, Ca^{2+} activated K^+ channels having a large unit conductance were activated and concomitantly the cell contracted slightly. A reduction in the pCa of the bathing solution from 6.0 to 9.0 abolished the opening of these channels. The relationship between open-probability and pCa in skinned cells appeared not to be significantly different from that in inside-out patches, suggesting that skinning by β -escin preserves receptor-operated cell responses. Application to skinned cells of 30 μ M acetylcholine (ACh) together with 1 mM GTP at pCa 7.0 elicited transient bursts of the channel openings which were similar to those observed in intact cells. Similar transient activation of these channels was also observed following application of 5 μ M $InsP_3$ to skinned cells. In contrast, 100 μ g/ml low molecular heparin failed to induce channel activity either in intact cells or in skinned cells, presumably due to heparin-induced block of the release of Ca^{2+} from intracellular stores. These results strongly suggest that this ACh effect on Ca^{2+} activated K^+ channels is mediated by $InsP_3$. Moreover, they demonstrate that skinning by β -escin is a valuable tool for investigating the regulation of ionic channel activity via signal transduction following receptor stimulation.

Tu-Pos29

CHARACTERISTICS OF FAST OUTWARD CURRENT IN CANINE COLONIC CIRCULAR MUSCLE. K.D. Thornbury, S.M. Ward and K.M. Sanders. (Intro. by: R. Mathias) Dept. Physiology, University of Nevada, Reno, NV 89557, USA.

Non- Ca^{2+} dependent outward currents were studied using whole cell voltage clamp in canine colonic circular muscle cells bathed in 1.8 mM Ca^{2+} , 1 μM nifedipine and 100 μM Ni^{2+} . At 26°C depolarizations of -40 to +20 mV (HP -80 mV) produced slowly activating outward currents which inactivated little over 500 msec. At 37°C activation of the current was much faster, taking 3.6 ± 0.8 ms (mean \pm s.e.m) to reach 90% peak at +20 mV, and 16.4 ± 2.6 ms at -20 mV (compared to 58.2 ± 15.2 and 111.6 ± 14.5 ms, respectively, at 26°C, $n=5$). The onset of the outward current overlapped with the transient inward Ca^{2+} current, suggesting that it may act as a brake on the upstroke depolarization of electrical slow waves of intact muscles, which only reach -20 mV. At 37°C the currents evoked by test pulses positive to -20 mV inactivated by 50% over 500 ms at +20 mV, although little inactivation was observed at -30 and -40 mV. When net currents were studied without blocking Ca^{2+} channels, depolarizations of -40 to -20 mV evoked transient inward current. At -20 mV this was followed by a large net outward current, but at -40 and -30 mV there was little net current after the initial inward current. When this was repeated in 1 μM nifedipine, voltage dependent outward current was unmasked at all three potentials. This suggests that the zero net current in the -40 to -30 mV range is due to a balance of sustained inward and outward currents. This balance is likely to create the plateau phase of electrical slow waves. The Ca^{2+} insensitive outward current was separated into two components, one of which was relatively insensitive to 4-aminopyridine and was inactivated by negative conditioning pulses ($V_{0.5} = -53$ mV), while the other was reduced by the drug and inactivated at more positive potentials ($V_{0.5} = -27$ mV). (Supported by NIH grants DK41315 and F05 TW0445)

Tu-Pos31

MEASUREMENT OF MEMBRANE POTENTIAL, CYTOSOLIC CALCIUM AND MUSCLE TENSION IN SMOOTH MUSCLE TISSUE. H. Ozaki, R.J. Stevens, D.P. Blondfield, N.G. Publicover and K.M. Sanders. Dept. Physiology, Univ. Nevada School of Medicine, Reno, NV 89557.

Microelectrode techniques and the fluorescent Ca^{2+} indicator, indo-1, were used to measure membrane potential, cytosolic Ca^{2+} ($[\text{Ca}^{2+}]_{\text{cyt}}$) and muscle tension simultaneously in canine antral smooth muscles. Responses of muscles from the myenteric and submucosal regions were compared since electrical activity and excitation-contraction coupling in these regions differ. The upstroke phase of electrical slow waves in both regions induced an increase in $[\text{Ca}^{2+}]_{\text{cyt}}$. In myenteric muscles the plateau phase of slow waves often caused either a further rise in $[\text{Ca}^{2+}]_{\text{cyt}}$ or maintenance of the level reached during the upstroke event. In submucosal muscles, the plateau phase was significantly smaller, and did not induce a second phase in the Ca^{2+} transient. Contractions were related to the amplitudes of Ca^{2+} transients. Acetylcholine (3×10^{-8} M - 10^{-6} M) increased the amplitude and duration of the plateau phase of slow waves in a concentration-dependent manner. ACh also increased the second phase of Ca^{2+} transients and contractile responses associated with the plateau potential. In submucosal muscles ACh induced a significant increase in the plateau phase of the slow wave and increased the corresponding phase of the Ca^{2+} transient. Nicardipine (10^{-6} M) inhibited plateau phase of slow waves and the associated increases in $[\text{Ca}^{2+}]_{\text{cyt}}$ and muscle tension. Bay k8644 (10^{-7} M) augmented the plateau potential and increased $[\text{Ca}^{2+}]_{\text{cyt}}$ and muscle tension. These results suggest that dihydropyridine-sensitive Ca^{2+} currents participate in the plateau potential. Cholinergic stimulation modulates $[\text{Ca}^{2+}]_{\text{cyt}}$ and therefore force by regulating the amount of Ca^{2+} entering cells through these channels. (Supported by DK 32176 and DK 40569)

Tu-Pos30

IONIC CURRENTS OF COLONIC LONGITUDINAL SMOOTH MUSCLE: AN ACTION POTENTIAL GENERATING MUSCLE. S.M. Ward, K.D. Thornbury, and K.M. Sanders. (Intro. by R. Harrington) Dept. Physiology, Univ. of Nevada, Reno, NV 89557.

The circular and longitudinal muscle layers of the colon differ in their electrical activity: circular muscles generate slow electrical events with plateau depolarizations and longitudinal muscles generate fast Ca^{2+} action potentials. These differences suggest a differential expression of ionic channels. Studies in isolated longitudinal colonic myocytes with the patch clamp technique showed substantial net inward currents averaging 564 ± 100 pA (at 0 mV, $n=12$) which rapidly reversed to outward currents averaging 280 ± 69 pA (at 0 mV). Little or no outward current was observed at potentials negative to -10 mV which is in striking contrast to circular muscle cells where net current occurs positive to -40 mV. Outward current peaked within 100 ms and then declined to a sustained level about 60% of the peak. The peak outward current was very susceptible to nifedipine (10^{-6} M) and TEA (1 mM), suggesting it was largely Ca^{2+} dependent. Bay-k 8644 (10^{-6} M) greatly increased the magnitude of the outward current. Outward currents were blocked with Cs^{+} -filled pipettes and 40 mM TEA in the bath solution to study inward currents. Inward current was activated positive to -50 mV, peaked at 0 mV and reversed at about +60 mV. The inward current was characterized by a large transient component which rapidly inactivated to a small amplitude, sustained component. A large portion of the transient phase was dihydropyridine-sensitive because nifedipine (10^{-6} M) caused a 90% reduction (at 0 mV) and Bay-k 8644 (10^{-6} M) caused about a 50% increase in the amplitude of the inward current. The sustained current was blocked by nifedipine. The activation of outward current at more positive potentials and robust inward currents may provide an explanation for the action potential generating capability of the longitudinal muscle layer. (Supported by NIH grants DK41315 and F05 TW0445)

Tu-Pos32

SODIUM REGULATION IN SMOOTH MUSCLE CELLS

Moore, E.D.W., and Fay, F.S. (Intro. by Joshua J. Singer) Dept. of Physiology, University of Massachusetts Medical Center. Worcester Ma, 01609.

We have undertaken a study of the regulation of the intracellular sodium concentration in single, enzymatically dissected cells from the stomach of the toad *Bufo marinus*. Intracellular sodium concentrations were measured with the Na^{+} -sensitive fluorescent dye SBFI. Images of cells were captured with a digital imaging microscope and a thermoelectrically-cooled CCD camera, several planes of each cell were obtained to allow a three-dimensional reconstruction. While the dye distributes non-uniformly throughout the cell, the ratio images are uniform and we report that the intracellular sodium concentration averages 13 mM ($N=27$). While local application of ouabain uniformly increased the sodium concentration, application of isoproterenol decreased the sodium concentration. The decrease in sodium concentration was complete in an average of 3 seconds, it could be blocked by removal of extracellular K^{+} or application of the non-specific β -antagonist pindolol. The response could be mimicked with either the adenylate cyclase stimulant forskolin or the non-hydrolyzable cAMP analogue, 8-Br-cAMP. These results indicate that the ISO induced decrease in $[\text{Na}^{+}]_{\text{i}}$ is the result of activation of the $\text{Na}^{+}\text{-K}^{+}$ ATPase. We estimate that there are 600 pumps/ μm^2 in the smooth muscle membrane. The relationship of the activity of the $\text{Na}^{+}\text{-K}^{+}$ ATPase to the activity of the $\text{Na}^{+}\text{-Ca}^{2+}$ exchanger will be presented and discussed. Supported by MDA and NIH (HL4523).

Tu-Pos33

AN INFLUX OF EXTRACELLULAR CALCIUM MODULATES AVP-EVOKED INOSITOL PHOSPHATE FORMATION IN A CULTURED ARTERIAL SMOOTH MUSCLE CELL LINE.

D.M. Berman and W. F. Goldman, Dept. Physiology, Univ. Maryland Med. School, Baltimore, MD 21201.

Agonist-mediated vascular smooth muscle cell (VSMC) activation entails inositol 1,4,5-trisphosphate (IP₃)-induced release of Ca²⁺ from the sarcoplasmic reticulum as well as an influx of Ca²⁺ from the extracellular fluid (ECF). We studied the effects of influxes of extracellular Ca²⁺ on AVP-induced inositol phosphate (IP) formation in an arterial smooth muscle cell line (A₇r₅). IP formation was measured for up to 60 sec after pretreating cells with 30 mM Li⁺ for 10 min. The AVP-induced increase in IP synthesis was evident within 5 sec, maximal IP levels were usually attained within 10-15 sec. Thereafter, IP synthesis declined although AVP remained present. The stimulation threshold for AVP was 1 nM and 100 nM AVP elicited maximal IP formation. In the absence of extracellular Ca²⁺ (0Ca²⁺, 1 μ M EGTA) or after blockade of voltage-gated Ca²⁺ channels (10 μ M verapamil), there was a 40%-50% decline in basal IP levels, and AVP-induced IP synthesis was markedly attenuated. Nevertheless, there was no significant difference in the stimulation threshold or the AVP concentration required to elicit maximal IP formation. Augmenting the influx of Ca²⁺ from the ECF also inhibited AVP-induced IP synthesis; however, the characteristics of the inhibition differed from those observed in the absence of Ca²⁺. Membrane depolarization (40 mM K⁺) or pretreatment with Bay-K-8644 (5 μ M), caused a shift to the right of the AVP dose-response curve. There was a tenfold increase in the stimulation threshold, although basal IP levels remained unchanged. These observations indicate that AVP-induced IP formation can be modified by varying the influx of Ca²⁺ from ECF. They suggest that an agonist-evoked influx of extracellular Ca²⁺ plays an important role in modulating IP formation during VSMC activation.

Tu-Pos35

ONE AND TWO DIMENSIONAL MODELS OF CALCIUM MOVEMENT IN SMOOTH MUSCLE CELLS. Gary J. Kargacin and Fredric S. Fay, Departments of Physiology, University of Calgary and University of Massachusetts

We have developed one and two dimensional computer models of Ca diffusion in smooth muscle cells that include known Ca regulatory processes and intracellular Ca buffering. These models predict that a significant Ca gradient can develop in cells and persist for several hundred milliseconds following influx of Ca from the extracellular space and release from intracellular storage sites. The presence of this gradient would lead to inhomogeneities in the rates at which processes controlled by Ca operate in different parts of a cell. For example the models predict that, while the gradient exists, Ca-ATPase rates would be higher at SR sites near the surface membrane than at those more centrally located. This could lead to an initial rate of Ca removal following cell stimulation that is faster than that predicted by the average intracellular [Ca] similar to what has been observed in experimental records. We have also used the models to explore the effect that the location of SR release and pump sites could have on Ca distribution in cells and on the overall rate of its uptake and release. Our results indicate that the uniformity of distribution of the SR and the spatial relationship between the SR release sites and pumping sites could be important determinants of the extent of temporal and spatial inhomogeneities of Ca in cells. Supported by NIH AR39678 and HL14523 and the Alberta Heritage Foundation.

Tu-Pos34

Na/H EXCHANGE IN STRIPS OF MESENTERIC ARTERY FROM SHR AND WKY RATS.

C.D. Foster, T.W. Honeyman and C.R. Scheld.

Dept. of Physiology, Univ. of Mass. Medical Center, Worcester MA. 01655.

Studies in cultured cells have suggested that one of the underlying abnormalities in hypertension is an increased activity of the Na/H antiporter. To investigate if these changes were present in intact tissues, we utilized strips (0.5 x 4mm) of mesenteric arteries from SHR and WKY rats, loaded with the pH sensitive dye BCECF (14 μ M). Strips were held at a fixed length within a 3ml cuvette and fluorescence emission was monitored at 530nm. The spectrofluorimeter was operated in the ratio mode and the excitation wavelength alternated between 440 and 505nm. Tissues were maintained by perfusing with HEPES containing buffers. Basal pH_i was not significantly different between the two strains, (SHR= 7.19 \pm 0.02; WKY= 7.24 \pm 0.02, n=4). Using a standard ammonium prepulse technique to acidify the preparation, the initial acidic pH_i was also not different (SHR= 6.818 \pm 0.009; WKY= 6.823 \pm 0.003, n=4). The pH_i recovery from this acid load was Na⁺-dependent and sensitive to amiloride analogues. This recovery was, however, significantly increased in SHR (1.413 \pm 0.34 x10⁻² pH units/min, n=4) versus WKY (0.94 \pm 0.31 x10⁻² pH units/min, n=5). Measurements of the intracellular buffering capacity in SHR and WKY mesenteric strips showed no significant differences. Therefore the increase in pH_i recovery following an acid load appears to be due to an alteration in the intrinsic capacity of the system and not due to changes in intracellular buffering. This is the first time such an abnormality has been detected "on line" in intact arteries.

Supported by NIH HL 41188.

Tu-Pos36

FOCAL APPLICATION OF VASOPRESSIN TO VASCULAR SMOOTH MUSCLE CELLS TRIGGERS CALCIUM WAVES AS REVEALED BY DIGITAL IMAGING MICROSCOPY.

L. A. Blatter and W. G. Wier, Dept. of Physiology, University of Maryland School of Medicine, Baltimore, MD 21201

Application of [Arg⁸]-vasopressin (AVP) to A7r5 cells, a smooth muscle cell line derived from rat thoracic aorta, can lead to oscillations of intracellular calcium ([Ca²⁺]_i). To measure [Ca²⁺]_i, fura-2 was introduced into cells either through a tight-seal microelectrode or by exposure of the cells to fura-2/AM. When spatially averaged [Ca²⁺]_i was measured (photomultiplier tube), the oscillatory response to AVP consisted of an initial large [Ca²⁺]_i-transient followed by several oscillations in [Ca²⁺]_i of decreasing amplitude. Digital imaging microscopy was used to study the spatial distribution of [Ca²⁺]_i during the application of AVP. The magnitude of the rise in [Ca²⁺]_i and the delay between exposure to AVP and onset of the rise in [Ca²⁺]_i are both dose-dependent. Bath application of AVP to A7r5 cell in a rapid superfusion system leads to a rise in [Ca²⁺]_i at the cell's periphery. The elevated [Ca²⁺]_i subsequently moves as a concentric wave towards the center of the cell. Focal application of AVP by means of pressure ejection from a micropipette causes a local increase of [Ca²⁺]_i, which spreads as a wave over the whole cell at a velocity of approximately 10-20 microns/sec. It has already been shown by others that AVP increases the intracellular level of inositoltrisphosphate (IP₃) which mediates the increase of [Ca]_i. 3-dimensional modelling of diffusion indicates that the [Ca²⁺]_i-waves initiated by focal application of AVP are unlikely to be due simply to diffusion of IP₃ from its site of production (IP₃ could diffuse and release Ca²⁺ from stores in other parts of the cell). It is also unlikely that diffusion of Ca²⁺ alone from the area of increased [Ca]_i is responsible for the observed spatial distribution of [Ca²⁺]_i. The velocity and the profile of the response ([Ca²⁺]_i-wave) to focally applied AVP indicate that a regenerative mechanism such as calcium-induced release of calcium is involved.

Tu-Pos37

SOME PROPERTIES OF SINGLE K⁺ CHANNELS OF FRESHLY DISPERSED GUINEA-PIG URETERAL MYOCYTES AND THEIR RELATION TO WHOLE-CELL K⁺ CURRENTS. J. L. Sul, S. Y. Wang and C. Y. Kao. Department of Pharmacology, SUNY Downstate Medical Center, Brooklyn, NY, 11203.

In freshly dispersed guinea-pig ureteral myocytes, the action potentials have a variable plateau on which are superimposed irregular fluctuations. In whole-cell recordings, an inward I_{K_A} has a very slowly inactivating phase, interrupted by current fluctuation which are outward at $V > +30$ mV. Such fluctuating currents are readily blocked by TEA (2 - 30 mM). Activities of single K⁺ channels have now been recorded in both cell-attached and in detached inside-out patches. These channels are manifested as random burst-openings of fairly large unit currents at $V > -10$ mV. At pCa of 9 and 8, the open probability (P_o) of this channel is usually less than 0.001 at 0 mV. The open-time histogram can be fitted with one exponential component, whereas the close-time histogram needs at least two components. In physiologically asymmetrical K⁺ distributions (135 mM, in/ 6 mM, out), the average unit conductance is 163 ± 7.5 pS (mean \pm SEM of 30 patches). The P_o of these channels is voltage-dependent, with an α -fold increase in P_o upon a +12 mV shift. It is highly sensitive to $[Ca^{2+}]_i$. When internal pCa is increased from 8 to 7, the voltage for $P_o = 0.5$ is shifted by -62.2 ± 10.2 mV ($n=5$). From HP of -50 mV, these channels are activated when the patch is step-depolarized to $V > -10$ mV. Summed and averaged current of single sweeps show a gradually developing and outwardly rectifying current, similar to the delayed rectifier current in other excitable cells. When averaged for 20 sweeps, the macroscopic current shows fluctuations similar to those seen in whole-cell recordings. When averaged for 60 to 100 sweeps, the macroscopic currents are smoothed. These observations suggest that the complex ionic currents and the complex action potentials of ureteral myocytes are due to a combination of a very slowly inactivating I_{K_A} and the opening of few Ca^{2+} -activated K⁺ channels. (Supported by NIH DK 39731).

Tu-Pos39

CONVERGENCE OF REFLEX PATHWAYS ACTIVATED BY DISTENSION AND MUCOSAL STROKING OF THE ISOLATED GUINEA-PIG ILEUM. T.K. Smith, J.C. Bornstein* and J.B. Furness. Centre for Neuroscience and Departments of Anatomy & Histology and of Physiology*, Flinders Medical Centre, Bedford Park, S.A., 5042, Australia. (Intro. by R. Paul)

The electrical responses to both distension and mucosal stroking were recorded from circular muscle cells and myenteric neurons of isolated guinea-pig ileum. Myenteric ganglia were exposed by sharp dissection of an area in the middle of an opened segment of guinea-pig ileum that was pinned flat with the mucosa uppermost over two hemispherical balloons. The balloons were located 20mm oral and anal to the recording area. Reflexes were evoked by either oral or anal distension or by brushing the mucosa. Both distension or mucosal brushing evoked in circular muscle cells excitatory junction potentials (EJPs) on the oral side and inhibitory junction potentials (IJP) on the anal side of the stimulus. These stimuli evoked a burst of fast excitatory postsynaptic potentials (fEPSPs) in about 40% of S neurons (52 neurons) located either oral or anal to the stimulus but not in AIJ cells (100 neurons). Those S-neurons that responded to distension usually responded to mucosal stimulation from the same side. The oral EJPs declined to zero with repetitive distension or stroking. However, during the rundown period of the EJP evoked by distension or stroking, stimulation of another anal site evoked a full EJP suggesting that the rundown occurs near the site of stimulation. Repetitive brushing over the distension site enhanced the EJPs and IJPs to distension despite rundown in the responses to brushing but not vice versa. The fEPSPs evoked in oral S neurons also declined with repetitive stimulation. Despite the rundown of fEPSPs to repetitive distension, mucosal brushing over the distension site evoked a burst of fEPSPs in 4 S-neurons tested for this phenomenon. These studies suggest that each stimulus activates different sensory neurons but many of the interneurons and final motor neurons may be common to both reflex pathways.

Tu-Pos38

STRETCH-ACTIVATED SINGLE-CHANNEL AND WHOLE-CELL CURRENTS IN ISOLATED VASCULAR SMOOTH MUSCLE CELLS.

Michael J. Davis, James A. Donowitz and John D. Hood, Department of Medical Physiology and Microcirculation Research Institute, Texas A&M University, College Station, TX 77843.

We tested the hypothesis that a stretch-activated cation channel (SAC) is involved in the contraction of vascular smooth muscle (VSM) following stretch. Single-channel and whole-cell patch-clamp techniques were used to record from enzymatically isolated porcine coronary artery cells. In single-channel experiments, membrane stretch was applied via suction through 5-12 MΩ patch electrodes. The cells were bathed in a solution of 140 mM K-aspartate or K-glutamate to depolarize the membrane, and in the absence of Ca^{2+} to reduce interference by Ca^{2+} -activated K⁺ channels; pipettes contained (in mM): 140 KCl, 2 MgCl, 10 HEPES, and 2 EGTA or 2 CaCl₂. Stretch-activated currents were observed in about 10% of cell-attached and inside-out patches during application of 20-60 mmHg suction. Suction increased the open probability of the channel without altering unitary conductance. The likelihood of observing SACs appeared to be increased by including physiologic levels of Ca^{2+} in the pipette. Unitary conductance to K⁺ under these conditions, as determined from amplitude histograms at various holding potentials, was ~40 pS; this value is comparable to values for SAC in other tissues. The channel was also permeable to Na⁺, Cs⁺, Ca^{2+} , and Ba²⁺.

To examine the possible role of SAC in the response of whole VSM cells to a more physiologic stretch, we used 2 additional patch-type pipettes to attach to the cell ends. Longitudinal stretch was applied using hydraulic manipulators while recording whole-cell current or membrane potential through a third patch electrode (1-5 MΩ). For this protocol, the cells were bathed in physiologic saline (PSS) and the recording electrode contained (in mM): 140 K-aspartate, 2 ATP, 2 MgCl, 10 HEPES, 2 EGTA. In unclamped cells, stretch (10-20% beyond slack length) often initiated cell contraction. Under current clamp, stretch depolarized the cell membrane (from $V_r = -55$ mV) and sometimes initiated action potentials. Under voltage clamp, stretch elicited an inward current (I_{sa}), which was characterized by both transient and sustained components. The reversal potential for I_{sa} in PSS was -15 mV, and is consistent with activation of a non-selective cation channel. Neither the amplitude nor activation threshold of voltage-operated Ca^{2+} channels was modified by stretch. These results, coupled with our previous observation (FASEB J 4:A844,1990) that high doses of nifedipine block only ~50% of the intracellular Ca^{2+} increase elicited by single-cell stretch, support a physiologic role for a non-selective cation channel in the response of VSM cells to stretch. Activation of this channel would allow direct Ca^{2+} entry and depolarize the membrane to recruit voltage-activated Ca^{2+} channels. Supported by HL-38104, AHA 881161, Texas ATRP 3177. MJD is an Established Investigator of the American Heart Association.

Tu-Pos40

Ca^{2+} ACTIVATED Cl^- CURRENTS IN RABBIT ESOPHAGEAL SMOOTH MUSCLE CELLS. H. Akbarali and W. Giles. Departments of Medicine and Medical Physiology, Faculty of Medicine, University of Calgary, Calgary, Alberta, Canada T2N 4N1.

Ca^{2+} currents (I_{Ca}) measured with whole-cell voltage clamp are often recorded in the presence of internal EGTA to minimize 'run-down'. This buffering of intracellular Ca^{2+} , however, may obscure other Ca^{2+} activated currents. In the rabbit esophageal tunica muscularis mucosae (TMM) cells, I_{Ca} recorded in the absence of EGTA usually runs down significantly within 15 mins after beginning whole-cell recordings. When no EGTA was used in the recording pipette, following the I_{Ca} transient, an outward current was elicited by depolarizations beyond 0 mV, and slowly decaying inward tail currents were recorded upon repolarization to the holding potential, -60 mV. In contrast, when EGTA (1 - 10 mM) was present, neither outward nor tail currents were recorded.

To examine further the characteristics of these outward and tail currents under stable recording conditions, we used the nystatin perforated patch technique. I_{Ca} of approx. 300 pA in peak amplitude was obtained in 2 mM $[Ca^{2+}]_i$ on depolarization to -10 mV from holding potential of -60 mV. The threshold for activation of I_{Ca} was near -30 mV and the current reversed at approx. +50 mV. Stable recordings could be obtained in most cells for over 1 hour. The outward and tail currents which were observed on depolarization and repolarization, respectively, were very similar to those observed in the absence of EGTA during standard whole cell recording. When $[Ba^{2+}]_i$ was used to replace $[Ca^{2+}]_i$, both the outward and the tails were abolished. The reversal potential of these tail currents was dependent upon the electrochemical gradient for Cl^- . In chloride substitution experiments (using aspartate), a negative shift was observed in high $[Cl^-]_i$ solution and a positive shift in low $[Cl^-]_i$ solution. Both the outward currents and tails were reversibly blocked by niflumic acid (10 μ M) without any significant change in I_{Ca} . These results demonstrate the presence of a substantial Ca^{2+} activated Cl^- current in the rabbit TMM. (Supported by the Alberta Heritage Foundation and the Canadian Heart Foundation).

Tu-Pos41

CA²⁺ CHANNEL BLOCKERS DISTINGUISH BETWEEN G-PROTEIN-COUPLED, PHARMACOMECHANICAL CA²⁺ RELEASE AND CA²⁺-SENSITIZATION IN SMOOTH MUSCLE

M. Gong, S. Kobayashi, A. V. Somlyo, and A. P. Somlyo
From the Department of Physiology, University of Virginia,
Charlottesville, VA22908

The effects of Ca²⁺ channel blockers on two modes of G-protein-mediated, pharmacomechanical coupling, Ca²⁺ release and modulation of Ca²⁺ sensitivity of the contractile apparatus, were investigated. Smooth muscles were permeabilized with *Staphylococcus* α -toxin or with β -escin to avoid effects due to block of sarcolemmal Ca²⁺ channels, while retaining receptor/G-protein coupling. In permeabilized portal vein smooth muscle, verapamil and nifedipine inhibited Ca²⁺ release induced by an α_1 -adrenergic agonist (phenylephrine) and by GTP γ S, but not that induced by inositol 1,4,5-trisphosphate (InsP₃). These Ca²⁺ channel blockers also did not block the phenylephrine- or GTP γ S-induced force development at constant cytoplasmic Ca²⁺ ("Ca²⁺-sensitization"). An α_1 -blocker (prazosin) inhibited both the Ca²⁺ releasing and "Ca²⁺-sensitizing" effects of phenylephrine, but not those of GTP γ S, nor did it block InsP₃-induced Ca²⁺ release. We conclude that Ca²⁺ channel blockers selectively uncouple the Ca²⁺ release, but not the Ca²⁺-sensitizing, component of pharmacomechanical coupling. These findings raise the possibility that pharmacomechanical Ca²⁺ release may be modulated by dihydropyridine binding proteins at the level of G-proteins/phospholipase C, and also indicate a divergence of the Ca²⁺-releasing and Ca²⁺-sensitizing effects at some step prior to phospholipase C. This work was supported by National Institutes of Health grant HL15835 to the Pennsylvania Muscle Institute and by 2 P01 HL19242-14.

Tu-VCR1

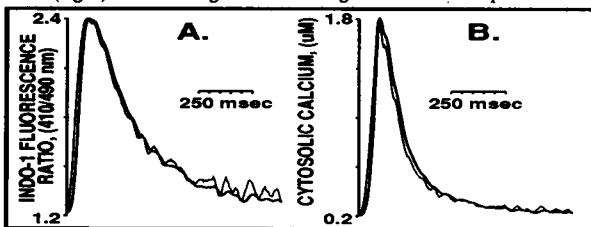
Thin Filament Motility: Effect of Myosin-Binding Fragments of Caldesmon
M.E. Hemric, Dave M. Warshaw, and J.R. Haeblerle, Department of Physiology and Biophysics, University of Vermont, Burlington VT 05405

Caldesmon has been shown to bind both actin and myosin and to form an actin-caldesmon-myosin complex (Hemric and Chalovich, (1988) *J. Biol. Chem.* 263, 1878-1885). The C-terminal, actin-binding region of caldesmon is a competitive inhibitor of myosin binding to actin; the N-terminal region binds specifically to the S1/S2 region of myosin. Haeblerle et al. (*Biophys. J.*, this volume) have utilized an "in vitro" motility assay to investigate the effects of caldesmon on the movement of unloaded rhodamine-phalloidin-labeled actin filaments over a surface of thiophosphorylated smooth muscle myosin. They found that intermediate concentrations of caldesmon (0.1 μ M) promote filament binding under high salt conditions (80 mM KCl, 30°C) without inhibiting filament velocity. They proposed that the formation of actin-caldesmon-myosin complexes tethers actin filaments to the myosin surface and promotes the productive interaction of actomyosin to generate filament motility. An alternate explanation for the increased filament binding is that caldesmon inhibits product release from myosin, and thereby, increases the number of high-affinity actomyosin complexes. To differentiate between these possible mechanisms, we have isolated chymotryptic myosin-binding fragments of chicken gizzard caldesmon and used these fragments in the motility assay to determine if binding of the N-terminal region of caldesmon to myosin is required for enhanced filament binding. Chicken gizzard caldesmon was digested for 5 min @ 25°C with chymotrypsin (1:800 weight ratio) and the myosin-binding fragments were isolated by myosin-affinity chromatography. The inability of the myosin-binding fragments to bind to actin was verified by actin-filament sedimentation assay. The addition of 0.75 mg/ml myosin-binding fragments to the flow cell, in the absence of intact caldesmon, had no effect on either actin filament binding or filament velocity; this suggested that the myosin binding fragments do not inhibit product release from actomyosin. This same amount of fragment, however, completely reversed the increased binding seen in the presence of 0.4 μ M intact caldesmon, presumably by competitive inhibition of intact-caldesmon binding to myosin. Taken together, these results demonstrate that the caldesmon-dependent increase in filament binding (1.) requires that caldesmon bind to both actin and myosin and (2.) is not due to inhibition of product release by caldesmon binding to actin or myosin. These findings, in agreement with those of Hemric et al. (*J. Biol. Chem.* 263: 1878-1885) and Haeblerle et al. (*Biophys. J.*, this volume), indicate that caldesmon enhances the binding of actin filaments to myosin by forming an actin-caldesmon-myosin complex. This in turn facilitates binding of actin to myosin, and consequently, cross-bridge cycling at high ionic strength.

Tu-Pos42

INFLUENCE OF PROBE KINETICS ON MEASUREMENT OF CALCIUM RELAXATION TIMES IN CARDIAC MYOCYTES
M.D. Stern, W.H. DuBell, H.A. Spurgeon, E.G. Lakatta (Intro. by Alexandre Fabiato). Gerontology Research Center, NIA, NIH, Baltimore, MD 21224

When calcium-binding fluorescent probes such as indo-1 and fura-2 are used to study the kinetics of calcium relaxation in skeletal and cardiac muscle cells, the finite rates of calcium binding and release by the probe might limit the accuracy of such studies, since it has been shown that fura-2 kinetics may be severalfold slower in the cytosolic milieu (in skeletal muscle) than in free solution. For dual-wavelength ratio probes, the effect of the probe kinetics can be expressed by means of a "kinetically corrected ratio", (bold curves) defined as the fluorescence ratio which, if used "naively" in the equilibrium calibration formulae, would give the true value of calcium. Theoretical analysis shows that the kinetically corrected ratio is given by $R_c = R - \{\beta(R_{max} - R)dR/dt\} / \{k_b(R_{min} - \beta R_{max}) - \beta dR/dt + (\beta - 1)k_b R\}$ where k_b is off-rate for calcium dissociation from the probe and β is the ratio of fluorescence at saturating $[Ca]/zero [Ca]$ at the wavelength used in the denominator of the fluorescence ratio R . Note that corrected ratio does not depend on K_d for calcium binding to the probe. Using indo-1 free acid microinjected into rat cardiac myocytes at 23°C, and assuming $k_b = 10 \text{ sec}^{-1}$, which is 12-fold less than measured rate in solution, the kinetic correction to the ratio (left) or the calculated calcium concentration (right) is still insignificant during the relaxation phase.

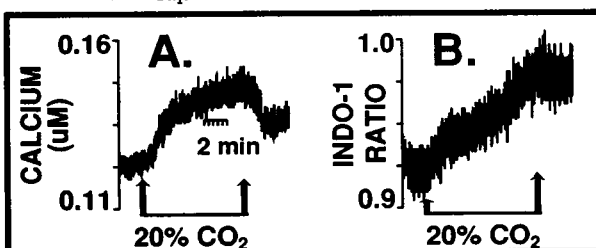


Tu-Pos44

ACIDOSIS INCREASES CYTOSOLIC AND MITOCHONDRIAL Ca^{2+} IN CARDIAC MYOCYTES

Giovanni Gambassi, Richard G. Hansford, Steven J. Sollott, Maurizio C. Capogrossi, Laboratory of Cardiovascular Science, Gerontology Research Center, NIA, NIH, Baltimore, MD 21224

The effect of acidosis on myocardial Ca^{2+} homeostasis is still largely undefined. Cytosolic $[Ca^{2+}]_i$ (Ca_i) appears to increase but both the source of such an increase in Ca_i and the effect of acidosis on mitochondrial free $[Ca^{2+}]_m$ (Ca_m) are unknown. We measured Ca_i in isolated rat left ventricular myocytes loaded with indo-1 free acid. We measured Ca_m in cells loaded with the ester derivative of indo-1 and pretreated with 200 μM Mn^{2+} for 50 min to quench the cytosolic indo-1 fluorescence. Cells were bathed in bicarbonate buffer with 1.5 mM $[Ca^{2+}]_o$, gassed with 5% (pH 7.36) or 20% CO_2 (pH 6.82). Acidosis for 10 min caused a progressive increase in Ca_i from $147 \pm 16 \text{ nM}$ to $202 \pm 22 \text{ nM}$, mean \pm SD, $n = 4$). A similar increase in Ca_i occurred with 5 μM ryanodine and no added Ca^{2+} with 0.1 mM EGTA in the bathing medium (Panel A) (from $108 \pm 19 \text{ nM}$ to $140 \pm 15 \text{ nM}$, $n = 6$). Ca_m also increased in response to acidosis (Panel B) and there was no effect of 10 μM ruthenium red (not shown). These results indicate that acidosis increases both Ca_i and Ca_m and suggest that a decreased Ca^{2+} binding to intracellular buffers, owing to increased H^+ activity, represents a major mechanism for the increase in Ca_i .

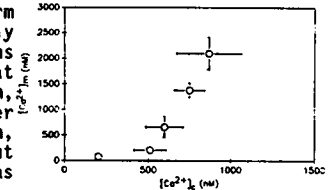


Tu-Pos43

DYNAMIC MEASUREMENT OF MITOCHONDRIAL $[Ca^{2+}]_m$ IN SINGLE CARDIAC MYOCYTES

Haruo Miyata, Howard S. Silverman, Richard G. Hansford, Steven J. Sollott, Edward G. Lakatta, Michael D. Stern. GRC, NIA, NIH and Johns Hopkins University, Baltimore, Maryland.

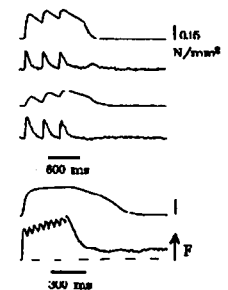
It has not previously been possible to measure mitochondrial calcium in living cardiac cells. Taking advantage of the fact that roughly 50% of indo-1 loaded by the acetoxymethyl (AM) ester partitions into cardiac mitochondria we measured twitch amplitude and the indo-1 fluorescence ratio (410/490 nm) in single rat ventricular myocytes following loading with the AM form. After 28 ± 10 min of perfusion with 100 μM manganese (Mn^{2+} , capable of quenching indo-1 fluorescence) fluorescence transients disappeared without a significant change in the electrically stimulated mechanical twitch amplitude. After Mn^{2+} exposure, fluorescence intensity was reduced by roughly 50%. After the disappearance of the cytosolic indo-1 transient superfusion with low Na^+ buffer increased the fluorescence ratio to levels which could reach R_{max} . The rise in the ratio was nearly abolished by pretreatment with ruthenium red, the potent blocker of the mitochondrial calcium uniporter. Calcium estimated assuming the unquenched dye is located in a single compartment was $80 \pm 15 \text{ nM}$ ($n=18$) during stimulation at 0.2 Hz. Steady state mitochondrial calcium was estimated during superfusion with buffers of gradually decreasing $[Na^+]$ and compared to cytosolic calcium levels in cells loaded with indo-1 free acid. The data confirm results obtained previously in mitochondrial suspensions suggesting that mitochondrial $[Ca^{2+}]_m$ is normally lower than cytosolic calcium, $[Ca^{2+}]_c$ (figure), but increases above $[Ca^{2+}]_c$ as the cell is calcium loaded.



Tu-Pos45

SIMULTANEOUS MEASUREMENTS OF ISOMETRIC FORCE AND FLUO-3 CALCIUM TRANSIENTS IN INTACT SINGLE MUSCLE FIBERS. C. Caputo and K.A.P. Edman. Department of Pharmacology, Lund University, Lund, Sweden.

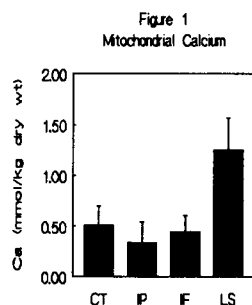
Calcium transients and isometric contractions were recorded from single muscle fibers loaded with fluo3 AM, at 5 to 10 °C. To diminish movement artefacts, care was taken to minimize lateral and rotational movements of the fibers. The experimental chamber was mounted on the stage of a microscope with epi-fluorescence attachment, with a low power objective (10x). The light source was a 100 W Hg-lamp with a stabilized power supply. The filter combination (excitation/dichroic/barrier) was 546/580/590. To load the dye, the fibers were bathed in a Ringer's solution containing 1 to 10 μM of dye at about 20 °C from 30 to 60 minutes. Fluorescence signals were recorded at 3 kHz with a photodetector, and were not calibrated. The delay between the calcium signal and tension development was about 8 ms. The upper records of the figure show that the calcium signals were not much affected by an hypertonic solution (150 mM added sucrose) that decreased appreciably tension. The lower record shows that during a mechanically fused tetanus (20 Hz), individual peak transients in the calcium signals could be observed that increased during the tetanus plateau due to a sustained increase in the calcium signal base line, maintained for many seconds after complete relaxation. In many cases, during the relaxation phase an extra component could be observed in the calcium signal probably caused by movement artefact. (Supported by the Swedish Medical Research Council).



Tu-Pos46

ELECTRON PROBE MICROANALYSIS OF MITOCHONDRIAL CALCIUM IN CONTRACTING CARDIAC MUSCLE - EFFECT OF INOTROPIC STIMULATION. M. Bond and C. S. Moravec, Cleveland Clinic Foundation, Cleveland, OH.

In order to determine whether increased energy demand in cardiac muscle (and increased energy production via activation of Krebs cycle enzymes) is associated with increased mitochondrial (MT) Ca^{2+} uptake, we have measured total MT Ca^{2+} by electron probe microanalysis in cryosections from hamster papillary muscles rapidly frozen during the response to several inotropic interventions. The contracting muscles were rapidly frozen at the peak rate of tension rise ($+d\text{T}/dt$)¹, shown to correspond to the peak of the free Ca^{2+} transient², under the following conditions: (1) control (CT); (2) 10^{-6} M isoproterenol (IP); (3) 3-fold increase in stimulation frequency (IF); (4) low (46.5 mM) Na^+ (LS). IP caused an increase in developed tension (DT) to 139% of CT; IF was accompanied by a decrease in DT to 62% of CT (negative force-frequency relationship). LS caused an initial increase in DT accompanied by a maintained increase in resting tension.



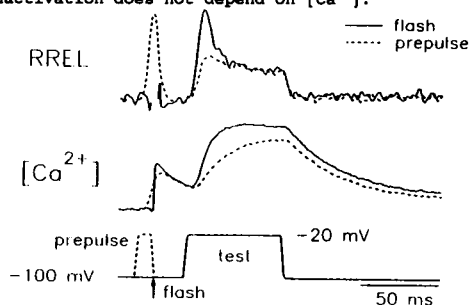
Results (figure 1) indicate that in contracting cardiac muscle, MT can take up Ca^{2+} in response to an increased Ca^{2+} load (by exposure to LS). However, under the inotropic conditions of β -adrenergic stimulation or increased frequency, MT do not take up Ca^{2+} . We therefore conclude that, with more physiological interventions which increase energy demand on the cell, mitochondrial Ca^{2+} changes are unlikely to play a significant role in the activation of mitochondrial metabolism.

1. Moravec C.S. and Bond M. Am J Physiol (in press).
2. Yue DT. Am J Physiol 252:H760-770,1987.

Tu-Pos48

USE OF "CAGED CALCIUM" IN SKELETAL MUSCLE TO STUDY CALCIUM-DEPENDENT INACTIVATION OF SR CALCIUM RELEASE David Hill and Bruce Simon. Dept. Physiology and Biophysics, UTMB, Galveston, TX 77550

Changes in $[\text{Ca}^{2+}]$ and charge movement were measured in frog skeletal muscle fibers (8°C) using the double vaseline gap voltage clamp. The internal solution contained 1 mM AP III as the calcium indicator, reduced $[\text{Mg}^{2+}]$ and 2 mM DM-Nitrophen, a compound which rapidly releases "caged" calcium upon photolysis with UV light. The effects of elevating $[\text{Ca}^{2+}]$ with either a prepulse or a UV flash-induced release of caged calcium on the rate of release of calcium (RREL) during a subsequent test pulse were studied. As shown previously (Schneider and Simon, 1988, J. Physiol. 405), a brief prepulse could substantially depress the inactivating component of release seen during a long test pulse, presumably by elevating $[\text{Ca}^{2+}]$ prior to the test pulse. Unexpectedly, when the same test pulse was preceded by a flash-induced elevation of $[\text{Ca}^{2+}]$ of the same magnitude as the depolarization induced release there was no depression of the test pulse. In some cases the flash-induced release potentiated the test release. Neither the prepulse nor the flash altered charge movement during the test pulse. Four possibilities will be considered: 1) $[\text{Ca}^{2+}]$ gradients exist when calcium is elevated with a prepulse but not with a flash. Thus, during the prepulse, the spatially averaged $[\text{Ca}^{2+}]$ determined from the dye may underestimate the $[\text{Ca}^{2+}]$ at the inactivation site. 2) Release channels must first open before calcium-dependent inactivation can occur. 3) DM-Nitrophen does not have access to the inactivation site. 4) inactivation does not depend on $[\text{Ca}^{2+}]$.



Tu-Pos47

THE EFFECTS OF ENFLURANE AND ISOFLURANE ON STIMULATED CHANGES IN $[\text{Ca}^{2+}]$ IN SINGLE CARDIAC CELLS.

Dixon W. Wilde, Ravi Gutta and Michael F. Haney. Dept. of Anesthesiology, University of Michigan Medical Center, Ann Arbor, MI 48109-0572

The effects of the volatile anesthetics enflurane and isoflurane on $[\text{Ca}^{2+}]_i$ were investigated in enzymatically isolated single, quiescent ventricular myocytes from the rat. Cells in suspension were loaded at room temperature with 4 μM FURA-2 AM for 10 minutes. Cells were placed in a controlled atmosphere, constant temperature superfusion chamber through which oxygenated Tyrode's solution (1.8 mM Ca^{2+}) passed. This chamber was placed on the stage of a Leitz Diavert inverted fluorescence microscope equipped with a computer driven excitation filter wheel. The wheel alternated between 340 nm and 380 nm excitation filters with a switch time of 150 msec. A fast sampling data acquisition system captured the voltage outputs from an MPV photomultiplier at a maximum rate of 40 $\mu\text{sec}/\text{point}$. Cells were stimulated in 3 ways; by superfusion with 15 mM caffeine, 50 mM K^+ or by direct, electrical membrane excitation. Anesthetics were supplied by Dräger vaporizer using 100% O_2 as carrier gas. Isoflurane reversibly reduced the caffeine stimulated Ca^{2+} transient in a dose-related manner. Isoflurane at 1% concentration reduced the caffeine transient from a control value of 170 nM to 33 nM. Enflurane had no effect on the caffeine-sensitive Ca^{2+} store at any concentration. Both isoflurane and enflurane reduced the K^+ -stimulated, tonic rise in $[\text{Ca}^{2+}]_i$. At concentrations of 0.5%, isoflurane and enflurane reduced the K^+ stimulated rise in $[\text{Ca}^{2+}]_i$ to 64 ± 10 and 55 ± 6 percent of control, respectively. Both agents were potent inhibitors of Ca^{2+} transients induced by electrical stimulation of the sarcolemma. Enflurane was more potent than isoflurane, reducing Ca^{2+} transients to 58 ± 17 percent of control at 0.25% concentration compared to 74 ± 4 percent of control by 1% isoflurane. Both anesthetics caused a significant incidence of spontaneous, phasic or tonic elevations in $[\text{Ca}^{2+}]_i$. These spontaneous events usually commenced during anesthetic washout and could be prevented or blocked by 1 mM nifedipine. The results suggest that isoflurane and enflurane affect sarcolemmal L-channel activity and may reduce $\text{I}_{\text{Ca}2}$, to cause a negative inotropic effect. Isoflurane, like halothane, appears to reduce the availability of activator Ca^{2+} from the sarcoplasmic reticulum.

Tu-Pos49

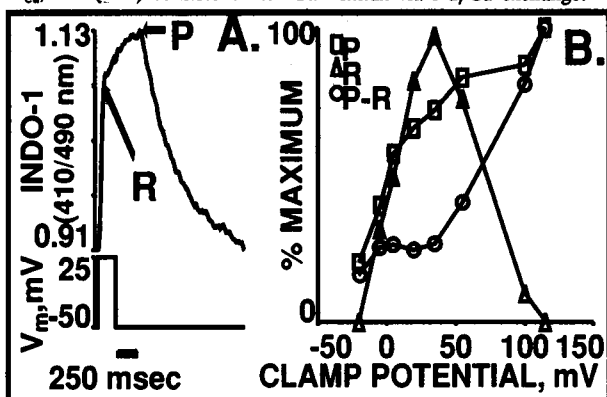
RE-EVALUATION OF THE DYNAMIC CALCIUM REQUIREMENTS FOR ACTIVATION OF RABBIT PAPILLARY MUSCLE CALCULATED FROM TENSION INDEPENDENT HEAT. Edward M. Blanchard and Norman R. Alpert, Univ of Vermont, Dept Physiology and Biophysics, Burlington, VT 05405

We have used tension independent heat (TIH) (1 mJ/g) generated by right ventricular papillary muscles of rabbits to calculate the dynamic calcium requirements for mechanical activation (Blanchard et al., 1990, Am J Cardiol 65:8G-11G). The estimated calcium turnover per twitch at 21°C, 0.2 Hz pacing rate, and 2.5 mM CaCl_2 in the Krebs solution was 52 nmol/g wet weight. One assumption underlying this calculation was that 87% of TIH was due to Ca transport by the sarcoplasmic reticulum (SR) with the remaining 13% attributable to the energy cost of electrical activation, i.e. Na transport. New experiments where TIH was measured as a function of solution calcium concentration indicate that the "Ca-independent" portion of TIH is much higher than 13% of control—about ~50% of control TIH (0.5 mJ/g) would remain if one extrapolates to zero solution calcium. This estimate of "Ca-independent" TIH is similar to the value measured by Gibbs and Vaughn (1968, J Gen Physiol 52:532-549) using different methods. Recalculation of Ca turnover with this new value for "Ca-dependent" TIH reduces the estimate for the dynamic requirements for 50% activation (determined from the twitch/tetanus ratio) to 30 nmol/g wet weight. Additional experiments measuring TIH in the absence and presence of 10 μM ryanodine support the idea that this concentration of ryanodine locks the Ca release channel of the SR in an open subconductance state. We also report that 5 mM 2,3-butanedione monoxime has no effect on SR Ca transport measured using homogenates of rabbit ventricle by the method of Pagani and Solaro (1984, Methods in Pharmacol 5:49-61). PHS 28001.

Tu-Pos50

TWO COMPONENTS OF THE CYTOSOLIC CALCIUM TRANSIENT IN SINGLE GUINEA PIG VENTRICULAR MYOCYTES. Harold A. Spurgeon, Gerrit Isenberg, Antti Talo, Michael D. Stern, Edward G. Lakatta. Gerontology Research Center, NIA, NIH, Baltimore, MD

Depolarization (-45 to +10 mV for 300 msec) of single guinea pig myocytes (23°) leads to a rapid, ryanodine sensitive increase of Ca^{2+} , Ca_i , indexed as the rapid component of the transient change in indo-1 fluorescence (R), followed by a slower increase to a peak (P) (Figure A). In the absence of pipette NaCl , both R and P exhibit a bell shaped dependence on membrane potential (-40 to +100 mV, not shown). With 10 mM NaCl in pipette, the R component retains a bell shape but the P component remains elevated at positive clamp potentials (Figure B, average of 3 cells); the difference between P and R increases monotonically with the membrane potential. The results indicate that two processes contribute to the increase in Ca_i following excitation: an R component, consistent with Ca^{2+} release from the SR induced by I_{Ca} , and (P-R) consistent with Ca^{2+} influx via Na/Ca exchange.



Tu-Pos52

Ca^{2+} MEASUREMENTS IN MYOTUBES GROWN FROM MUSCLES OF NORMAL AND DYSTROPHIC (mdx) MICE Anthony J. Bakker, Stewart I. Head, David A. Williams & D. George Stephenson, Department of Zoology, La Trobe University, Bundoora, Victoria, 3083, Australia.

Duchenne muscular dystrophy is a debilitating degenerative muscle disease that has recently been shown to be associated with the lack of the protein dystrophin. The mdx strain of mice also lack dystrophin and muscle fibres isolated from these animals have been found to exhibit elevated cytosolic free Ca^{2+} levels (Turner, Westwood, Regen & Steinhardt, 1988, *Nature*, 335: 735-738). In this study we investigated the Ca^{2+} homeostatic abilities of myotubes derived from mdx and normal murine skeletal muscle.

Cytosolic Ca^{2+} levels were measured with Fura-2 (free acid) loaded into the cells via ionophoresis. The resting membrane potential (RMP) was monitored in both groups to ensure the myotubes were at a similar stage of differentiation. The myotubes were bathed in Tyrode solution containing 2.5 mM CaCl_2 and all experiments were undertaken at room temperature (22°C).

The resting cytoplasmic free Ca^{2+} levels in mdx myotubes (151 ± 43 nM, $n=23$) (mean \pm SD) were significantly higher than those observed in control mouse myotubes (81 ± 32 nM, $n=27$) (t-test, $p < 0.001$). No significant difference was found between the RMP of mdx myotubes (-36 ± 10 mV) and the control myotubes (-33 ± 7 mV).

These results suggest that Ca^{2+} homeostasis is perturbed not only in the muscle cells from adult mdx mice but also in the mdx myotubes in culture.

Tu-Pos51

RATIOMETRIC CONFOCAL IMAGING OF pH FLUCTUATIONS IN ISOLATED CARDIAC MYOCYTES.

Stephen H. Cody, Philip N. Dubbin & David A. Williams, Department of Physiology, The University of Melbourne, Parkville, Victoria, 3083, Australia.

The coupling of laser-scanning confocal microscopy and new dual-emission fluorescent indicators for pH offers great potential for quantitative ratiometric intracellular imaging with high spatial and temporal resolution.

Individual cardiac myocytes, enzymatically isolated from rat left ventricle were loaded with the pH-sensitive fluorophore SNARF-1 (incubation with esterified derivative) at 25°C for 30 min. We employed a laser scanning confocal microscope (Biorad Lasersharp, MRC-500) configured for dual channel emission detection. Cells were excited with the 488 or 514nm band of the Argon-ion laser with the emission spectrum split to separate detectors at the isosbestic point (605nm) by a modified dichroic mirror/filter block added to the standard system. The thickness of the optical sections contributing to each detector (generally 1-5µm) was matched by using equivalent confocal apertures in the emission pathways. Image pairs were background corrected and ratio images generated by pixel-by-pixel division. Absolute intracellular pH levels were calibrated by treatment of individual cells with nigericin in high $[\text{K}^+]$ solutions.

Ratio images of SNARF-1 fluorescence in individual myocytes indicated that in the majority of cells cytosolic pH levels were relatively uniform. In the remaining cells small pH gradients existed between cytosol, nucleus and perinuclear regions. There were no significant pH changes accompanying the propagated spontaneous contractile waves that occur in these cells, confirming our previous observations with other indicators. Fatiguing electrical field stimulation (1 Hz, 50 msec, 8 nominal volts) resulted in a significant decrease in intracellular pH with a pH drop of 0.2 pH units (acidification) evident after 5 min.

These techniques provide dynamic spatial information on the intracellular pH changes occurring within single living cells.

Tu-Pos53

ABSORBANCE AND FLUORESCENCE SIGNALS FROM THE Ca^{2+} INDICATOR FLUO-3 IN INTACT TWITCH FIBERS FROM FROG MUSCLE. A. B. Harkins, Nagomi Kurebayashi, S. Hollingworth and S. M. Baylor, Department of Physiology, University of Pennsylvania Medical Center, Philadelphia, PA.

The free-acid form of fluo-3 (Minta, Kao and Tsien, 1988) was pressure-injected into single fibers and four indicator-related signals were measured (16°C): absorbance (A) and fluorescence (F) in fibers at rest, and changes (ΔA and ΔF) in response to action potential stimulation. A and ΔA were used to estimate the total fluo-3 concentration in myoplasm ($[\text{D}_T]$), the change in Ca^{2+} -fluo-3 concentration during activity ($\Delta[\text{CaD}]$), and thus the fraction of the indicator driven into the Ca^{2+} -bound form ($\Delta f_{\text{CaD}} = \Delta[\text{CaD}]/[\text{D}_T]$). From the in vitro measurement of $F_{\text{max}}/F_{\text{min}}$ (the ratio of Ca^{2+} -bound to Ca^{2+} -free F for the indicator) and the in vivo measurement of $\Delta f_{\text{CaD}}/(\Delta F/F)$, a resting value of $\sim 0.02-0.04$ was estimated for f_{CaD} . The average peak value of Δf_{CaD} was $0.30 (\pm 0.02 \text{ SEM})$, a value much smaller than expected given (i) the Ca^{2+} -fluo-3 dissociation constant measured in vitro ($0.5 \mu\text{M}$), (ii) the time course of fluo-3's ΔF signal (time to peak, 13 ms; time of half-width, 33 ms), and (iii) the amplitude (ca. $10 \mu\text{M}$) and time course (time to peak, 6 ms; time of half-width, 8-9 ms) of the myoplasmic free $[\text{Ca}^{2+}]$ transient as estimated with other Ca^{2+} indicator dyes. The results can be reconciled under the assumption that, in myoplasm, the effective dissociation constant of fluo-3 for Ca^{2+} is increased \sim ten-fold over the in vitro value. This increase is likely related to the finding that in the muscle fiber at least 70% of fluo-3 is bound to myoplasmic constituents. Nevertheless, because of fluo-3's large value of $F_{\text{max}}/F_{\text{min}}$ (20-40) and remarkable insensitivity of ΔF to changes in pH or Mg^{2+} , fluo-3 appears to report information about myoplasmic $[\text{Ca}^{2+}]$ not readily obtained with other Ca^{2+} indicators. For example, 20 s after a brief (50-200 ms) high-frequency (50-100 Hz) tetanus, $[\text{Ca}^{2+}]$ appears to be elevated by $\sim 30\%$ above its resting level of $\sim 0.1-0.2 \mu\text{M}$. This slow return of $[\text{Ca}^{2+}]$ to baseline evidently reflects processes other than the dissociation of Ca^{2+} from parvalbumin, for which the rate constant at 16°C is about 0.8 s^{-1} (Hou et al., 1990).

Supported by NIH 17620.

Tu-Pos54

A METHOD FOR $[Ca^{2+}]_i$ QUANTIFICATION USING AEQUORIN IN THE DOG HEART CONTINUOUSLY PERFUSED WITH BLOOD.

K. Harada, A. J. Meuse, Y. Kagaya, A. Franklin, R. G. Johnson, R. Weintraub, W. Grossman and J. P. Morgan. Harvard-Thorndike Laboratory, Beth Israel Hospital, Boston, MA 02215.

Aequorin (AEQ), a bioluminescent Ca^{2+} indicator, has been successfully used for the detection of intracellular calcium ($[Ca^{2+}]_i$) levels in various preparations. We have previously described a method for recording $[Ca^{2+}]_i$ in the buffer-perfused dog heart (Biophys J, 57:173a). In order to establish the method in a large animal model under more physiologic conditions, we used the isolated dog heart continuously perfused with blood (30°C) and directly measured the absolute values of $[Ca^{2+}]_i$. In 8 dog hearts, AEQ was introduced by macroinjection into a 15 mm² area of LV subepicardium during blood perfusion at 30°C. No interference by blood with recording the light signal was detected in these experiments. Simultaneous recordings were made of ECG, LV pressure, perfusion pressure, and AEQ generated light signals.

Results: 1) $[Ca^{2+}]_i$ was calculated using the fractional luminescence technique: diastolic $[Ca^{2+}]_i$ levels were 0.30 ± 0.10 μ M and peak systolic $[Ca^{2+}]_i$ were 0.64 ± 0.13 μ M. The beat-to-beat changes of the light signals were shown during short term force-frequency responses. 2) Peak systolic $[Ca^{2+}]_i$ levels linearly responded to the extracellular calcium levels. 3) Isoproterenol increased the peak systolic $[Ca^{2+}]_i$, but shortened the time course of the transient. 4) $[Ca^{2+}]_i$ increased to micromolar levels during transient global ischemia, returning to the baseline values upon reperfusion.

Conclusions: These data confirm the qualitative changes and quantitative values reported for $[Ca^{2+}]_i$ in the buffer-perfused ferret heart (Circ Res 1989; 65:1029). Moreover, our results indicate that the aequorin-loaded blood perfused dog heart is a suitable large animal model for studying the effects of ischemia/hypoxia and ventricular fibrillation on $[Ca^{2+}]_i$ handling. (Support: HL-31117, HL-01611, HL-07371, and a Grant-in-Aid and Fellowship from the American Heart Association)

Tu-Pos56

CALCIUM CURRENTS AND CALCIUM TRANSIENTS DURING EXCITATION CONTRACTION COUPLING IN GUINEA PIG VENTRICULAR MYOCYTES.

JORGE ARREOLA, ROBERT T. DIRKSEN, RU-CHI SHIH, DANIEL J. WILLIFORD AND SHEY-SHING SHEU. Department of Pharmacology, School of Medicine and Dentistry, University of Rochester, Rochester, NY 14642.

Heart excitation-contraction coupling is triggered through the opening of Ca^{2+} channels by membrane depolarization. Furthermore, sarcoplasmic reticulum Ca^{2+} release is dependent upon the magnitude and kinetics of the Ca^{2+} current (I_{Ca}). Therefore, precise knowledge of trans-sarcolemmal Ca^{2+} influx and the type(s) of Ca^{2+} channel(s) involved during the physiologic action potential (AP) is essential to completely understand both processes. We characterized the properties of the I_{Ca} using a voltage clamp protocol that simulates an AP. I_{Ca} shows a fast activation during the upstroke of the AP, followed by a slow component during the AP plateau. Maximum I_{Ca} was 7.62 ± 1.03 pA/pF for the fast component and 2.88 ± 0.45 pA/pF for the slow component. Maximum Ca^{2+} conductance was 195 ± 24 pS/pF. The maximum flux of Ca^{2+} through Ca^{2+} channels was $1.75 \pm 0.25 \times 10^{-18}$ moles/pF. L- and T-type Ca^{2+} channels are both activated by the AP clamp. Fura-2 fluorescence measurements of the Ca^{2+} transient confirm a Ca^{2+} -induced Ca^{2+} release by I_{Ca} . In addition, β -adrenoceptor stimulation enhances both the fast (69%) and the slow component (88%) of the I_{Ca} . The increase in I_{Ca} by isoproterenol is associated with an increase in the amplitude ($56 \pm 18\%$) and an acceleration of the relaxation phase (50% relaxation time change from 0.41 ± 0.05 s in control to 0.22 ± 0.04 s with isoproterenol) of the Ca^{2+} transient. In conclusion, the AP clamp allows the characterization of the relationship between I_{Ca} and Ca^{2+} release under a more physiologic condition. J.A. supported by AHA (88-120F).

Tu-Pos55

CHANGES OF INTRACELLULAR CALCIUM AND pH DURING FATIGUE IN ISOLATED MOUSE MUSCLE FIBRES.

David G. Allen and Håkan Westerblad, Department of Physiology, F13, University of Sydney, N.S.W. 2006, Australia.

The decline of tension during repetitive activity in skeletal muscle has frequently been attributed to increased concentrations of hydrogen and phosphate ions. These ions may depress tension both by reducing the maximum Ca^{2+} -activated force and by reducing the Ca^{2+} -sensitivity of the contractile proteins. We have studied the role of reduced intracellular pH (pH_i) for the tension reduction in fatigue produced by repeated tetanic stimulation of intact, single fibers dissected from a mouse muscle. pH_i and the myoplasmic Ca^{2+} concentration ($[Ca^{2+}]_i$) were measured with the fluorescent dyes BCECF and fura-2, respectively; maximum Ca^{2+} -activated tension was assessed by tetanic activation in the presence of 10 mM caffeine. In the fatigued state tetanic tension in the presence of caffeine was reduced by about 20% and the $[Ca^{2+}]_i$ required to obtain 50% of the original tetanic tension was almost doubled. pH_i declined by only about 0.1 units during fatiguing stimulation and thus reduced pH_i appears to be of minor importance for the tension reduction. Using skinned skeletal muscle fibers, Godt and Nosek (1989; J Physiol 412, 155-180) have shown that an elevation of the phosphate ion concentration to 15 mM causes a reduction of the maximum tension and the Ca^{2+} -sensitivity similar to those observed here. We therefore suggest the present findings to be due to increased phosphate ion concentration.

Fatigued fibers (tetanic tension reduced to about 30% of the original) also showed a reduced tetanic $[Ca^{2+}]_i$. Thus, in addition to the depression of maximum tension and Ca^{2+} -sensitivity, the tension reduction in severe fatigue is caused by impaired Ca^{2+} release from the sarcoplasmic reticulum.

Tu-Pos57

DIABETES-RELATED CHANGES IN CELL LENGTH AND FREE MYOPLASMIC CALCIUM DURING CONTRACTION IN ISOLATED RAT MYOCYTES.

F.M. Siri, R. Aronson, E. Sonnenblick and F. Fein. Albert Einstein College of Medicine, Bronx, New York.

Diabetes generally slows myocardial contraction, although peak shortening is often preserved. The cellular basis for this abnormality was examined by measuring myoplasmic free calcium (Ca), using Fura-2, and cell length (L) in single myocytes isolated from control rat hearts (C) and from hearts of diabetic rats (D). Myocytes were driven at 1 Hz in normal Tyrode's (2.4 mM $CaCl_2$), while perfused at either 30°C or 37°C. 12 cells from 3 control hearts and 12 cells from 3 diabetic hearts were assessed. In each group 6 were studied at 30°C and 6 at 37°C. Means \pm S.D.:

	TEMP	dCa/dt	dL/dt	TCa	TSHORT	PEAK Ca	PSHORT
C	30	13 \pm 4	1.22 \pm .52	40 \pm 9	156 \pm 32	250 \pm 53	10 \pm 4
D	30	9 \pm 2	1.12 \pm .39	77 \pm 36	160 \pm 19	199 \pm 59	11 \pm 4
C	37	13 \pm 9	1.17 \pm .75	32 \pm 13	88 \pm 8	219 \pm 156	6 \pm 4
D	37	9 \pm 2	0.48 \pm .40	46 \pm 23	100 \pm 31	124 \pm 53	4 \pm 3

Diabetes tended to reduce estimated Ca at the peak of contraction (PEAK Ca) and to cause a greater decrease in peak shortening (PSHORT, %) with increased temperature, but these changes were not significant. Time from onset of contraction to PEAK Ca (TCa, ms) was significantly prolonged by diabetes, and time to PSHORT (TSHORT, ms) showed a similar trend. Maximal rate of Ca rise (dCa/dt, nM/ms) was significantly slower in D, corresponding to a similar, but non-significant trend in maximal rate of cell shortening (dL/dt, cell lengths/s). Perfusion at 37°C significantly reduced PSHORT, TCa and TSHORT in C and D, and tended to reduce dL/dt in D. All significances by F-test, $P < 0.05$. These data demonstrate that diabetes significantly slows the Ca transient in single myocytes. These changes in Ca kinetics are accompanied by similar trends in contraction. Further studies are needed, using inotropic agents and other drive rates, to assess the full range of myocyte contractile abnormalities with diabetes, and their correlation with the Ca transient.

Tu-P058

THE RELATIONSHIP BETWEEN MEMBRANE POTENTIAL AND CALCIUM RELEASE IN MALIGNANT HYPERTHERMIA SUSCEPTIBLE SKELETAL MUSCLE MEASURED BY FURA2-AM AND CALCIUM SELECTIVE MICROELECTRODES

J.R. Lopez, M. Alfonso and P.D. Allen; CBB, IVIC Caracas Venezuela and Dept of Anesthesia, Brigham & Women's Hospital, Boston, MA 02115

Malignant Hyperthermia (MH) is a pharmacogenetic myopathy triggered by inhalational anesthetics and depolarizing muscle relaxants. We have studied the relationship between membrane depolarization induced by sub-contraction concentrations of potassium (K^+) and calcium release measured by means of the fluorescent dye FURA2-AM (F2AM) and calcium selective microelectrodes (CSM). Intact intercostal muscle bundles were removed under ketamine-pentothal anesthesia from Control (Yorkshire) swine and MH susceptible (Pietrain) swine. The resting $[Ca^{2+}]_i$ in MH skeletal fibers was 300 ± 20 nM ($M \pm SEM$, $n=10$) measured by CSM and 80 ± 10 ($n=16$) by F2AM. Determinations of V_m and $[Ca^{2+}]_i$ by CSM in the presence of K^+ 10mM showed a partial depolarization (-62 ± 3.24 mV) which was associated with an increment in $[Ca^{2+}]_i$ to 1330 ± 200 nM ($n=8$). Determination of $[Ca^{2+}]_i$ with F2AM showed a $[Ca^{2+}]_i$ of 310 ± 50 nM ($n=13$). Experiments conducted in control skeletal muscle showed qualitatively but not quantitatively similar results. Sarcoplasmic $[Ca^{2+}]_i$ was increased in the presence of high extracellular K^+ by a factor of 2.9 instead of the factor of 4.3 observed in MH susceptibles. These results show for the first time that the amount of calcium release in response to sub contraction K^+ in MHS fibers is greater than in control which might be related to some alteration in the coupling mechanism between the t-tubule and the sarcoplasmic reticulum. In addition, it shows that determination of $[Ca^{2+}]_i$ using F2AM seems to underestimate $[Ca^{2+}]_i$. (Supported by NSF and Angelini Pharmaceuticals.)

Tu-P059

EARLY AND LATE ANTIPYRYLAZO III SIGNALS CONSISTENT WITH DECREASED MYOPLASMIC $[Mg^{2+}]$ DURING AND AFTER DEPOLARIZATION OF FROG SKELETAL MUSCLE FIBERS. V. Jacquemond, M.G. Klein and M.F. Schneider, Dept. of Biological Chemistry, Univ. of Maryland Sch. of Medicine, Baltimore, MD 21201

Cut segments of single fibers containing both fura-2 and antipyrilazo III (AP III) were voltage clamped in a double Vaseline gap (holding $V = -100$ mV, $3.8-4.5$ μm /sarcomere, $8-10^\circ C$). Absorbance signals at 700 and 590 nm were corrected for intrinsic components (recorded at 850 nm) and used to calculate myoplasmic $[Ca^{2+}]$ and $[Mg^{2+}]$ transients. Control 590 nm absorbance records exhibited a small continuous increase with time due to dye entry from the end pool solution. 200 ms depolarizing pulses to 0 or +20 mV produced large positive $\Delta[Mg^{2+}]$ signals, presumably due to Ca^{2+} for Mg^{2+} exchange on parvalbumin during elevated $[Ca^{2+}]$. Well after the pulse a negative phase of $\Delta[Mg^{2+}]$ was often observed. In 27 fibers mean $\pm SEM$ $\Delta[Mg^{2+}]$ 24 s after the pulse declined to -25 ± 4 μM , even after correction for the small increase in 590 nm absorbance due to dye entry. $\Delta[Mg^{2+}]$ remained negative for records up to 45 s long. $\Delta[Mg^{2+}]$ signals were also monitored in fibers heavily injected with BAPTA to eliminate the rise in $[Ca^{2+}]$ during the pulse (Jacquemond et al, these abstracts) and the consequent rise in $[Mg^{2+}]$. In 7 out of 13 fibers containing sufficient BAPTA to suppress $\Delta[Ca^{2+}]$ to $< 10\%$ of the pre-injection control we observed an early decrease in $[Mg^{2+}]$ during 200 ms depolarizing pulses. In principle, both the early and late changes could be due to an increase in myoplasmic $[H^+]$. However, both changes were observed in fibers containing the pH buffer PIPES as major anion in the internal solution. If the signals reflect a decline in $[Mg^{2+}]$ they could be due to Mg^{2+} entry into the sarcoplasmic reticulum (Somlyo et al, J. Biol. Chem., 260:6801, 1985) in exchange for some of the released Ca^{2+} .

Tu-P059

CALCIUM RELEASE IMAGING OF THE CROSS SECTION OF ISOLATED SKELETAL MUSCLE FIBERS FROM THE FROG. M. Rozycka and H. Gonzalez-Serratos. Biophysics Department, Univ. of Maryland School of Medicine, Baltimore, MD 21201

Fluorescence image analysis of skeletal muscle cells done from views taken from a plane parallel to the long axis of the muscle fibers, as is done with commercially available microscopes, has serious drawbacks: a large component of the fluorescence image come from out of focus fluorescence (above and below the plane of focus) and the lens effect produced by the quasi cylindrical shape of the muscle cell. To avoid these problems, an optical system has been built with which cross section images perpendicular to the long axis are obtained. The optical system consisted of a 150 W xenon lamp with a collecting lens, a variable slit placed in front of the collecting lens. A sharp image of the slit was created at the plane of the object position at 90° in respect to the long axis of the muscle cell. A second variable slit placed at the focal plane of the condenser permits the control convergence of light on the fiber. By choosing the proper combination of numerical apertures and focal lengths of the collecting and condenser lenses, one can optimize the size, intensity and minimum degree of blurring of the illuminating area. The optical axis of a viewing microscope fitted with an image intensifier and a CCD camera is placed along the long axis of the fiber. To avoid light absorption by the muscle tendon, the fibers were bent 90° in front of the viewing microscope. The cells were loaded with the Ca indicator fluo-3 (AM form) and the magnitude and fluorescence images of Ca releases was collected in a magnetic disc. The excitation and barrier filter combination were 510 and 518 nm respectively. With this optical system clear images of Ca release from the cross section area were obtained. They showed that Ca release was not homogenous in the cross section. The degree of heterogeneity depended on whether Ca was released by electrical stimulation, caffeine exposure or K depolarization. The maximal fluorescence needed to calculate $[Ca^{2+}]$ was done in situ at the end of the experiment with a 20 mM Ca solution containing 0.1 mM of the A-23187 calcium ionophore. (Supported by a grant from the NIH RO1 NS17048).

Tu-P061

SPATIAL DISTRIBUTION OF Ca^{2+} SIGNALS VISUALIZED BY CONFOCAL MICROSCOPY IN INTACT ISOLATED CARDIAC MYOCYTES. Santi, C. and Hernández-Cruz, A. Dept. Biophysics. Sch. of Med. Montevideo, Uruguay and Dept. Neurosci., Roche Inst. Mol. Biol. Nutley NJ, 07110 USA.

Depolarization-induced intracellular $[Ca^{2+}]$ transients in cardiac myocytes result from 1) Ca^{2+} influx through sarcolemmal voltage-gated channels, 2) Ca^{2+} release from sarcoplasmic reticulum (SR) and 3) Ca^{2+} influx through Na^+/Ca^{2+} exchanger operating in reverse mode. Here we examine whether the spatial distribution of Ca^{2+} signals varies when the contribution of these sources of Ca^{2+} is preferentially activated or inhibited.

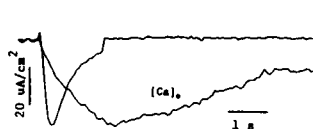
We used laser confocal microscopy of fluo-3-loaded guinea pig cardiac myocytes to obtain digital fluorescence images and spatially averaged recordings of variations in $[Ca^{2+}]_i$ associated to brief (50 ms to 2 s) membrane depolarizations with pulses of high K^+ . Ratio images obtained by dividing stimulated over resting cell images (S/R ratio) revealed large spatial heterogeneities, with different regions sometimes exhibiting four-fold differences. The largest changes apparently occurred near the cell membrane and in regions of lower resting fluorescence. The mean S/R ratio values varied considerably from cell to cell (range 1.06 to 2.01; mean 1.446 ± 0.067 S.E.; $n = 16$). On average, ryanodine (20 μM) reduced by $42 \pm 6.2\%$ the stimulus-associated changes in Ca^{2+} (range 22 to 64 %; $n = 7$). By comparison verapamil (10 μM) reduced these changes by 80 % (range 69 to 84 %; $n = 5$). The overall spatial distribution of Ca^{2+} changes was not significantly affected by these maneuvers. The small Ca^{2+} transient remaining in the presence of verapamil and ryanodine suggest a modest contribution of the Na^+/Ca^{2+} exchanger (less than 15%) under normal conditions. However, its contribution increased considerably during exposure to 30 μM ouabain or low external Na^+ , presumably because of a shift in the equilibrium potential for the exchanger. TTX (20 μM) did not reduce the mean S/R ratio, either in normal cells or in cells exposed to verapamil and low Na^+ . Therefore our results do not support a Ca^{2+} release from the SR triggered by Na^+ influx through TTX sensitive Na^+ channels.

Tu-Pos62

EXTRACELLULAR CALCIUM TRANSIENTS IN SKELETAL MUSCLE OF THE FROG

Sándor Györke and Philip Palade, Dept. Physiology and Biophysics, UTMB, Galveston, TX 77550

The low affinity Ca^{2+} indicators tetramethylmurexide (TMM) and carboxyarsenazo (CA) were used to measure changes in extracellular Ca^{2+} concentration in single voltage-clamped cut fibers and whole intact muscles optically. In cut fiber experiments external solutions contained 2.2 mM TMM or 8 mM CA, 5 mM Ca^{2+} and 115 mM TEA MeSO_3 ; the internal solution contained 10-70 mM Cs_2EGTA (to prevent movement), 3 mM MgATP, 5 mM Na_2PCr and 100-10 mM CsAsp. On application of depolarizing pulses which elicited I_{Ca} , a slow transient decrease in external $[\text{Ca}^{2+}]$ was measured (see Fig.). The time course of the falling phase and the amplitude of the signals correlated closely with the time



course and amplitude of the I_{Ca} , indicating that the optical signals represent depletion of Ca^{2+} from T-tubules during I_{Ca} . No significant regular changes in $[\text{Ca}^{2+}]_o$ have been measured in whole

muscles kept in Ringer solution with 0.5 mM Ca^{2+} , 3 mM Mg^{2+} and 2.2 mM TMM or 2 mM Ca^{2+} and 5 mM CA during low or high frequency prolonged direct extracellular electrical stimulation. The signal was measured simultaneously at two different wavelengths and corrected for movement artifacts. According to estimates made from the size of the T-tubular Ca transients in single fibers, alterations in T-tubular Ca^{2+} concentration in whole muscle during prolonged activity must be less than 0.1 mM. This makes it unlikely that fatigue is caused by accumulation or depletion of Ca^{2+} in the T-system.

Tu-Pos64

INFLUENCE OF ENDOTHELIN ON INTRACELLULAR Ca^{2+} TRANSIENTS AND CONTRACTIONS IN AEQUORIN-LOADED FERRET MYOCARDIUM.

JX Wang, G Paik, ZH Qiu, AJ Meuse and JP Morgan, Department of Medicine, Harvard Medical School, Boston, MA 02215.

The Ca^{2+} -sensitive bioluminescent indicator aequorin (AEQ) was chemically loaded into ferret papillary muscles ($n=20$). Endothelin (ET) [3×10^{-9} M to 10^{-7} M] produced dose-dependent increases in the AEQ signal (avg. 31%) and force generation (avg. 64%). The peak AEQ light (Peak $[\text{Ca}^{2+}]_i$)-peak tension curve generated by varying ET concentrations was steeper and shifted to the left (Compared to the curve generated by varying $[\text{Ca}^{2+}]_o$). The effect of ET on the amplitude of the AEQ signal was much less than the effect of $[\text{Ca}^{2+}]_o$ for similar levels of increased force generation. In another way, 10^{-7} M ET shifted the peak AEQ light-peak tension curve (generated by varying $[\text{Ca}^{2+}]_o$) upward and the maximum activated force was also increased about 12%. The contractions were prolonged while the time course of the Ca^{2+} transient was not changed in the presence of ET. The function of the sarcoplasmic reticulum (SR) was decreased in the presence of 6 μM ryanodine while 10^{-7} M ET increased the force generation (avg. 40%) without increasing the intracellular peak Ca^{2+} either during isometric twitches or during tetanus. In addition, β -receptor blockade with (\pm)-bupranolol (3×10^{-7} M) or α_1 -receptor blockade with prazosin (5×10^{-8} M) did not influence the effect of ET on Ca^{2+} transients and/or force generation. In saponin-skinned preparations ET did not exert these myocardial effects. These results suggest that the positive inotropic and negative lusitropic effects of ET on intact ferret myocardium are predominantly due to an increase in the Ca^{2+} -sensitivity of the myofilaments although Ca^{2+} release from SR is also increased. We postulate that an ET receptor-second messenger pathway may be the mechanism by which ET exerts its myocardial effects. (Support: HL-31117, HL-01611, HL-07371, and a Grant-in-Aid and Fellowship from the American Heart Association)

Tu-Pos63

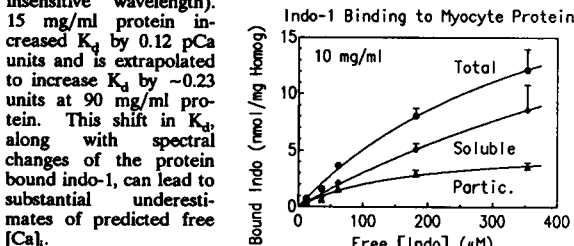
HETEROGENEOUS DISTRIBUTION OF THE INTRAMITOCHONDRIAL Ca^{2+} CONCENTRATION AND MEMBRANE POTENTIAL IN CULTURED NEONATAL RAT VENTRICULAR MYOCYTES. MEI-JIE JOU, LAN BO CHEN AND SHEY-SHING SHEU. Department of Pharmacology, University of Rochester School of Medicine and Dentistry, Rochester, NY 14642 and Dana Farber Cancer Institute, Harvard Medical School, Boston, MA 02115.

Morphological and biochemical studies have shown that within a cardiac myocyte there are several different populations of mitochondria, which may serve different physiological functions. This study demonstrates that the intramitochondrial free Ca^{2+} concentration ($[\text{Ca}^{2+}]_m$) and membrane potential (m.p.) are quite heterogeneous in neonatal rat ventricular myocytes after two weeks of culture. The distribution of $[\text{Ca}^{2+}]_m$ and m.p. was revealed by fura-2 fluorescence digital imaging microscopy and a tetrachloro-1,1',3,3'-tetraethylbenzimidazole carbocyanine iodide (denoted JC-1, Polaroid Co., Cambridge, MA) respectively. Above a certain concentration, monomers of JC-1 form a nematic phase (J-aggregates). The monomers fluoresce in the green and the J-aggregates in the red range. In fluorescent ratio images of fura-2, we found the highest Ca^{2+} concentration was originated from the mitochondria located at perinuclear area. The intermediate level of Ca^{2+} concentration was originated from the mitochondria located in the intermyofibrillar space or underneath the sarcolemmal membrane. In fluorescent JC-1 images, the mitochondria in the perinuclear region showed mostly in green color which indicated the m.p. was low. However, the mitochondria from the intermyofibrillar space or subsarcolemmal area showed mostly in red color which implied the m.p. was high. We conclude that there are at least two populations of mitochondria in cultured neonatal rat ventricular myocytes. The mitochondria that possess higher concentrations of Ca^{2+} appear to have lower membrane potential.

Tu-Pos65

INDO-1 IN VENTRICULAR MYOCYTES IS MOSTLY BOUND TO PROTEIN AND HAS ALTERED Ca BINDING PROPERTIES. *L. Hove-Madsen & D.M. Bers, Division of Biomedical Sciences, Univ. of Calif., Riverside, 92521 and *Univ. of Aarhus, 8000 Aarhus C, Denmark.

The fluorescent calcium indicator Fura-2 has been shown to bind significantly to cellular protein in skeletal muscle, causing a change in spectral characteristics and the K_d for Ca (Konishi *et al.*, *Biophys J* 54: 1089-1104, 1988). We studied the binding of indo-1 to soluble and particulate protein extracted from cardiac myocytes. We incubated homogenate with indo-1 and measured the distribution of indo-1 in protein fractions obtained by centrifuging the homogenate (177,000xg, particulate pellet) and filtration of the resultant supernatant (10 kDa cutoff, soluble protein). Parallel measurements with ^{14}C -sucrose (assumed not to bind to protein) allowed correction for free indo-1 trapped in the particulate and soluble protein fractions. Increasing homogenate protein with excess indo-1, caused a linear increase in both fluorescence anisotropy and indo-1 binding to protein. Binding of indo-1 to soluble and particulate fractions obtained from 10 mg total homogenate protein/ml at increasing free [indo-1] is shown in the figure. Assuming a total of 90 mg/ml protein inside a cardiac myocyte dialysed with a 100 μM indo-1 solution, 449 μM indo-1 or 82% of the total indo-1 is estimated to be bound. Thus, the $[\text{Ca}]_i$ buffering effect of 100 μM indo-1 in a patch pipette may be much greater than expected. The change in K_d for Ca binding to indo-1 was determined at different protein concentrations. Free $[\text{Ca}]$ was controlled by a 1mM EGTA buffer and monitored with calcium sensitive minielectrodes. The K_d was computed from the ratio of fluorescence at 480/445 nm (where the latter is a Ca -insensitive wavelength).



Tu-Pos66

EVIDENCE FOR THE BEAT-DEPENDENT ACTIVATION OF THE Na/Ca EXCHANGER IN HEART BY Ca_i

Robert A. Haworth, Atilla B. Goknur, Douglas R. Hunter (Intro. by H. Komai)

Department of Anesthesiology, University of Wisconsin, Madison WI 53792 USA

Electrical stimulation of isolated adult rat heart cells in suspension resulted in an accelerated rate of Na/Na exchange across the sarcolemma, as measured from ^{22}Na fluxes. Flux rates returned to normal within seconds of ceasing stimulation. The increased rate was inhibited by tetrodotoxin (TTX) or verapamil (V). The inhibition by TTX could be overcome by BAY K 8644 or isoproterenol. The stimulation-induced efflux was not inhibited by ouabain, but required extracellular Ca . Mn would not substitute for Ca .

A similar rate of ^{22}Na efflux to that induced by excitation could also be induced by KCl addition. This was inhibited by V but not by TTX.

In cells loaded with Na by incubation with ouabain in the absence of Ca , addition of low levels of Ca also induced an accelerated rate of Na/Na exchange. This was prevented by V, but V was ineffective when added after Ca . Dichlorobenzamil or ATP depletion, on the other hand, prevented and reversed the induction of Na/Na exchange by Ca .

We conclude that 1) Ca_i activates Na/Na exchange through the Na/Ca exchanger in heart, as in squid axon; 2) the extent of such Na/Na exchange is a measure of the activity of the Na/Ca exchanger; 3) the absence of such exchange in cells at rest indicates that at rest the exchanger is inactive; 4) the induction of such exchange by electrical stimulation suggests that the exchanger becomes activated by the excitation-dependent rise in Ca_i ; and 5) ionic fluxes through the exchanger during excitation are much larger than those through channels.

Tu-Pos67

Na/Ca EXCHANGE MEDIATED CONTRACTIONS IN FELINE VENTRICULOCYTES.

H. Bradley Nuss and Steven R. Houser. Temple University School of Medicine, Department of Physiology, Philadelphia, PA.

The hypothesis of this study is that calcium entry via Na/Ca exchange during depolarization is sufficient to activate contraction in feline ventriculocytes. Voltage clamp experiments were performed on isolated feline ventricular myocytes in the presence of verapamil (10^{-6} M) to block L-type calcium current with 2-4 megohm pipettes containing 20 mM Na (to enhance Na/Ca exchange activity). In one series of experiments the duration of depolarization to +60 mV from a holding potential of -40 mV was varied between 100 msec and 1000 msec. Conditioning beats to +10 mV for 500 msec (0.5 Hz) were interposed between each test pulse. The duration of contraction varied directly with the duration of depolarization. The magnitude of shortening increased as the duration of depolarization to +60 mV increased between 100 msec and 500 msec. Depolarizations longer than 500 msec did not further increase the magnitude of shortening. In a second series of experiments, cells were stimulated to contract with repeated depolarizations to +60 mV (0.5 Hz). After five depolarizations to +60 mV of 100 msec (or 500 msec) duration, the duration of the very next depolarization was increased to 500 msec (or decreased to 100 msec). In both cases, when the duration of the depolarization was changed there was an immediate change in the duration and magnitude of shortening without evidence of positive (or negative) staircase phenomenon. These results are consistent with the idea that sufficient Ca can enter the cell via Na/Ca exchange to directly activate the contractile elements.

Tu-Pos68

THE LOCOMOTION OF FISH KERATOCYTES VIEWED AS A FRACTAL PROCESS?

J. Lee, A. Ishihara and K. Jacobson. Dept. Cell Biology and Anatomy, University of North Carolina at Chapel Hill, N.C. 27599.

A new model of cell locomotion is proposed that views cell movement in an analogous way to a 2-D fluid flow. It incorporates the idea that cell movements or "flows" can be fractal processes in that they may occur in a similar way over a range of size and time scales.

Fish keratocytes move rapidly in a smooth continuous way by extension of a flat, semicircular shaped lamella. Since the shape and size of the lamella remains virtually constant during locomotion a radial "flow" is assumed to occur outwards from the perinuclear region. Vector addition of this flow to the forward movement of the cell results in flow vectors that are at a tangent to the cell edge. Computer simulation of this resultant flow predicts that points on the cell edge will exhibit a motion similar to that of a vortex pair. Thus points on the cell edge to the right of the line of cell movement appear to move in a clockwise direction while those to the left move in an anticlockwise direction. Experimental observations of surface ridges and ventral regions of close cell contact to the substratum both display this behavior in locomoting cells. In addition the edge of the extending lamella appears to be composed of a number of smaller similar shaped edges which are composed of yet smaller self similar parts. This supports the idea that lamellar extension is a fractal process since it is occurring over a range of size scales during locomotion. This approach could offer a way of unifying observations at the molecular and cellular levels and so lead to a major advance in our understanding of cell locomotion. Supported by NIH GM35325 and the International Human Frontier Science Program Organisation.

Tu-Pos70

A SENSITIVE MEASURE OF NEUTROPHIL CORTICAL TENSION. R. M. Hochmuth and D. Needham, Department of Mechanical Engineering and Materials Science, Duke University, Durham, N. C. 27706.

The current view of the "passive" neutrophil is that an outer cortex surrounds a viscous cytoplasm and that this cortex maintains a small persistent tension of ~ 0.035 dyn/cm (Evans and Yeung, 1989 Biophys J. 56:151-160). The "passive" cell is spherical and always recovers to a spherical shape after large deformation. This behavior contrasts with the formation of solid-like projections that are associated with pseudopod activity and cell "activation". The origin of the cortical tension is at present unknown, but indications are that it may be related to the sensitivity of a given cell to external stimulation and the "passive - active" transition. In order to characterize further this feature of the neutrophil we have developed a sensitive measure of cortical tension as a function of area dilation of the highly ruffled membrane. A single cell is aspirated into a slightly tapered pipet and allowed to recover to its resting spherical shape in the larger lumen of the pipet. An extremely small positive pipet pressure (10 dyn/cm²) is then applied and the cell is driven down the pipet until it comes to rest in the taper. A step increase in pipet pressure drives the cell to a new equilibrium position. Several such equilibrium measurements are made on a given cell with increasing pipet pressure. Each equilibrium position represents a balance between the cortical tension in the membrane and the pressure drop across the cell. Membrane tension is calculated at each pressure as a function of membrane area dilation. Initial experiments show that for area dilations of $\sim 30\%$ the cortical tension ranges from 0.01 dyn/cm to 0.06 dyn/cm. It can be constant for some cells but has also been observed to increase by a factor of two for other, apparently "passive", cells. We are currently evaluating the response of neutrophils to various agents, including cytochalasin D, in an attempt to obtain a truly "passive" baseline as a control for F-actin polymerization and cell "activation". Supported by NIH-HL23728

Tu-Pos69

NANOMETER-SCALE MAMMALIAN CELL MOTIONS MEASURED ELECTRICALLY. C.R. Keese and I. Giaever, School of

Science, Rensselaer Polytechnic Institute, Troy, NY 12180

Mammalian fibroblasts are cultured on small gold electrodes carrying weak AC current. When cells attach and spread on these surfaces, the electrode impedance at 4000 Hz increases by as much as a factor of 7 for confluent layers. When the impedance is tracked as a function of time, fluctuations are observed that are a direct measure of cell motions*. Surprisingly, these fluctuations continue even when the cell layer becomes confluent. To understand the type and magnitude of motion being detected we have modeled the interaction of cultured cells with the electrode surface in detail. The main point of the model is that current can flow underneath the cells at low frequencies, and at high frequencies a substantial fraction of the current flows through the cells because of the capacitance of the cell membranes. This model accurately describes the impedance of the cell-covered electrode as a function of the applied AC frequency from 10 Hz to 100,000 Hz. By comparing the measured impedance fluctuations with those calculated, it is clear that average motions of the cell layer of the order of one nanometer can be inferred from these measurements.

*Giaever, I. and C.R. Keese, *Physica D* 38, 128-133 (1989)

Tu-Pos71

The Change of Spectrin Distribution by Treatment with Unsaturated Free Fatty Acids is Correlated with Membrane Organization in Lymphocytes. Merek Langner, Frank D. Stephen, Sek-Wen Hui*, and Elizabeth A. Repasky. Departments of Molecular Immunology and Biophysics*. Roswell Park Cancer Institute, Buffalo, NY 14263.

Spectrin, a major component of the erythrocyte cytoskeleton, is found in various distribution patterns among lymphocytes (Repasky *et al.* JCB 99: 350, 1984; Black *et al.* JCB 106: 97, 1988). It is seen as a large cytoplasmic aggregate in some resting lymphocytes while in others it is associated with the cell membrane. It has previously been shown that treatment of tissue derived lymphocytes with various unsaturated free fatty acids (uFFA) results in a change in the distribution of some cytoskeletal proteins. Actin, α -actinin, myosin, and tubulin have been shown to be reorganized after uFFA treatment (Hoover *et al.* Mole. Cell Bio. 1: 939, 1981). We have shown that this treatment causes the disruption of spectrin aggregates in tissue derived lymphocytes as well as in an established T cell hybridoma, DO11.10, in which almost all cells express their spectrin in the aggregated form. This effect was not seen using a saturated FFA, stearic acid. We have utilized fluorescent techniques to ascertain the membrane organization of the lymphocyte after treatment with uFFA. Using pyrene-phosphotidylethanolamine excimer/monomer ratio, MC 540 fluorescence enhancement, and pyrene-phosphotidylcholine quenching with rhodamine-6G as determinants of FFA perturbation of lymphocyte membranes, we have found that treatment of DO11.10 cells with 10 μ g/ml of uFFA e.g. linoleic, oleic, arachidonic, and elaidic acid is sufficient to cause significant changes in measured membrane parameters whereas saturated free fatty acids, such as stearic and nonadecanoic do not. From these results, we hypothesize that a change in the distribution of a cytoskeletal protein, in this case spectrin, can be correlated with changes in the plasma membrane. Supported by NIH grant AI26612.

Tu-VCR2

MYOSIN-I MOVES ACTIN FILAMENTS OVER A PURE LIPID SUBSTRATE. Henry G. Zot and Thomas D. Pollard Johns Hopkins Medical School. Baltimore MD.

Acanthamoeba myosin-I binds to glass coated with nitrocellulose or a phospholipid bilayer and moves fluorescent actin filaments in the assay of Kron and Spudich (1986, *PNAS* 83:6272). Actin filaments bind to these myosin-I-treated surfaces in the absence of ATP, but gliding movements require both ATP and myosin-I heavy chain kinase. The velocity of gliding was 0.7 $\mu\text{m}/\text{sec}$ over both surfaces. During the assay new motile filaments continuously attached to the lipid surface but not to albumin treated nitrocellulose. This may be due to a reversible association of myosin-I with the lipid. After exposure of albumin coated glass to myosin-I, some actin filaments bound but did not move even with kinase and ATP. Interaction with membranes has a major effect on the actin-activated ATPase of myosin-I. Myosin-I alone is highly activated by low concentrations of actin filaments due to the crosslinking of filaments that results from an ATP-insensitive actin binding site on the tail of myosin-I (Lynch, T.J. et al., 1986, *JBC* 261:17156). The presence of NaOH stripped amoeba membranes eliminates the activation of the ATPase at low actin concentrations, presumably by preventing crosslinking, but not at high actin concentrations. These reconstitution experiments establish that myosin-I, myosin-I kinase, actin filaments, ATP, and a lipid bilayer constitute the minimum requirements for myosin-I mediated movement of actin filaments and membranes relative to each other.

Tu-Pos72

CALSEQUESTRIN POSSESSES HIGH-AFFINITY Ca^{2+} -BINDING AS REVEALED BY THE USE OF AN AMINO-REACTIVE COVALENT FLUORESCENCE PROBE. E. Ullmann, M. Végh and L. G. Mészáros, Semmelweis Univ. Med. School; Dept. of Biochem., 1088. Budapest, Hungary

Calsequestrin (CS) is an intraluminal protein found in the terminal cisternae of the sarcoplasmic reticulum (SR). Since being capable of binding a large amount of Ca^{2+} (~40 mol/mol) with low affinity ($K_d=1 \text{ mM}$), CS is believed to function as a Ca^{2+} -buffer in the SR lumen. Our results reported here suggest, however, that CS also has high-affinity Ca^{2+} -binding sites(s).

Purified CS (containing only a few % of contaminating proteins as analyzed by electrophoresis) was labeled with a covalent fluorophore (Succinimidyl-12-(N-methyl-N-(7-Nitrobenz-2-oxa-1,3-diazol-4-yl)) aminododecanoate). The labeled protein was identified as CS by determining twelve amino acid residues of the N-terminal sequence. The facts that 1) the time course of the increase in fluorescence intensity upon incorporation of the probe into CS was monophasic and 2) that only one cyanogen-bromide fragment carried the fluorescence label suggest that only a single lysine residue was modified. Furthermore, since the fluorescence of the probe, besides increasing in its intensity, was slightly red-shifted upon reacting with the $-\text{NH}_2$ group on the protein, the reactive lysine most probably sits in a hydrophobic environment within the polypeptide. The fluorescence intensity of the probe attached to CS was altered in a Ca^{2+} -dependent fashion: in addition to the low-affinity Ca^{2+} -binding sites, the titration curve also revealed the existence of a previously not detected Ca^{2+} -binding site with high affinity ($K_d=8-11 \mu\text{M}$).

This suggests that CS might play a more active role than that of simply buffering the Ca^{2+} concentration in the SR lumen.

Tu-Pos74

DIFFERENTIAL EXPRESSION OF THE RYANODINE AND INOSITOL TRISPHOSPHATE RECEPTORS, DURING MYOGENESIS. J.A. Airey, M.D. Baring, and J.L. Sutko, Department of Pharmacology, University of Nevada, Reno, NV 89557

We have investigated the expression, during myogenesis, of the intracellular calcium release channels, the ryanodine receptor (RR) and the inositol trisphosphate receptor (IP_3R), in two myogenic murine cell lines. The non-fusing BC_{3}H_1 cells, which lack MyoD1 expression, and the normally fusing C2C12 cells, which in low external calcium also do not fuse, were used. The RR is not detectable in proliferating myoblasts, maintained in high serum, in either cell line, but is seen after the concentration of the serum is lowered, and increases in abundance during differentiation. Since the RR is expressed in both fusing and non-fusing cells, neither fusion nor MyoD1, is required for the expression of the RR protein in these cells. The addition of either bFGF (90 ng/ml) or TGF- β 1 (5 ng/ml), growth factors that block differentiation, prevents the expression of the RR. In contrast to the RR, the IP_3R is expressed in proliferating BC_{3}H_1 and C2C12 myoblasts, as well as during differentiation in both the fused and non-fused cells. Additionally, neither growth factor blocked the expression of the IP_3R . The different time courses of expression of these intracellular calcium release channels suggests that they may have different roles in these two myogenic cell lines.

Tu-Pos73

NONMAMMALIAN VERTEBRATE SKELETAL MUSCLES EXPRESS TWO TRIAD JUNCTIONAL FOOT PROTEIN ISOFORMS. E. Olivares, S. Tanksley, J. Airey, C. Beck*, Y. Ouyang*, T. Deerinck*, M. Ellisman and J. Sutko. Depts. of Pharmacol., Univ. Nevada, Reno, NV 89557; *Bacteriol. and Biochem., Univ. of Idaho, Moscow, ID 83843; *Neurosci., Univ. of California, San Diego, La Jolla, CA 92093

Mammalian skeletal muscles express a single ryanodine receptor (RR) isotype, while avian muscles have two isoforms of this protein. We investigated whether either case is representative of muscles from other vertebrate classes. We identified two RR in bullfrog and toadfish muscles on the basis of (i) co-purification with [^3H]epi-ryanodine binding; (ii) similarity in size to avian muscle RR; (iii) recognition by anti-RR antibodies. The bullfrog and toadfish RR exist as homo-oligomers comprised of unique subunits. In addition, immunocytochemical localization established that the bullfrog muscle isoforms coexist in the same muscle cells. The RR isoforms in either bullfrog and chicken muscles have comparable [^3H]epi-ryanodine binding capacities; while those in toadfish muscle differ in their levels of binding. Additionally, chicken thigh and breast muscles differ in the relative amounts of the two isoforms they contain, being similar in breast muscle and markedly different in thigh muscle. In conclusion, two RR isoforms are present in amphibian, avian and piscine skeletal muscles. This may represent a general difference in the architecture and/or a functional specialization of the triad junction in mammalian and nonmammalian vertebrate muscles.

Tu-Pos75

THE M_r 95 kDa PROTEIN OF THE SKELETAL MUSCLE TRIAD JUNCTION LINKING THE DIHYDROPYRIDINE AND RYANODINE RECEPTORS IS A MULTIMER LINKED BY DISULFIDE BRIDGES. A.H. Caswell, J-P Brunschwig, K.C. Kim, and N.R. Brandt, Department of Molecular and Cellular Pharmacology, University of Miami School of Medicine, Miami, FL.

We have recently proposed that the triad junction is composed of a triad of proteins. The junctional foot protein (JFP) and the dihydropyridine receptor (DHPR) both bind to an intrinsic M_r 95 kDa protein of the sarcoplasmic reticulum terminal cisternae (TC) membrane in protein overlays. That 95 kDa protein, immobilized on Sepharose, specifically extracts the JFP, the α subunit of the DHPR and an M_r 170K Stains-All blue protein from triads dissolved in non-denaturing detergents. The 95 kDa protein interactions persist at 0.5M salt. A monoclonal antibody was prepared against the 95 kDa protein and the distribution of the antigen was determined for intact triads and subfractions of triads prepared after disruption and centrifugation. The proportion of 95 kDa protein by Elisa assays for heavy TC:strong triads:TC/triads:longitudinal reticulum:T-tubules is 27:10:10:0.7:1 while ryanodine binding in the same organelles is 24:9:10:1:1. In reducing SDS gels the protein has an M_r app of 95 kDa. On non-reducing gels, the 95 kDa protein exists almost entirely as multimers; 2 to ~12 unit homopolymers have been resolved. We have not detected in non-reducing SDS gels any binding of a biotinylated disulfide reagent at the same M_r as that of the 95 kDa protein. Dithiothreitol and β mercaptoethanol but not glutathione at 10 mM cause partial reduction in intact membranes, though reduction is still incomplete at 1 M. The sedimentation velocity of non-denatured protein in rate zonal centrifugation is a linear function of the size of the multimer, indicating that the 95 kDa protein forms polymers only by disulfide bridges. These observations strongly suggest that the 95 kDa protein exists as a disulfide-linked multimeric complex in the native TC membrane. Our data are not consistent with the triad junction being identical to a 106 kDa Ca^{2+} release channel described by Salama et al. Support by NIH grants AR 21601 and HL 36029.

Tu-Pos76

Identification of a Distinct Isoform of the 53-kilodalton Glycoprotein in Brain and Cardiac Muscle Kimberly L. Boyd, Atsushi Mizushima, and Howard C. Kutchai, Department of Physiology, University of Virginia School of Medicine, Charlottesville, VA 22908.

The 53-kilodalton glycoprotein (GP-53) exists together with sarcoplasmic reticulum Ca^{2+} -ATPase in skeletal, cardiac, and smooth muscle cells. The nucleic acid and deduced amino acid sequence of a GP-53 has been determined from the skeletal muscle (Leberer et al. *JBC*, 264: 3484-3493, 1989). However the structure and function of this widely distributed protein is not well understood. Biochemical data suggests that GP-53 is membrane associated and modulates the coupling of Ca^{2+} transport and ATP hydrolysis of the Ca^{2+} -ATPase function (Kutchai & Campbell. *Biochem.* 28: 4830-4839, 1989). In order to further elucidate the functional significance of GP-53, analysis of conserved sequences between distinct isoforms from different cell types and organisms would be useful.

We initially synthesized an oligonucleotide probe, 5'-A-ATT-(G/C)CT-ICA-IAC-IGT-IAC-CAA-ITA-3', corresponding to amino acids #187-#195 of the rabbit skeletal muscle GP-53. Since this probe did not hybridize to any tissue RNA isolated from chicken, using this oligonucleotide probe we obtained a rabbit partial cDNA clone (1.9kb cDNA encoding from amino acid #146 to #454 of GP-53) by screening a rabbit skeletal muscle cDNA library. The 1.9kb cDNA fragment was then used to identify chicken GP-53 analogues in skeletal muscle, cardiac, and brain cDNA libraries. Initial sequencing and restriction mapping analysis of several overlapping cDNAs suggests that there are two different isoforms of GP-53, one in skeletal muscle, and the other in brain and cardiac muscle. [This work was supported by Grant -In-Aid from AHA, VA Affiliate to HCK]

Tu-Pos78

AMINO ACID SEQUENCE OF CHICKEN CALSEQUESTRIN DEDUCED FROM cDNA: COMPARISON OF CALSEQUESTRIN AND ASPARTACTIN. Paul J. Yazaki, Sergio Salvatori, and A. Stephen Dahms, Molecular Biology Institute and Rees-Stealy Research Foundation, San Diego State University, San Diego, CA 92182.

Calsequestrin is the major Ca^{2+} -binding protein involved in the sequestration of Ca^{2+} within the terminal cisternae of the skeletal muscle sarcoplasmic reticulum. Previously, we have reported partial amino terminal sequence from adult chicken calsequestrin isolated from fast-twitch skeletal muscle. This partial sequence shows homology with mammalian calsequestrins contained in the Protein Identification Resource data bank and most importantly, complete identity with a putative laminin-binding protein of the extracellular matrix, aspartactin.

Presently, we have used this amino terminal and consensus sequence data to synthesize oligonucleotide primers for polymerase chain reaction (PCR). Direct DNA sequencing of asymmetric PCR products have revealed the cDNA sequence for the coding region of adult mature chicken calsequestrin. The amino acid sequence deduced from this cDNA matches tryptic peptide fragments from chicken calsequestrin and is identical to the amino acid sequence of aspartactin. Based on this complete cDNA sequence there can be no doubt that calsequestrin and aspartactin are the same protein.

In addition, chicken skeletal muscle calsequestrin has been shown to have a lower Ca^{2+} binding ability compared to mammalian isoforms. We have performed a multiple sequence alignment with known calsequestrin isoforms to determine possible differential Ca^{2+} binding sites. Studies on dimer formation employing cross-linking agents will be discussed. This research was supported by the National Science Foundation grants DCB 8613881 and INT 8515846, and the California Metabolic Research Foundation.

Tu-Pos77

PARTIAL PURIFICATION AND CHARACTERIZATION OF TRANSVERSE TUBULAR MEMBRANE 85KD GLYCOPROTEIN

H.B. Cunningham, R.C. Domingo, C. Jachec-Schmidt, J.J. Kang, R.A. Sabbadini, and A.S. Dahms. Departments of Chemistry and Biology, Molecular Biology Institute and Rees-Stealy Research Foundation, San Diego State University, San Diego, CA 92182-328

The transverse tubule (TT) of chicken skeletal muscle contains a very active (~250 $\mu\text{mol/hr/mg}$) MgATPase. The enzyme exhibits a host of distinguishing features, including: 1) unusual kinetic properties, 2) insensitivity to FITC and vanadate, 3) modulation by phorbol esters and diacylglycerols, and 4) sensitivity to detergents. An important characteristic of the chicken T-tubule MgATPase is its ability to be stimulated by lectins that can bind to the inner core of complex type oligosaccharide chains, including ConA, PHA-E, Lentil and WGA. In purified chicken T-tubule preparations a minor glycoprotein of Mr 85 kD (85 kD-GP) is reactive to stimulatory lectins on western blots. To date, the only polypeptide that can be associated with the MgATPase is the 85 kD glycoprotein. Partial purification of the 85 kD-GP has thus far been accomplished using the non-ionic detergent Triton X-114. Integral membrane proteins have been shown to partition preferentially into the detergent-rich phase while soluble proteins partition into the aqueous phase. The 85 kD glycoprotein of purified chicken T-tubules is highly enriched in the detergent-rich phase as well as the insoluble phase, indicating a possible integral membrane origin. Under these conditions the lectin-protected ATPase co-purifies with the 85kD-GP. Deglycosylation with Endo H reduced the 85kD-GP to Mr 75,000. N-Glycanase reduced the 85 kD-GP to Mr 65,000, consistent with results obtained by complete chemical deglycosylation with TFMSA. O-Glycanase treatment had no effect. These preliminary results indicate that the 85kD-GP contains both high mannose/hybrid and complex N-linked oligosaccharides, and no O-linked oligosaccharides. (Supported in part by NSF DMB 8613881, NSF INT 8515846, and the California Metabolic Research Foundation.).

Tu-Pos79

COVALENT LABELING OF CALCIUM BINDING DOMAINS IN SARCOPLASMIC RETICULUM ATPASE WITH ACRYLODAN. Sergio S. Serpa, Andrea D. Batista, Sergio Verjovski-Almeida and Sergio T. Ferreira

Departamento de Bioquímica, Instituto de Ciências Biomédicas, Universidade Federal do Rio de Janeiro, RJ 21944, Brazil.

The thiol reactive fluorescent probe acrylodan is being used to covalently label the Ca^{2+} -ATPase of sarcoplasmic reticulum. Under appropriate reaction conditions, it is possible to modify up to 7-8 cysteine residues per ATPase molecule. The fluorescence emission of acrylodan-ATPase indicates that the probe is located in hydrophobic regions of the protein, suggesting that cysteine residues in membrane-spanning segments of the ATPase are preferentially labeled. Presence of calcium in the reaction mixture causes a significant decrease in the rate and maximal level of labeling. In addition, the fluorescence emission of acrylodan-ATPase is sensitive to the concentration of calcium in the medium. The extent of high affinity calcium binding to ATPase previously labeled with acrylodan is decreased by 50% with respect to control unlabeled ATPase, as measured by column equilibration with radioactive calcium. These results suggest that acrylodan labels cysteine residues which are at or close to a high-affinity calcium binding site located in a transmembrane ATPase domain. Attempts are currently under way to locate the site(s) of attachment of acrylodan in the ATPase molecule.

Supported by CNPq, FAPERJ and FINEP (Brazil).

Tu-Pos80

UNFOLDING OF THE CA-ATPASE OF SARCOPLASMIC RETICULUM INDUCED BY UREA AND MONITORED BY FLUORESCENCE RESONANCE ENERGY TRANSFER. D. J. Bigelow, J. J. Chon, C. Sumbilla and G. Inesi, Dept. of Biochem., University of Maryland School of Medicine, Baltimore, Maryland, 21201.

Fluorescence resonance energy transfer (FRET) between spectroscopic probes bound to the Ca-ATPase was used to directly measure three-dimensional structural changes involved in unfolding of the native protein. FRET was measured during step-wise denaturation with urea between probes bound to specific residues predicted to lie both within the bilayer and on the cytoplasmic "head" of the Ca-ATPase. These probes include: (1) the iodoacetamide-directed probe, IAEDANS modifying proximal cysteines (670 and 674) of the nucleotide binding (B) domain; (2) FITC that modifies lysine 515 also of the B domain, and (3) several maleimide-directed probes that modify cysteines of the A₁ domain. In addition to these probes of the cytoplasmic portion of the protein, we have probed transmembrane protein sequences using intrinsic tryptophans as well as the fluorescent carbodiimide, N-cyclohexyl-N'-(4-dimethylamino-naphthyl) carbodiimide (NCD-4), bound to transmembrane residues of the A₁ domain. In contrast to conventional measurements of local structure, FRET measurements demonstrate (1) differential sensitivity between measurements obtained from probes located on different portions of the protein, (2) detection of structural changes at low urea concentrations, (3) better correlation with the effects of unfolding on the partial reactions of the enzymatic cycle, and (4) allows a more straightforward mechanistic interpretation of the data.

Tu-Pos82

FUNCTIONAL EXPRESSION OF INTRACELLULAR ORGANELLAR CALCIUM PUMP ISOFORMS. Jonathan Lytton¹, Marisa Westlin¹, Scott E. Burk², Gary E. Shull², David H. MacLennan³, and Michael R. Hanley⁴. ¹Brigham and Women's Hospital, Boston, MA, ²Univ. of Cincinnati College of Med., ³Univ. of Toronto, and ⁴MRC Molecular Neurobiology Unit, Cambridge, U.K.

Intracellular calcium stores in all cells are maintained, in part, by an ATP-dependent calcium pump. We have recently used molecular cloning techniques to identify two novel isoforms encoding organellar calcium pumps. One isoform (SERCA2b) was produced from an alternatively spliced transcript of the cardiac/slow-twitch muscle sarcoplasmic reticulum Ca-ATPase gene (Lytton and MacLennan, (1988) *J. Biol. Chem.* 263: 15024; Gunteski-Hamblin *et al.* (1988) *ibid.*: 15032). The other isoform (SERCA3) was encoded by a separate gene (Burk *et al.* (1989) *J. Biol. Chem.* 264: 18561). We have expressed the proteins encoded by these cDNA molecules, as well as by others, in COS cells and assayed their function by monitoring oxalate-dependent calcium uptake and calcium-dependent ATPase activity in microsomal fractions isolated from the transfected cells. The stoichiometry of calcium pumping was similar for all isoforms. Their apparent affinity for calcium varied, however, such that SERCA2b had the highest affinity, followed by the cardiac muscle isoform, and then SERCA3 with the lowest affinity. Vanadate inhibited the different isoforms with a potency which was inversely related to their apparent calcium affinities. Thapsigargin (TG), a non-TPA type tumor promoter, has been shown to discharge calcium stores from a variety of cell types. Recently it has been suggested that TG elicits its response by specifically inhibiting the endoplasmic reticulum (ER) calcium pump (Thastrup *et al.* (1990) *Proc. Natl. Acad. Sci. U.S.A.* 87: 2466). We have characterized further the interaction of TG with its target, and found that it inhibited each of the intracellular calcium pump isoforms with a similar nanomolar affinity. TG was without effect on either Na,K-ATPase or plasma membrane Ca-ATPase activities, and is thus a highly specific inhibitor of all the known organellar calcium pumps. These data indicate the mechanistic similarity and the subtle functional differences among structurally distinct intracellular calcium pumps, thus highlighting the question of the physiological role of these different molecules.

Tu-Pos81

SPECIFIC LABELING OF THE FOOT PROTEIN MOIETY OF THE TRIAD WITH A NOVEL FLUORESCENT PROBE: APPLICATION TO THE STUDIES OF CONFORMATIONAL CHANGES OF THE FOOT PROTEIN.

J.-J. Kang^a, A. Tarscafalvi^a, E. Fujimoto^b, Z. Shahrokhi^c, S. B. Shohet^c, and N. Ikemoto^{a,d} (a, Dept. Muscle Res., Boston Biomed. Res. Inst., Boston, MA 02114; b, Pierce Chemical Co. c, Univ. Calif. San Francisco d, Dept. Neurol. Harvard Medical School, Boston, MA)

We used a novel cleavable photoaffinity cross-linking reagent with the structure Azido-MCA(7-azido-4-methyl coumarin-3-acetic acid)-S-S-R(sulfosuccinimidylpropionate) developed with the help of Pierce Chemical Co. (vis Thevenin *et al.*, abstract this meeting) to examine the function of foot protein in microsomes. The cross-linker was conjugated with polylysine which specifically binds to the foot protein of sarcoplasmic reticulum (SR) and induces a rapid Ca²⁺ release from SR (Cifuentes, Ronjat, and Ikemoto, Arch. Biochem. Biophys. 273, 554, 1989). The polylysine conjugate was then mixed with muscle microsomes enriched with triad vesicles and photolysed for covalent labeling. It was then washed with β-mercaptoethanol. Fluorescence examination of SDS gels of the treated vesicles showed that the fluorescent probe was incorporated selectively into the foot protein. Since in this system, Ca²⁺ release is regulated by cytosolic [Ca²⁺], probably because of Ca²⁺-dependent conformational changes of the foot protein, we investigated the fluorescence intensity of the labeled foot protein as a function of [Ca²⁺]. Fluorescence intensity first increased as the [Ca²⁺] was raised from 1 μM to 11 μM (ΔF/F₀ = 11-12%), and then decreased upon further increase of [Ca²⁺], showing a bell-shaped [Ca²⁺]-dependence similar to that of Ca²⁺ release. These results suggest that the fluorescent probe appears to have been incorporated into the release trigger-binding region of the foot protein and to be serving as a reporter of the conformational change of the foot protein. (Supported by grants from NIH, MDA and AHA).

Tu-Pos83

PURIFICATION AND IDENTIFICATION OF ENDOPLASMIN (GRP94) FROM CANINE CARDIAC SARCOPLASMIC RETICULUM (SR).

S.E. Cala and L.R. Jones, Department of Medicine, Krannert Institute of Cardiology, Indiana University School of Medicine, Indpls., IN 46202.

A number of proteins have been described recently that, like calsequestrin, are localized to the SR lumen, and can be visualized in SDS-gels by the carbocyanine dye Stains-All. While several of these proteins are muscle specific, luminal SR proteins that are also found in ER have now been described. The COOH-termini of many of these luminal ER/SR proteins (reticuloplasmins) terminate with the sequence Lys-Asp-Glu-Leu (KDEL). We have isolated a major 100 kDa Stains-All blue-staining SR protein (Cala and Jones, *J. Biol. Chem.* 258:11932, 1983) from canine cardiac SR vesicles using a procedure involving solubilization by 100 mM Na₂CO₃, and purification by chromatography on phenyl-agarose, DEAE-Sephacel, and heparin-agarose. N-terminal sequencing of CNBr peptides determined that two peptides of 16 and 17 residues in length were 87% and 100% identical, respectively, to the reticuloplasmin, endoplasmic reticulum glucose-regulated protein M_r = 94,000 (GRP94). Endoplasmic reticulum was shown to be a constituent of both free and junctional SR using a novel ryanodine-dependent density shift of cardiac SR vesicles.

Tu-Pos84

DETECTION OF THE JUNCTIONAL FOOT PROTEIN DURING DEVELOPMENT OF EMBRYONIC CHICKEN CARDIAC MUSCLE. S.M. Dutro, J.L. Sutko*, C.F. Beck, J.A. Airey* & W.R. Trumble. Dept. Bact. & Biochem. University of Idaho, Moscow, Idaho; *Dept. Pharmacol., University of Nevada, Reno, Nevada.

We have investigated the expression of the foot protein during the development of the avian embryonic heart using monoclonal antibodies made against the skeletal foot protein (Airey *et al.* J. Biol. Chem. 265(24):14187, 1990). The foot protein can be detected from day E4 to day E20 in chick embryonic cardiac muscle. A monoclonal antibody which reacts with two different skeletal isoforms, α and β , cross-reacts with chick cardiac preparations in both Western blots and immunoprecipitations. A monoclonal antibody specific to only one skeletal isoform, β , also cross reacts with chick cardiac preparations. Although the embryonic heart begins to beat at approximately 33-38 hours, we have been unable to detect the foot protein with either immunoprecipitations or Western blots prior to day E4. Although two isoforms of the foot protein are present in skeletal muscle, only one isoform is detected in chick cardiac tissue (from sucrose gradient density centrifugation and SDS-PAGE analysis). Avian cardiac tissue is similar to mammalian cardiac tissue in this respect. We conclude that only one isoform of the foot protein can be detected from day E4 to day E20 of embryonic development of the avian heart.

Tu-Pos86

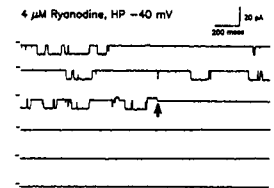
ANTIBODIES AGAINST THE 53 KDa GLYCOPROTEIN INHIBIT THE ROTATIONAL DYNAMICS OF BOTH THE Ca^{2+} -ATPase AND THE 53 KDa GLYCOPROTEIN IN THE MEMBRANE OF SARCOPLASMIC RETICULUM. James E. Mahaney^a, Christopher Weiss^b, Charles M. Grisham^a, and Howard Kutcher^a. Biophysics Program and ^aDepartment of Chemistry and ^bDepartment of Physiology, University of Virginia, Charlottesville, VA 22903.

The aim of this study is to better define the relationship of the 53 KDa glycoprotein (GP-53) of the sarcoplasmic reticulum (SR) to other SR proteins and its disposition with respect to the SR membrane. We investigated the effects of antibodies against GP-53 on the rotational dynamics of maleimide spin-labeled (MSL) proteins of SR of rabbit skeletal muscle. Our labeling protocol resulted in 1.6 ± 0.3 moles spin label bound per 10^5 g SR protein. MSL was bound principally to the Ca^{2+} -ATPase (1.3 mol MSL/mol Ca^{2+} -ATPase) and to GP-53 (0.9 mol MSL/mol GP-53). Using saturation-transfer electron paramagnetic resonance (ST-EPR), we found that the effective rotational correlation time (τ_r) of these proteins increased 5-fold upon preincubation of MSL-SR with an antiserum against the GP-53, while preincubation of MSL-SR with preimmune serum had no effect. Preincubation of MSL-SR with a monoclonal antibody (mAb) against the GP-53 produced a 4-fold increase in the apparent τ_r of the MSL-SR proteins compared to controls. These effects showed a marked Ca^{2+} dependence: the increase in τ_r of the MSL-SR proteins preincubated with anti-GP-53 antibodies in 500 μM Ca^{2+} was 3- to 6-fold greater than that of MSL-SR preincubated with antibodies in 5 mM EGTA. The binding of MSL and anti-GP-53 antibodies to GP-53 in intact, right-side-out SR is consistent with GP-53 being an integral membrane protein with part of its protein mass exposed on the cytosolic SR surface. Spectral simulations indicate that the increases we observed in τ_r caused by the anti-GP-53 mAbs are much too large to be accounted for by effects on τ_r of GP-53 alone. We infer that the rotational rate of Ca^{2+} -ATPase was also diminished by anti-GP-53 mAbs. This suggests an interaction between GP-53 and Ca^{2+} -ATPase in the SR membrane. (Supported by grants from NIH, NSF, and Amer. Heart Assn., Virginia Affiliate.)

Tu-Pos85

HIGH MOLECULAR WEIGHT PROTEINS IN THE NEMATODE *C. elegans* DISPLAY $[^3\text{H}]$ RYANODINE BINDING ACTIVITY AND FORM A ~500 pS CHANNEL IN PLANAR LIPID BILAYERS. Young-Kee Kim, Hector H. Valdivia, Ed B. Maryon*, Philip Anderson*, and Roberto Coronado. Department of Physiology, and *Department of Genetics, University of Wisconsin, Madison WI 53706

The nematode *C. elegans* is an excellent model organism to study the structure, assembly and function of muscle proteins at the genetic, structural, and biochemical levels. As a first step towards a genetic analysis of ryanodine receptors in this organism, we assessed the binding of $[^3\text{H}]$ ryanodine in solubilized homogenates of wild-type, ryanodine-sensitive nematodes. CHAPS-solubilized membrane fragments were layered on top of a 5X-20X (w/v) linear sucrose gradient and centrifuged at 55,000 g. Gradient fractions were monitored for $[^3\text{H}]$ ryanodine binding activity and SDS-PAGE gel electrophoresis. Binding activity was negligible at the top (5X) of the sucrose gradient and peaked at 18X to 19X sucrose. The fraction containing the highest $[^3\text{H}]$ ryanodine binding activity showed one major band of M.W. > 300 kDa in addition to a few low M.W. proteins. When incorporated into planar lipid bilayers, this fraction formed a 500 pS channel that also showed frequent transitions to a 133 pS subconductance state. Ryanodine (4 μM) completely inhibited the transitions between the two states and locked the channel into a permanently open, low-conductance state (see arrow). These results demonstrated the presence of a high-molecular weight, ryanodine-sensitive channel protein that may underlie Ca^{2+} release in muscle cells of *C. elegans*. The ligand binding and planar bilayer assays will be used to establish the phenotype of genetically altered ryanodine receptors in *C. elegans* mutants. Supported by NIH, MDA and AHA.



Tu-Pos87

POSTNATAL MATURATION OF DICARBOXYLIC ANION STIMULATED Ca^{2+} UPTAKE IN RABBIT SARCOPLASMIC RETICULUM. D.J. Fisher, C.A. Tate & S. Phillips. Departments of Pediatrics & Medicine, Baylor College of Medicine, Houston, TX, 77030, and Department of Pharmacology, University of Houston.

Previous reports have demonstrated that Ca^{2+} uptake by fetal cardiac sarcoplasmic reticulum (SR) membranes is diminished compared to adults. As all of the measurements were performed in the presence of cotransported dicarboxylic anions (DCA) such as maleate which themselves augment SR Ca^{2+} transport, the purpose of these experiments was to determine if the previously reported diminished Ca^{2+} transport in the fetus was related to diminished Ca^{2+} pumping, to DCA cotransport, or to both. Studies were performed on simultaneously isolated cardiac SR membranes from 29 day gestation fetal rabbits (term= 31 d) and their mothers. PIPES, to which cardiac SR is essentially impermeable (J Biol Chem 257:7704, 1982), was used as the control anionic buffer. The maximum Ca^{2+} uptake with Pipes was 29 and 39 nmoles/mg in fetal and mature SR, respectively (mean of n=4). Maleate and succinate stimulated earlier attainment of maximum Ca^{2+} uptake compared to that observed with PIPES in both fetal and mature SR; however, augmentation of maximum Ca^{2+} uptake by these DCA's in the fetal SR was trivial. In contrast, maleate and succinate increased maximum Ca^{2+} uptake by 32 and 15% in the SR from mature hearts (n=4). Ca^{2+} -ATPase activity, measured under identical reaction conditions, increased 29 and 17% by maleate and succinate in fetal SR, and 60 and 40% in mature SR (n=2). Measurement of maximal DCA cotransport, measured by ATP-dependent ^{14}C -succinate uptake in the presence of calcium, is in progress. These data demonstrate that the reduced Ca^{2+} transport by fetal SR can be related to dicarboxylic anion cotransport dependent as well as independent mechanisms. Supported by grants from the American Heart Association, Texas Affiliate (#90G-221) and from the NIH (#AG06221).

Tu-Pos88

MAGNESIUM DETERMINES CALCIUM SENSITIVITY OF GTP HYDROLYSIS BY CARDIAC SARCOPLASMIC RETICULUM.

C. Tate, B. Eikenburg, G. Shin, G. Taffet, R. Bick, and M. Entman. Sec. Cardiovas. Sci., Dept. of Med., Baylor College of Med., Dept. of Pharmacol., Univ. of Houston, Texas

Previously we demonstrated in cardiac SR that at 10 mM Mg and 1 mM NTP, unlike ATP hydrolysis, GTP hydrolysis is not Ca-sensitive sensitive; does not involve a Ca-sensitive phosphoenzyme; and is not inhibited by FITC. Like ATP, though, GTP induces Ca accumulation. In the present study, when Mg was lowered to 1 mM, GTP hydrolysis was similar to ATP hydrolysis: (1) Ca-stimulated GTPase activity was observed with a K_m for Ca of 1 μ M; (2) Ca-sensitive acylphosphoenzyme was formed from GTP and was abolished by FITC; and (3) ATP- and GTP-induced Ca accumulation was not affected by lowering Mg. Despite these similarities, these differences existed: (1) Ca-stimulated ATPase activity was rapidly inhibited at pCa 5.5; Ca-stimulated GTPase activity was stable from pCa 5.5-3.5. (2) Unlike Ca-stimulated ATP hydrolysis, Ca-stimulated GTP hydrolysis was not augmented by A23187. These data suggest that the calcium binding site(s) which stimulates GTP hydrolysis at low Mg is distal to the site which inhibits the Ca-stimulated ATPase activity. Supported by HL13870, AG06221, and AG0048.

Tu-Pos90

EFFECTS OF THE INTRACELLULAR MILIEU CHANGES ASSOCIATED WITH HYPOXIA IN SKINNED CARDIAC MUSCLE: INHIBITION OF SARCOPLASMIC RETICULUM (SR) Ca^{2+} UPTAKE AND REVERSAL OF THE PUMP AT LOW ATP. Yu Zhu & Thomas M. Nosek. Dept. Physiology & Endocrinology, Medical College of Georgia, Augusta, GA 30912-3000.

Short term (2 min) hypoxia causes a rapid decline in cardiac contractility that is accompanied by intracellular milieu changes, i.e., increases in inorganic phosphate (Pi), ADP, and AMP and decreases in creatine phosphate (CP) and ATP (Kammermeier et al., *J. Mol. Cell. Cardiol.* 14:267, 1982). We tested the effects on SR Ca^{2+} transport of solutions mimicking such intracellular milieu changes. SR Ca^{2+} content was estimated by measuring the magnitude of the caffeine-induced contracture in saponin-skinned rat papillary muscle. SR Ca^{2+} uptake was inhibited by solutions mimicking the hypoxic milieu only at short loading times (<60 sec, an $11 \pm 4\%$ inhibition at 7 sec) and at $[Ca^{2+}] > 1 \mu$ M. The inhibitory effect on SR Ca^{2+} uptake of hypoxic solutions was primarily due to the effect of elevated [Pi] (from 0.88 to 17.38 mM). At the longer loading times (> 30 sec), the ability of Pi to precipitate Ca^{2+} within the SR overcame its inhibitory effect on SR Ca^{2+} uptake. In longer term hypoxia, the myocardium begins to go into contracture as intracellular ATP is depleted and intracellular Ca^{2+} increases (Allen and Orchard *Circ. Res.* 60:153, 1987). To determine the effect of the hypoxic milieu changes at low ATP, we exposed the Ca^{2+} -loaded SR for 60 sec to a rigor solution containing zero ATP and zero CP (to inhibit Ca^{2+} uptake by the SR Ca^{2+} -ATPase) and 10 mM Mg^{2+} (to block the SR Ca^{2+} channel). This rigor solution had no effect on the Ca^{2+} content of the SR. Elevating Pi in the rigor solution to 17.38 mM or ADP to 0.7 mM (conservative values for long term hypoxia) had no effect on Ca^{2+} content. However, when elevated Pi and ADP were present in the rigor solution, we found a reduction to $58 \pm 12\%$ (n=5) of the control SR Ca^{2+} content. This reduction is most likely due to reversal of the SR Ca-pump. Pump reversal was inhibited by the addition to the rigor solution of 6 mM AMPPCP, a non-hydrolyzable ATP analog. We conclude that the changes in milieu with short term (2 min) hypoxia can depress contractility by inhibiting the Ca^{2+} -ATPase. At longer term hypoxia when [ATP] is reduced to low levels, these milieu changes can elevate intracellular Ca^{2+} by reversing the SR Ca^{2+} -pump. Support: NIH HL/AR 37022 and Am. Heart Assoc. - Ga. Affiliate (TMN).

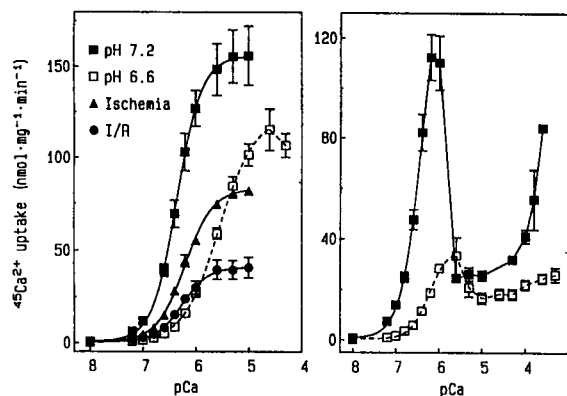
Tu-Pos89

THE EFFECT OF ACIDOSIS AND ISCHEMIA ON SR CALCIUM UPTAKE BY ADULT RAT CARDIOMYOCYTES. CM Hohl, AA Garleb, DK Wimsatt, GP Brierley, RA Altschuld. Dept. of Physiological Chemistry, Ohio State Univ., Columbus, OH.

In the presence of efflux inhibitors (30 μ M ruthenium red, 10mM procaine) in Na^+ -based medium (pH 7.2, 37°C, 50mM P_i , 10mM MgATP), $^{45}Ca^{2+}$ uptake by the sarcoplasmic reticulum (SR) of digitonin-lysed rat myocytes as a function of free $[Ca^{2+}]$ was saturable with a V_{max} of 160 $nmol \cdot mg^{-1} \cdot min^{-1}$ and $K_{0.5}$ of 0.45 μ M (Fig 1). Lowering pH to 6.6 shifted the $K_{0.5}$ to 2.75 μ M and decreased V_{max} by 28%. Preincubation of cells under N_2 , 20 mg/ml, 1 hr, 37°C (ischemia), with or without reoxygenation (I/R), greatly reduced V_{max} but had little effect on $K_{0.5}$. Fig 2 shows SR $^{45}Ca^{2+}$ uptake in the absence of efflux inhibitors at pH 7.2 and pH 6.6. The results indicate that acidosis lowers SR Ca^{2+} affinity whereas ischemia and reoxygenation decrease the capacity for Ca^{2+} accumulation. Supported by NIH HL-36240.

Fig 1

Fig 2



Tu-Pos91

MODULATION OF THE CONFORMATIONAL COUPLING BETWEEN THE TRANSMEMBRANE HELICES AND NUCLEOTIDE SITES ON THE Ca -ATPase BY THE PHOSPHOLIPID ENVIRONMENT. T.C. Squier and D.J. Bigelow. Dept. of Biochem., Univ. of Kansas, Lawrence, KS 66045.

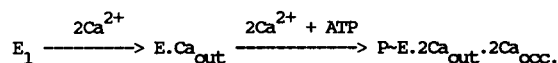
Utilizing frequency-domain fluorescence spectroscopy to measure the lifetime and anisotropy decays associated with both the intrinsic tryptophans and covalently bound FITC fluorophores on the Ca -ATPase, we have investigated the calcium-dependent structural changes associated with enzyme activation. We observe changes in both the lifetime, anisotropy, and solvent accessibility of these fluorophores upon calcium binding, indicating a long range structural change coupling the high affinity calcium sites at the level of the phospholipid bilayer and the distant nucleotide binding region sensed by the FITC chromophore. Upon modulation of the phospholipid environment with a small amount of monomristoyl phosphatidylcholine these calcium-dependent lifetime and anisotropy changes are abolished. Under these conditions there are no significant changes in the ATPase's transport activities or the solvent accessibility of the tryptophan or FITC fluorophores relative to the native membrane - indicating that there are no significant changes in the ATPase's tertiary structure and ruling out direct interactions between FITC and monomristoyl phosphatidylcholine. We suggest that in native membranes these calcium-dependent changes result from an amplification of changes in the mobility of these fluorophores and/or changes in the interactions between neighboring ATPase chains by modulating the resonance energy transfer efficiency between homologous fluorophores (i.e., homotransfer). The modulation of this calcium-dependent structural change by the phospholipid environment is relevant to the effective coupling mechanism of the ATPase, whereby calcium binding to the high affinity sites destabilizes the phosphoenzyme intermediate. Completed in part at the Center for Fluorescence Spectroscopy in Baltimore, Maryland.

Tu-Pos92

SIMULTANEOUS Ca BINDING TO AND OCCLUSION WITHIN THE SARCOPLASMIC RETICULUM Ca-PUMP WHICH CONTRADICTS THE $E_1 - E_2$ MODEL. L. G. Mészáros and J. Bak, Med. Coll., Georgia, Dept. Physiol. Endocrinol., Augusta, GA 30912

The kinetics of Ca^{2+} uptake, formation of the phosphorylated intermediate of the Ca-ATPase (EP) and the hydrolysis of ATP in rabbit skeletal muscle sarcoplasmic reticulum (SR) were investigated in the presence of mM Mg^{2+} . It was found by using the rapid filtration and the stopped-flow techniques that during the initial, rapid phase of uptake two calcium ions per enzyme previously bound to the high affinity and outward oriented sites are being occluded in a Ca-ionophore-inaccessible space within the interior of the pump protein. It was also shown that in parallel with the occlusion process two additional calcium ions must bind to the abandoned, therefore, newly available high-affinity sites. This indicates that four binding sites on the enzyme are simultaneously occupied by Ca^{2+} . Furthermore, they also indicate that two types of Ca^{2+} binding sites (i.e. the high-affinity outward oriented sites and the occluded ones) coexist, which contradicts a principal feature of the generally accepted $E_1 - E_2$ model.

The scheme below illustrates the elementary steps that could account for the Ca^{2+} uptake kinetics as observed:



Tu-Pos94

CORRELATION OF CARDIAC CALCIUM PUMP ACTIVITY WITH SUCCESSIVE INCORPORATION OF PHOSPHATE INTO PHOSPHOLAMBAN
Colyer, J. & Wang, J.H. "introduced by M.P. Walsh"
Cell Regulation Group, Dept. of Medical Biochemistry, University of Calgary, Calgary, Alberta T2N 4N1.

An understanding of the link between phospholamban phosphorylation and changes in cardiac sarcoplasmic reticulum calcium transport has remained qualitative due to difficulties in the expression of phosphorylation in molar terms. The situation is further complicated in that phospholamban is a homopentamer and as such one needs to correlate activity with overall stoichiometry and with the contribution made by individual molecular species (mono- to penta-phosphorylated) present at each stoichiometry.

Phosphorylation of phospholamban by the cAMP-dependent protein kinase results in the generation of 6 electrophoretically distinct species of the pentamer, containing 0 to 5 moles phosphate inclusive. Immunquantification of the relative concentration of each provides a method for determination of molar phosphorylation stoichiometry in isolated SR membranes and of the molecular species which comprise this phosphoprotein. We have applied this technique to study the relationship between Ca-ATPase activity and phospholamban phosphorylation. At low free Ca^{2+} (0.1 μM), full phosphorylation of phospholamban (5 mol/mol) resulted in a three-fold stimulation of control Ca-ATPase activity (where phospholamban was dephosphorylated). Generation of a range of phosphorylation stoichiometries (0.4-3.5 mol/mol) by PKA-mediated thiophosphorylation produced degrees of stimulation of ATPase activity predicted by a linear progression from non-phosphorylated to fully phosphorylated samples. No deviation from this relationship was observed dispelling the notion that either positive or negative cooperation exists between phosphorylation of phospholamban and stimulation of calcium transport. In addition, since the reaction mechanism employed by the cAMP-dependent protein kinase is random, one can conclude that each incorporation of a phosphate moiety contributes equally to stimulation of calcium pump activity.

Tu-Pos93

AlF_4^- AS AN ANALOG OF P_i ON THE SR Ca^{2+} -ATPASE

A. Troullier, J.L. Girardet, Y. Dupont

DBMS/BMC, CENG, 85 X, 38041 Grenoble Cedex (France)

Aluminofluorides have long been known to influence the activity of enzymatic systems like transducin of retinal rod outer segments and other G-proteins. It has been suggested that AlF_4^- acts as an analog of inorganic phosphate. We have investigated the aluminofluorides action on the sarcoplasmic reticulum Ca^{2+} -ATPase. As already reported, we confirm that aluminofluorides inhibit the pump activity. We have performed intrinsic tryptophan fluorescence measurements to study the mechanism of aluminofluorides binding to the ATPase. When the enzyme is in its E_2 calcium free conformation, we show that:

- * AlF_4^- is the most reactive of the various aluminofluoride complexes;
- * the binding of AlF_4^- on E_2 results in stabilizing the E_2 conformation of the Ca^{2+} -ATPase, inhibiting its return to E_1 upon addition of Ca^{2+} ;
- * the complexation is a quasi irreversible reaction with $k_+ = 2.5 \cdot 10^3 \text{ M}^{-1} \text{ s}^{-1}$ and $k_- < 10^{-1} \text{ s}^{-1}$. This slow process is magnesium dependent with an affinity of 0.5 mM, similar to the phosphorylation reaction with P_i . In the presence of DMSO, the rate of inhibition by AlF_4^- is greatly increased, showing a striking analogy with the phosphorylation by P_i .

This demonstrates that AlF_4^- acts as a quasi irreversible analog of P_i and confirms that the formation of the acyl-phosphate bound is related to a large change of water activity in the catalytic site rather than to the solvation of the phosphate.

Tu-Pos95

REGULATION OF SKELETAL SARCOPLASMIC RETICULUM Ca^{2+} -ATPase BY PHOSPHOLAMBAN AND NEGATIVELY CHARGED PHOSPHOLIPID. G. Szymanska, E. Amler, W.J. Ball and E.G. Kranias. Department of Pharmacology and Cell Biophysics, University of Cincinnati, Cincinnati, OH 45267-0575

The purified Ca^{2+} -ATPase from skeletal muscle sarcoplasmic reticulum (SR) was reconstituted in proteoliposomes containing phosphatidylcholine (PC). When reconstitution occurred in the presence of PC and phosphatidylserine (PS), (50:50 mol%) both the V_{max} and the affinity of the Ca^{2+} -pump for calcium were increased. These changes in Ca^{2+} -pump properties were correlated with changes in membrane viscosity, as monitored by the probe 1(4-trimethyl-ammoniumphenyl)6-phenyl-1,3,5-hexatriene (TMA-DPH). Reconstitution of the Ca^{2+} -ATPase, using PC:PS, resulted in phospholipid vesicles with a higher order parameter ($S = \sqrt{r/r_0}$) of the fluorescent probe TMA-DPH in the bulk phase ($S=0.810$), than reconstitution using PC ($S=0.773$). However, opposite changes were observed for phospholipids of the enzyme annulus. Sensitized fluorescence of TMA-DPH, with tryptophyl residues of Ca^{2+} -ATPase as donors, revealed a higher anisotropy in PC ($r=0.35$) than in PC:PS ($r=0.29$) vesicles. These findings suggest that negatively charged PS may influence both the membrane lateral pressure and the immediate environment of the Ca^{2+} -ATPase. The skeletal SR Ca^{2+} -ATPase, reconstituted into either PC or PC:PS proteoliposomes was also found to be regulated by exogenous phospholamban (PLB). Inclusion of PLB into the proteoliposomes was associated with significant inhibition of the initial rates of Ca^{2+} -uptake, while phosphorylation of PLB by the catalytic subunit of cAMP-dependent protein kinase reversed the inhibitory effects. The effects of PLB on the reconstituted Ca^{2+} -ATPase were similar in either PC or PC:PS proteoliposomes, indicating that inclusion of negatively charged phospholipid may not affect the interaction of PLB with the skeletal SR Ca^{2+} -ATPase. (Supported by NIH HL26057, HL22619 and HL32214 (WJB)).

Tu-Pos96

PHOSPHOLAMBAN-PHOSPHATASE IN CARDIAC SARCOPLASMIC RETICULUM. N.A.E. Steenaart, J. Di Salvo, E.G. Kranias. Department of Pharmacology and Cell Biophysics, University of Cincinnati, Cincinnati, OH 45267-0575

Phospholamban, the putative regulator of the Ca^{2+} -pump in cardiac sarcoplasmic reticulum (SR), can be phosphorylated by three different protein kinases at distinct sites. Phosphorylation is associated with stimulation of Ca^{2+} -uptake, and dephosphorylation may occur by an endogenous phosphatase and reverse the stimulatory effects of the protein kinases. To characterize the protein phosphatase activity, associated with sarcoplasmic reticulum, the membranes were solubilized with n-octyl- β -D-glucopyranoside and the extracted phosphatase activity was purified by sequential chromatography on DEAE-Sephacel, polylysine-agarose, heparin-agarose and DEAE-Sephadex. A single peak of phosphatase activity was eluted from each column. The enzymatic activity was purified over 1,000-fold and it could dephosphorylate the sites on phospholamban phosphorylated by either cAMP-dependent or calcium-calmodulin-dependent protein kinase(s). Enzymatic activity was inhibited by inhibitor-2 and by okadaic acid (I_{50} : 10-20 nM). The sensitivity of the phosphatase to inhibitor-2 or okadaic acid was similar for the two sites on phospholamban, phosphorylated by the cAMP-dependent and the Ca^{2+} -calmodulin-dependent protein kinases. Phospholamban phosphatase activity was enhanced (40%) by Mg^{2+} or Mn^{2+} (3 mM) while Ca^{2+} (0.1-10 μM) had no effect. These characteristics suggest that a type 1 phosphatase is associated with cardiac sarcoplasmic reticulum, which can dephosphorylate the sites on phospholamban phosphorylated by either the cAMP-dependent or the Ca^{2+} -calmodulin-dependent protein kinase, and this phosphatase may participate in regulation of the sarcoplasmic reticulum function in cardiac muscle (Supported by NIH HL26057 and HL22619).

Tu-Pos97

ACTIVATION OF PROTEIN KINASE C IN VIVO BY α_1 -ADRENERGIC AGONISTS IS NOT ASSOCIATED WITH PHOSPHORYLATION OF PHOSPHOLAMBAN. L. Talosi, I. Edes and E.G. Kranias. Department of Pharmacology and Cell Biophysics, University of Cincinnati, Cincinnati, OH 45267-0575

The calcium pump in cardiac sarcoplasmic reticulum is regulated by a low molecular weight phosphoprotein, called phospholamban. Phospholamban can be phosphorylated by cAMP-dependent, Ca^{2+} -calmodulin-dependent and Ca^{2+} -phospholipid dependent protein kinases *in vitro*. Cyclic AMP-dependent and Ca-calmodulin dependent phosphorylation of phospholamban has been also shown to occur *in vivo*, in intact hearts. To determine whether protein kinase C can also phosphorylate phospholamban *in vivo*, beating hearts were perfused with modified Krebs-buffer containing ^{32}P -phosphate and treated with an α_1 -agonist, phenylephrine, to activate protein kinase C. Control hearts were perfused under identical conditions but in the absence of this agent. Perfusion of hearts with phenylephrine resulted in redistribution of the protein kinase C activity from the cytosol to the membrane fraction, suggesting the activation of the enzyme *in vivo*. Examination of ^{32}P -incorporation into various fractions revealed that there was no increase in the degree of phosphorylation of phospholamban in the sarcoplasmic reticulum. However, in the same hearts there was a significant increase in the ^{32}P -incorporation into a 28 kDa cytosolic protein. Similar findings were obtained using phorbol 12-myristate, 13-acetate (PMA) and 1,2-dioctanoyl-glycerol (D8G) in the perfusate, which directly activated protein kinase C intracellularly. These findings indicate that, although phospholamban is phosphorylated by protein kinase C *in vitro*, it does not appear to be a substrate for this enzyme in the intact beating heart. (Supported by NIH HL26057 and HL22619).